EFFECTS OF IMMUNE COMPLEXES ON GLOMERULAR ENDOTHELIAL CELLS: IMPLICATIONS FOR LUPUS NEPHRITIS

WANG LINLIN

Ph.D

The Hong Kong Polytechnic University

2017

The Hong Kong Polytechnic University

Department of Health Technology and Informatics

Effects of Immune Complexes on Glomerular Endothelial Cells: Implications for Lupus Nephritis

WANG Linlin

A thesis submitted in partial fulfilment of the requirements for the degree of Doctor of Philosophy

June 2017

CERTIFICATE OF ORIGINALITY

I hereby declare that this thesis is my own work and that, to the best of my knowledge and belief, it reproduces no material previously published or written, nor material that has been accepted for the award of any other degree or diploma, except where due acknowledgement has been made in the text.

_____ (Signed)

WANG Linlin _____(Name of student)

Abstract

Lupus nephritis (LN) is a common and severe complication of systemic lupus erythematosus, with poor prognosis. Lupus nephritis can lead to permanent renal damage and is the major cause of morbidity and mortality in lupus patients. Although multi-factors have been proved to be involved in disease pathogenesis, including the genetic, environmental, and immunological factors, the precise mechanisms of renal impairments are still not thoroughly understood.

Glomerular endothelial cells (GECs) is one type of the renal parenchymal cells and plays important roles in maintaining the integrity of the tripartite renal filtration barrier, which is the structural foundation of renal function. GEC injury and dysfunction will unavoidably affect renal physiology. There is accumulating evidence revealing vascular lesions and endothelial cell injury in LN. However, GECs has been little studied and the underlying pathways for GEC injury in LN remain unknown. Immune complex (IC) formation is one characteristic of LN. Detection of specific autoantibodies and ICs is among the criteria for disease diagnosis. Immune complexes can exist in the circulation or be deposited in tissues. In the kidney, ICs are mainly deposited in subendothelial, subepithelial, or mesangial areas. Since the kidney is a vessel-rich organ and receives approximately 1/5 of the resting cardiac output, GECs are constantly exposed to the circulating ICs or GECs can maintain contact with ICs that deposit in the subendothelial

areas. This IC challenge may impair GEC function. Thus, we aimed to investigate the effects of ICs on GECs *in vitro* and try to understand the details of GEC injury in LN. In the present project, we used heat-aggregated gamma globulin (HAGG) to substitute the ICs. TNF-alpha was also used to simulate the inflammatory microenvironments in the kidney in LN. Cultured human GECs were incubated with HAGG alone or in combination with TNF-alpha. Different aspects of endothelial cell functions were evaluated.

We first investigated the effect of HAGG on autophagy in GECs. Autophagy is a highly conserved catabolic process to degrade cytoplasmic contents through lysosomes. Autophagy presents at basal level and can be activated in response to different stresses. Autophagy is required for maintaining cell homeostasis and exhibits cytoprotective roles in many cell types. Impaired autophagy is reported in many diseases and pathological conditions. Our results showed that HAGG incubation led to decreased LC3 conversion, increased p62 expression, and decreased fluorescence intensity of LC3 puncta staining. Incubation with HAGG also significantly increased the phosphorylations of the key nodes in the mTOR-dependent pathways, including mTOR, p70s6k, 4E-BP-1, and Akt. Therefore, our results indicated that autophagy was suppressed by HAGG in GECs, through an Akt/mTOR-dependent pathway.

Next, we evaluated the characteristic cell functions in GECs under HAGG stimulation. Results showed that HAGG treatment changed GEC morphology, induced apoptosis and suppressed cell viability. For tube formation assay, HAGG led to decreased number of

junctions and number of meshes, suggesting inhibited angiogenesis. Moreover, HAGG induced intracellular NO productions in GECs, partly through the Akt-eNOS pathway. Mimicking the inflammatory condition, combination of HAGG and TNF-alpha led to obvious cell morphological changes, further decreased cell viability, increased apoptosis, increased NO production, and decreased ability for tube formation.

To investigate the possible relationship between autophagy and endothelial cell functions, we used autophagic regulators, rapamycin and 3-Methyladenine, to stimulate and inhibit autophagy respectively. Akt was a key molecule when considering the interaction between autophagy and NO production. Incubation with HAGG activated Akt, which could subsequently activate eNOS and induce NO production in GECs. Meanwhile, activated Akt phosphorylated mTOR and eventually suppressed autophagy.

In conclusion, HAGG incubation can affect endothelial cells functions, including autophagy, cell morphology, cell viability, NO production, and angiogenesis. These effects of HAGG on GECs functions, especially under inflammatory microenvironment, are implicated in the renal damage in LN patients. Since renal injury is the most important predictor of mortality in SLE patients, it is important to translate these findings to drug development and treatment strategies to improve the prognosis of LN.

Publications

Scientific Journal Papers

Wang LL and Law HKW (2015), The Role of Autophagy in Lupus Nephritis. International Journal of Molecular Sciences 16(10): 25154-25167.

Wang LL and Law HKW (2017), Immune complexes suppressed autophagy in glomerular endothelial cells. (Submitted to Cellular Immunology, CIMM-17-247)

Refereed Conference Abstracts

Wang LL, Law HKW. Heat-aggregated Gamma Globulins Suppress Autophagy and Induce Injuries in Glomerular Endothelial Cells. 1st International Congress of Chinese Nephrologists (ICCN), 11-13 December 2015, Hong Kong, China. Published in Hong Kong Journal of Nephrology 17(2): S57, October 2015 (Poster presentation).

Wang LL, Law HKW. Suppressed autophagy in glomerular endothelial cells under TNF-alpha and immune complex stimulation, International Congress of Immunology (ICI) 2016, 21-26 August 2016, Melbourne, Australia (Poster presentation).

Awards

ICI-FIMSA travel awards for International Congress of Immunology 2016.

Acknowledgements

During my PhD journey, I owe a debt of gratitude to a lot of people. First of all, I would like to express my sincere appreciation to my chief supervisor Dr. Helen Ka Wai LAW. Dr. LAW understands my desires and fears, and my merits and demerits. She supports me to design this project combining my previous clinical experiences and the unresolved research question. She gives me a balanced training between learning and research, and always encourages me to learn from different people. She supported me to attend the Croucher Summer Course 2014 "Advances in Immunology in Health and Disease", the 8th HKU-Pasteur Immunology Course 2015, and the Basic Immunology Course in the ICI 2016, through which I gained systematic knowledge about immunology progresses from the invited distinguished scholars and was inspired by the participants. Her patience, encouragements, constructive criticisms and suggestions, supports me to conquer the challenges and complete my PhD study. Her enthusiasm for scientific research, rigorous scholarship, and hard work, have set an excellent example for me. It is my great honour and luck to be supervised by her.

I would like to thank Prof. Shea-ping YIP, Prof. Iris BENZIE, Prof. Benjamin Y. M. YUNG, Dr. Parco M. F. SIU, Dr. Tony S. S. TO, Dr. Cesar S. C. WONG, Dr. Xiang ZHOU, Dr. Chien-ling HUANG, Dr. Patrick Y. M. LAI, Dr. Gilman K. H. SIU, Dr. Jung Sun YOO, Dr. Michael T. C. YING, and Dr. Lawrence W. C. CHAN, for their valuable comments, suggestions and instructions for my study. Prof. BENZIE also spend her precious time to review my manuscript.

I would like to thank Ms. Aileen C.M. WONG, Ms. Brenda WONG, Ms. Michelle Ng, Ms. Joey C. Y. CHIU, Ms. Grace L. H. TANG, Ms. Christine W. Y. LI, Mr. Paul P. S. FAN, Ms. Nicki W. M. KWAN, for their professional technical assistance. I am thankful for Dr. Karen Y. J. Gu from Department of Applied Biology and Chemical Technology, for her expertise on confocal microscopy. I also appreciate Ms. Kathy Y. K. KWAN, Mr. Tommy P. S. CHAN, Ms. Doris S. L. KWOK, Ms. Fiona S. W. LEUNG, Ms. Candy S. C. YUNG, and Mr. David W. L. LAU in the general office and staff in the research office, for their assistance to help me complete my study smoothly.

I appreciate all my friends in this department. They are smart, diligent, energetic, and humorous. They inspire and motivate me. Discussions with them always lead to insights into the problems and creative ideas. Experiences shared by them are very helpful. Their friendships are my cherished treasure.

Finally, I would like to express my greatest appreciation to my parents. They always have my back and trust me more than myself. Their love and supports are my source of courage. Special thanks go to Dr. WANG, for his company and tolerance.

[This work was partially supported by grants to my supervisor Dr. Helen Law: (i) Early Career Scheme from Research Grants Council of the Hong Kong Special Administrative Region, China (RGC#589413). (ii) Departmental Research Fund, Department of Health Technology and Informatics, and (iii) Internal Grant for Eligible PIs (G-YBK0 and G- YBPL), The Hong Kong Polytechnic University.]

Table of Contents

List of Figures

Lists of Tables

List of Abbreviations

3MA	3-mehtyladenine
4E-BP-1	eIF4E-binding protein 1
AAVE	Autoantibodies to VE-cadherin
AECA	Anti-endothelial cell antibody
AF4	Asymmetrical flow field flow fractionation
AFS	Autophagosomal formation site
ALD-DNA	Activated lymphocytes-derived DNA
AMPK	AMP-activated protein kinase
Angs	Angiopoietins
APOL1	Apolipoprotein L1
APS	Anti-phospholipid syndrome
AT1-AA	Angiotensin II type 1 receptor-activating autoantibody
ATF6α	Activating transcription factor 6 α
Atgs	Autophagy-related proteins
ATP	Adenosine triphosphate
BCA	Bicinchoninic acid
BCR	B cell receptor
BH4	Tetrahydrobiopterin
BSA	Bovine serum albumin

CaMKII	Calmodulin-dependent protein kinase II
CaMKK2	Calmodulin-dependent protein kinase kinase 2
CDARS	Clinical Data Analysis and Reporting System
CDKN1B	Cyclin-dependent kinase inhibitor 1 B
CII	Type II collagen
CMA	Chaperone-mediated autophagy
CQ	Chloroquine
CSTAR	Chinese SLE Treatment and Research group
DEPTOR	DEP domain containing mTOR-interacting protein
DLS	Dynamic light scattering
DNA-PK	DNA-dependent protein kinase
DRAM1	DNA damage regulated autophagy modulator
EC	Endothelial cell
eIF4F	eukaryotic translation initiation factor 4F
Epac	Exchange protein directly activated by cAMP level
EPC	Endothelial progenitor cell
ER	Endoplasmic reticulum
ESL	Cell surface layer
ESRD	End-stage renal disease
FAD	Flavin adenine dinucleotide
FIP200, RB1CC1, Atg17	FAK family kinase-interacting protein of 200 kD
FMN	Flavin mononucleotide

GAP	GTPase-activating protein
GBM	Glomerular basement membrane
GC	Gluanylyl cyclase
GEC	Glomerular endothelial cell
GEF	Guanine nucleotide exchange factor
GFB	Glomerular filtration barrier
GFR	Growth factor-reduced
GSK3β	Glycogen synthase kinase 3β
GWAS	Genome-wide association studies
HAGG	Heat-aggregated gamma globulin
HCQ	Hydroxychloroquine
HMGB1	High-mobility group box 1
Hsc70	Heat shock cognate 70
HUVEC	Human umbilical vein endothelial cells
IBD	Inflammatory bowel disease
IC	Immune complex
ICAM-1	Intercellular adhesion molecule-1
IMPase	Inositol monophosphoatase
IP3	Inositol 1,4,5-trisphosphate
IRE1α	Inositol-requiring protein 1α
IRGM	Immunity-related GTPase family M
IRS1	Insulin receptor substrate 1

ISN/RPS	International Society of Nephrology/ Renal Pathology Society
JNK	c-Jun N-terminal kinases
LAMP-2A	Lysosome-associated membrane protein-2A
LIR	LC3-interacting region
LKB1, STK11	Liver kinase B1, STK11
LN	Lupus nephritis
LRP	Low-density lipoprotein receptor-related protein
MAP1LC3, LC3	Microtubule-associated proteins 1A/1B light chain 3
MAPK	Mitogen-activated protein kinase
MAPKAP1, mSIN1	Mitogen-activated protein kinase associated protein 1, or SAPK-interacting 1
MCP-1	Monocyte chemoattractant protein-1
MFI	Mean fluorescence intensity
MHC	Major histocompatibility complex
mlST8	mammalian lethal with SEC thirteen 8
MNK1	MAPK-activated protein kinase 1
MTMR3	Myotubularin-related phosphatase 3
mTOR	mammalian or mechanistic target of rapamycin
NADPH	Nicotinamide adenine dinucleotide phosphate
NET	Neutrophil extracellular trap
NO	Nitric oxide

NOS	NO synthase
NTA	Nanoparticle tracking analysis
NZB/W mice	Hybrid mice cross between the New Zealand Black Female and New Zealand White Male mice
p62, SQSTM1	Sequestosome 1
PBS	Phosphate buffer saline
PDCD4	Programmed cell death 4
PDK1	3-phosphoinositide-dependent protein kinase 1
PECAM-1, CD31	Platelet endothelial cell adhesion molecule
PEG	Polyethylene glycol
PERK	Protein kinase RNA-like ER kinase
PH domain	Pleckstrin homology domain
PHLPP	PH-domain leucine-rich-repeat-containing protein phosphatases
PI	Propidium iodide
PI3KC3, Vps34	class III phosphatidylinositol 3-Kinsase, or Vacuolar protein sorting 34
PIP2	Phosphatidylinositol 3,4-bisphosphate
PIP3	Phosphatidylinositol 3,4,5-triphosphate
PKA	Protein kinase A
PKB, Akt	Protein kinase B, a serine/threonine-specific protein kinase
PKC	Protein kinase C

PLC	Phospholipase C
PlGF	Placenta growth factor
PP2A	Protein phosphatase 2A
PRAS40	Proline-rich Akt substrate of 40 kD
PROCTOR	Protein observed with Ricto
PTEN	Phosphatase and tensin homolog
PTPN22	Protein tyrosine phosphatase non-receptor type 22
RAGE	Receptor for advanced glycation end products
RAPTOR	Regulatory-associated protein of mTOR
Rheb	Ras-homolog enriched in brain
RICTOR	Rapamycin-insensitive companion of mTOR
RNI	Reactive nitrogen intermediate
ROS	Reactive oxygen species
S6K	40S ribosomal S6 kinase
SDS-PAGE	Sodium dodecyl sulfate-polyacrylamide gel electrophoresis
SEC	Size exclusion chromatography
SLE	Systemic lupus erythematosus
SLEDAI	Systemic Lupus Erythematosus Disease Activity Index
SLICC	Systemic Lupus International Collaborating Clinics
SMR	Standardized mortality ratios
SPS	Sub-podocyte space
STK36	Serine/threonine kinase 36

sVEGFR-1, sFlt-1	soluble vascular endothelial growth factor receptor 1, or soluble Fms-like tyrosine kinase-1
TBC1D7	TBC 1 domain family, member 7
TCR	T cell receptor
TLR	Toll-like receptor
TNF	Tumor necrosis factor
TSC	Tuberous sclerosis complex
UBA domain	Ubiquitin-associated domain
ULK1	Uncoordinated 51-like kinase 1
VCAM-1	Vascular cell adhesion molecule-1
VEGF	Vascular endothelial growth factor

Chapter 1 Introduction

1.1 Systemic lupus erythematosus and lupus nephritis

Systemic lupus erythematosus (SLE, or lupus) is a prototype of chronic autoimmune inflammatory disease characterized by loss of tolerance against nuclear self-antigens, polyclonal autoantibodies production, immune complexes (ICs) formation, and deposited in different part of the body, leading to detrimental inflammation and multi-organ injuries (Lech and Anders, 2013). Besides, SLE can lead to fatigue, pain, sleep disturbance and neurological/psychiatric outcomes, particularly anxiety and depression. It has a considerable impact on the quality of life of patients and their ability to carry out normal daily activities, resulting in a high prevalence of disability (25–57%) (Schmeding and Schneider, 2013). The latest classification of SLE as illustrated in Table 1.1, contains 11 clinical and 6 immunological criteria. Meeting 4 criteria (at least include 1 clinical and 1 immunological criterion, or have kidney biopsy proven as lupus nephritis) is needed for the classification of SLE. The sensitivity and specificity of this criteria is 97% and 84%, respectively (Goldblatt and O'Neill, 2013).

Table 1.1 Updated classification criteria for SLE from the Systemic Lupus International Collaborating Clinics (SLICC) group

(Adapted from Petri et al., 2012)

Clinical criteria
Acute cutaneous lupus
Chronic cutaneous lupus
Oral ulcers
Non-scarring alopecia
Synovitis in two or more joints (includes tenderness and 30 minutes of early morning stiffness)
Serositis
Renal: urine protein-to-creatinine ratio or 24 hour collection representing 500 mg protein/24 hours
Neurological
Haemolytic anaemia
Leucopenia
Thrombocytopenia
Immunological criteria
Antinuclear antibodies
Anti-double-stranded DNA (anti-dsDNA)
Anti-Smith antibody
Antiphospholipid antibody
Low complement
Direct Coombs test in the absence of haemolytic anaemia

Although the term “lupus erythematosus” was firstly used by physicians to describe the skin lesions that resembled a “wolf’s bite” in the 13th century, the pathogenesis and mechanisms of SLE remains unclear (Tsokos, 2011) till now. The overall incidence and prevalence of SLE mainly range from 1 to 25 cases per 100,000 people per year and 20 to 200 cases per 100,000 people, respectively (Danchenko et al., 2006; Mok, 2011; Li et al., 2012; Goldblatt and O'Neill, 2013; Yeh et al., 2013; Arnaud et al., 2014; Lim et al., 2014; Jarukitsopa et al., 2015; Tsioni et al., 2015; Rees et al., 2016). Women are more frequently affected, as the female:male ratio is around 9:1 (Borchers et al., 2010; Borchers et al., 2012). People of African, Hispanic, or Asian ancestry tend to have increased prevalence and more severe organ involvement. The current treatments for SLE are mainly corticosteroids, immunosuppressants and biologic therapies. These treatments are only partially effective, and at the cost of considerable side effects. Survival of SLE patients has significantly improved in the past half century. The 10-year survival of patients increased from approximately 50% in the 1950s to over 90% in the 2000s (Goldblatt and O'Neill, 2013). However, increased longevity will extend patients’ exposure to immunosuppressant agents and inflammatory insults. This might retard further advancement of survival in these patients.

Among the multi-organ injuries, renal involvement, called lupus nephritis (LN), is one of the most common and severe complications of SLE. LN affects 30-60% of adults and 70% of children lupus patients (Carreno et al., 1999; Maroz and Segal, 2013; Davidson, 2016; Hanly et al., 2016). The prevalence and incidence of LN is 30.9 per 100,000 and 6.9 per

100,000 person-years respectively based on US Medicaid population (Feldman et al., 2013). Proteinuria is the characteristic feature of LN. Microscopic hematuria can also be found commonly in LN patients. About one-half of the LN patients have reduced glomerular filtration rate (a key indicator for renal functions) (Saxena et al., 2011). LN may lead to permanent renal damage and chronic kidney diseases. It is also the major cause of morbidity and mortality in lupus patients (Maroz and Segal, 2013). Histological lesions in LN can be divided into 6 classes according to the World Health Organization (WHO) and the International Society of Nephrology/Renal Pathology Society) (ISN/RPS) classifications (Table 1.2 and 1.3). The proliferative forms, including Class III and IV, are the main classes of LN patients, and will progress to chronic renal failure if appropriate immunosuppressive treatments have not been provided. About 10-30% of severe LN patients (WHO Class III and above) progress to end-stage renal disease (ESRD) within 15 years after diagnosis (Maroz and Segal, 2013). Till now, the mechanisms for renal injuries in LN are unclear. The therapy is still non-specific and far from interfering with the cause of the disease. The outcome of LN is not satisfied. The complete remission rate of proliferative renal diseases in LN patients remains less than 50%. The 10-year survival rates of LN patients range from 68%-98.2% (Borchers et al., 2012). The mortality in LN patients is ~6 times higher than that in general population [The standardized mortality ratios (SMR) of LN patients range from 5.9-6.8 (Faurschou et al., 2010; Yap et al., 2012b)]. LN patients who progress to ESRD have an even higher SMR of 26.1 (Yap et al., 2012b).

Table 1.2 World Health Organization (WHO) morphologic classifications of LN (modified in 1982)

(adapted from Weening et al., 2004)

Class I	Normal glomeruli
	a) Nil (by all techniques)
	b) Normal by light microscopy, but deposits by electron or immunofluorescence microscopy
Class II	Pure mesangial alterations (mesangiopathy)
	a) Mesangial widening and/or mild hypercellularity (+)
	b) Moderate hypercellularity (++)
Class III	Focal segmental glomerulonephritis (associated with mild or moderate mesangial alterations)
	a) With “active” necrotizing lesions
	b) With “active” and sclerosing lesions
	c) With sclerosing lesions
Class IV	Diffuse glomerulonephritis (severe mesangial, endocapillary, or mesangio-capillary proliferation and /or extensive subendothelial deposits)
	a) Without segmental lesions
	b) With “active” necrotizing lesions
	c) With “active” and sclerosing lesions
	d) With sclerosing lesions
Class V	Diffuse membranous glomerulonephritis
	a) Pure membranous glomerulonephritis
	b) Associated with lesions of category II (a or b)
	c) Associated with lesions of category III (a-c)
	d) Associated with lesions of category IV (a-d)
Class VI	Advanced sclerosing glomerulonephritis

Table 1.3 Abbreviated International Society of Nephrology/Renal Pathology Society (ISN/RPS) classification of lupus nephritis (2003)

(adapted from Weening et al., 2004)

Class I	Minimal mesangial lupus nephritis
Class II	Mesangial proliferative lupus nephritis
Class III	Focal lupus nephritis[a]
Class IV	Diffuse segmental (IV-S) or global (IV-G) lupus nephritis[b]
Class V	Membranous lupus nephritis[c]
Class VI	Advanced sclerosing lupus nephritis

Note:

[a]Indicate the proportion of glomeruli with active and with sclerotic lesions.

[b]Indicate the proportion of glomeruli with fibrinoid necrosis and cellular crescents.

[c]Class V may occur in combination with Class III or IV, in which case both will be diagnosed.

For local information, although recent national wide survey of SLE patients was lacking, the prevalence of SLE in China was estimated to be 30-70 cases per 100,000 people. Different prevalence has been reported from different research groups, for example, 70.1/100,000 people in Huang's report (Zeng et al., 2008), 37.7/100,000 people in Xiang's review (Xiang and Dai, 2009), and 0.03% in Li's report (Li et al., 2012). In Taiwan, the recent average prevalence of SLE reported in 2013 was 97.5 per 100,000 people (Yeh et al., 2013). Results from Chinese SLE Treatment and Research group (CSTAR) showed that 47.4% of SLE patients presented with nephropathy (Li et al., 2013a). In Hong Kong, SLE is also not an uncommon rheumatic disease. Data from the Clinical Data Analysis and Reporting System (CDARS) revealed that from 1999 to 2008, the prevalence and annual incidence of SLE are estimated to be 0.1% and 6.7/100,000 people, respectively. The 10-year survival of SLE patients is 83%. Kidney is also the most frequently disease-affected organ (Mok, 2011).

1.2 Immune complexes in the pathogenesis of lupus nephritis

Immune complexes are central players in the pathogenesis and tissue injury in SLE (Tsokos, 2011). The existence of circulating ICs in the serum and their correlation with disease activity have been proven in many experiments since the late 1970s (Hay et al., 1976; Theofilopoulos et al., 1976; Zubler et al., 1976; Casali et al., 1977; Harkiss et al., 1979; Abrass et al., 1980; Kingsmore et al., 1989). The constitutions of ICs are complex. They usually contain autoantigens such as nucleic acids, nucleic acids-associated proteins, and corresponding autoantibodies. The impaired clearance of apoptotic cells taken by

phagocytes in SLE patients results in secondary necrosis, and subsequently the release of nuclear autoantigens from the nuclei of these secondary necrotic cells. The generation of corresponding autoantibodies targeting against these nuclear autoantigens leads to the formation of ICs. The size and composition of ICs influence their consequent effects (Doekes et al., 1984; Nangaku and Couser, 2005). When an antigen bears oligo- or excess multi-valent epitopes, ICs tend to be small and soluble. Small ICs are inefficient to activate following complement pathway or Fc receptors mediated pathways and are relatively inert. When with equivalent antigen/antibody ratio, cross-linking is extensive to form large insoluble ICs, which have high affinity for Fc receptors and ability to activate complement pathways, thus facilitate their rapid removal from the circulation by phagocytosis. Medium-sized complexes that are less well-cleared but can activate sequencing immune responses. These are the ones that deposit on target organs, such as the skin and kidney, resulting in end organ damage.

1.2.1 Autoantibodies and immune complexes

Lupus nephritis is regarded as a typical example of IC-mediated glomerulonephritis. The presence of various autoantibodies and the corresponding ICs is required for pathogenesis of LN:

Anti-dsDNA antibody is one of the most important autoantibody related to LN. Autoantibodies against DNA were first described in 1957. Nearly 70–96% of the patients with LN were identified to have circulating anti-dsDNA antibodies, compared to 0.5% in patients with other autoimmune diseases or in normal controls (Grootscholten et al., 2007;

Yung and Chan, 2012). In lupus, circulating levels of anti-dsDNA antibodies correlate with disease activity in many experiments and clinical results (Isenberg et al., 2007). Anti-dsDNA antibodies are closely linked with nephritis development. Many typical manifestations of LN can be imitated in non-autoimmune mice either by administrating human or murine anti-dsDNA antibodies intraperitoneally or by inoculating the mice with the transgene that encodes the secreted form of an IgG anti-DNA antibody (Yung and Chan, 2012). When anti-C1q antibodies co-exist with anti-dsDNA antibodies, accelerated development of renal disease is observed (Nowling and Gilkeson, 2011).

Anti-endothelial cell antibodies (AECAs) are other important autoantibodies related to LN. They exist in a high percentage of lupus patients, especially during disease flares. Concentration of serum AECAs also correlates with the severity of LN and they are indicators for endothelial dysfunction (Yung and Chan, 2012).

1.2.2 Immune complex deposition in kidney

Immune complex deposition is observed in all pathogenic classes of LN (Table 1.2 and 1.3). ICs mainly deposit at subepithelial, subendothelial, or mesangial areas. How ICs deposit in the kidney is not fully understood yet, however, the mechanism is critical for LN pathogenesis. There are three models postulated for the deposition (Nangaku and Couser, 2005; Nowling and Gilkeson, 2011). **The first model** suggests that kidney damage is caused by passively trapped circulating ICs. Kidney receives one quarter of the cardiac output and circulating ICs are delivered at a high rate in this organ. The glomerular capillary walls also present highly negative charge that facilitates the

localization of positively charged macromolecules, including ICs. **The second postulated model** considers the binding of autoantibodies to intrinsic non-DNA glomerular antigens. For example, anti-dsDNA antibodies can cross-react with a wide spectrum of targets that from intracellular structures, renal cell membranes or the extracellular matrix, including annexin II, alpha-actinin, laminin or heparan sulphate (van Bavel et al., 2008; Goilav and Putterman, 2015; Rekvig, 2015). Then *in situ* ICs are formed. **The third model** proposes the binding of autoantibodies to chromatin materials present in the glomerular matrix. Chromatin materials released from apoptotic or necrotic cells can be entrapped within the glomerular matrix where they serve as "planted antigens" and anti-dsDNA antibodies can bind with these chromatin materials (Yung and Chan, 2012).

In addition, a silencing of renal *DNaseI* gene is observed in LN (Zykova et al., 2010; Seredkina and Rekvig, 2011). This enzyme is the major endonuclease in kidney. The loss of enzyme activity in LN leads to further accumulation of chromatin fragments in glomeruli and enhances the deposition of chromatin fragment-anti-dsDNA antibodies ICs.

How do deposited ICs lead to glomerular inflammations and injuries? Some current explanations include: (1) ICs can bind with Fc receptors through the Fc end. Genome-wide association studies (GWAS) revealed that Fc receptor genes *FCGR2A, 3A,* and *3B,* are susceptibility genes for human LN (Brown et al., 2007; Mohan and Putterman, 2015). The LN-associated FcγRIIA R131H polymorphisms (rs1801274) decreased binding affinity for IgG2 and reduced clearance of IgG2-containing ICs (Li et al., 2013b). The

LN-associated FcγIIIa V176F polymorphism (rs396991) showed lower affinity for IgG1 and IgG3. The loss of copy number in *FCGR3B* may confer risk of LN and could reduce the expression of this receptor on cell surface. In addition, the nucleic acid-containing ICs can also activate Toll-like receptor (TLR) 7/9 pathways via its nucleic acid components and enhance the inflammatory response (Barrat et al., 2005). Specifically, TLR7/9 antagonists have therapeutic effects on murine LN (Sun et al., 2007). (2) ICs can activate the complement pathways, which can generate complement cleavage product C5a to attract immune cells, activates complement receptors on renal cells to release cytokines, and forms the membrane attack complex (MAC) to kill renal cells (Birmingham and Hebert, 2015). (3) ICs deposition in renal compartment can also activate the coagulation cascades, facilitate the infiltration of acute and chronic inflammatory cells, and induce productions of pro-inflammatory cytokines or fibrosis from resident and infiltrating cells (Yung and Chan, 2012). Therefore, the effects of IC in renal system injury are multifactorial.

1.3 Glomerular endothelial cell dysfunction is another key process in the pathogenesis of lupus nephritis

Glomerular endothelial cell (GEC) is a kind of renal parenchymal cells that participates in the formation of glomerular filtration barrier (GFB). GECs injuries will impair GFB properties and renal functions. In LN patients, ICs can deposit in subendothelial areas or circulate in the blood, both of which have access to contact with GECs. Therefore, GEC functions may be affected by ICs and contribute to the LN mechanisms.

1.3.1 Normal GEC structure

Glomerular endothelial cells line the innermost of glomerular capillaries. They are extremely flattened cells, with a height around the capillary loop of about 50-150 nm. They have large fenestrated area, with diameter around 60-80 nm, covering 20-50% of the whole cell surface (Satchell and Braet, 2009) (Figure 1.1). In the cell-to-cell junction, GECs express typical endothelial function markers, including platelet endothelial cell adhesion molecule (PECAM-1, CD31) and cadherin-5. GEC surfaces are covered by a mesh-like negatively charged structure, called the endothelial cell surface layer (ESL), which is mainly composed of glycocalyx and a much looser associated layer. The ESL, GECs, together with the glomerular basement membrane (GBM), the podocytes, and sub-podocyte space (SPS), which are arranged in the order from the capillary lumen to the urinary space, constitute the five distinct layers of the GFB (Figure 1.2) (Arkill et al., 2014). The GFB components interact closely with each other (Menon et al., 2012). GECs, together with podocytes, synthesize laminins during glomerular development, becoming an important source for GBM proteins (St John and Abrahamson, 2001). The GFB is the structural foundation for renal function. Proteinuria, which is the clinical feature of LN, results from GFB impairments. However, unlike the podocytes and GBM, the importance of GECs has been neglected for a long time.

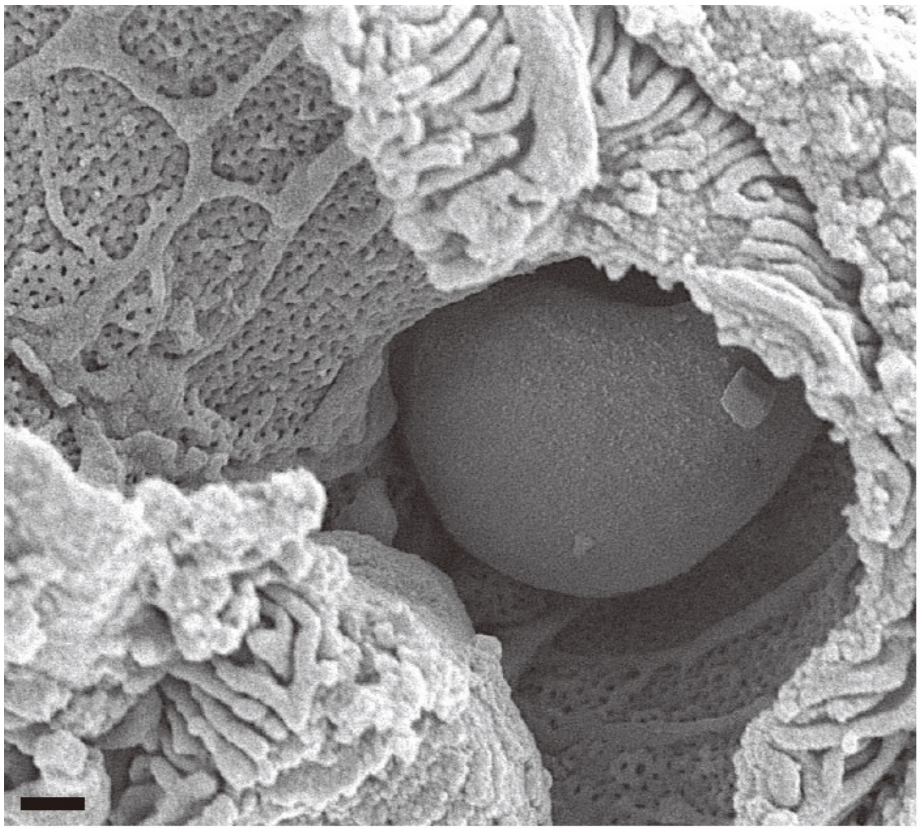

Figure 1.1 Scanning electron micrograph demonstrating the fenestrated endothelial surface of a glomerular capillary from a normal mouse kidney.

(Adapted from Haraldsson et al., 2008)

Note: Scale bar: 1 μm.

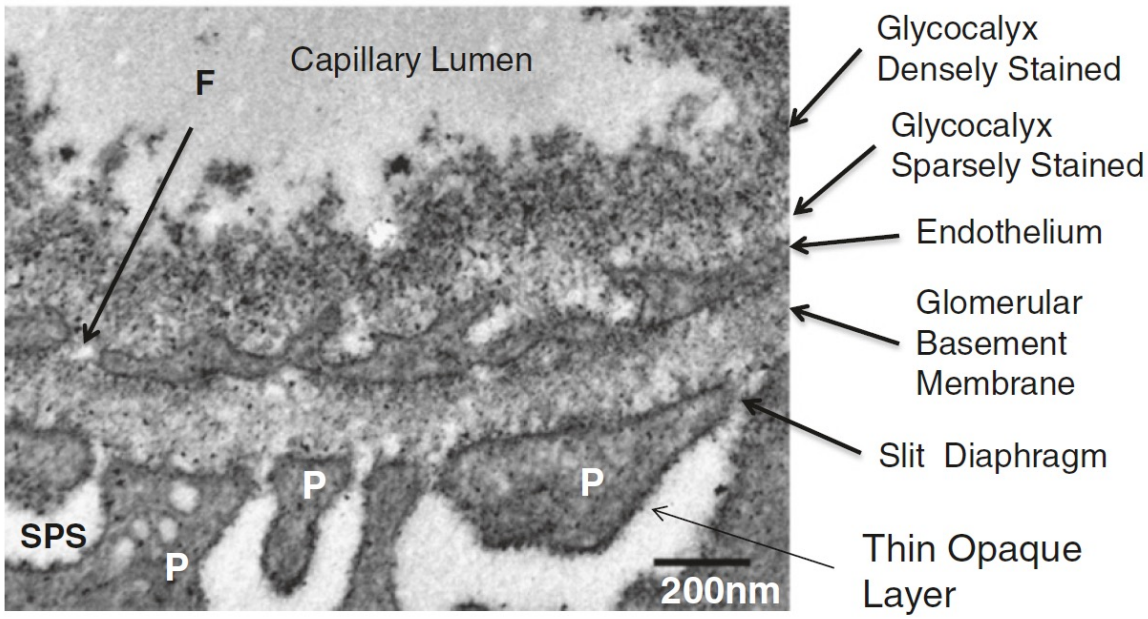

Figure 1.2 Transmission electron microscopy of the five layers of the glomerular filtration barrier from a perfusion fixed rat glomerulus.

(Adapted fromArkill et al., 2014)

From the capillary lumen to the urinary space: cell surface layer (glycocalyx and the loose associated layer), endothelium, glomerular basement membrane, podocytes, and the SPS. Magnification: 24,500 times. Abbreviations: P: podocyte, F: fenestration, SPS: sub-podocyte space.

1.3.2 Endothelial cell functions and dysfunctions

Even though not much is known for GECs, we can first see the common characteristics and functions of the general endothelial cells (ECs). Endothelial cells are heterogeneous, and spatial and temporal dynamic (Aird, 2005). The structures and functions of ECs vary greatly in different vascular beds (Aird, 2007; Yano et al., 2007). Commonly, **normal ECs** are metabolically active and participate in multitudes of physiological functions, including regulating vasomotor tone, vascular permeability, thrombosis, fibrosis, inflammatory responses, immunity, and new vessel formation (Fogo and Kon, 2010). Under stresses and stimulations, such as physical damage, invading pathogen infections, pro-inflammatory cytokines, abnormal metabolic products, and various diseases, ECs become activated and dysfunctional. Endothelial "**dysfunction"** represents a deviation from normal to a vasoconstrictive, procoagulant, platelet-activating, and antifibrinolytic state. This pathophysiological condition is characterised by increased expression of luminal adhesion molecules [such as intercellular adhesion molecule-1 (ICAM-1), vascular cell adhesion molecule-1 (VCAM-1), E-selectin, P-selectin, and PECAM-1], pro-inflammatory cytokines [such as tumor necrosis factor-alpha (TNF-alpha), interleukin-1, interleukin-6, interleukin-8, and interferon-γ] and pro-thrombotic factors [thrombomodulin (CD141), tissue factor (CD142)], as well as increased oxidative stress, abnormal vascular tone modulation, and disassembly of cell-cell junctions (Deanfield et al., 2007; Fogo and Kon, 2010; Zhang et al., 2010; Rajendran et al., 2013). These molecules can be used as markers for evaluating EC functions.

Especially, nitric oxide (NO) is essential for EC functions and maintaining vascular homeostasis. Low levels of NO which is within the physical range can dilate blood vessels by activating guanylyl cyclase (GC)-cGMP pathways in neighbouring smooth muscle cells (Denninger and Marletta, 1999). Besides regulation of vascular tone, NO contributes to inhibit vascular inflammations. Nitric oxide downregulates the expressions of adhesion molecules and inhibits leukocytes adhesion to vessel walls (Kubes et al., 1991; Armstead et al., 1997). In addition, NO inhibits platelet activation and aggregation, displaying antithrombotic effects (Wang et al., 1998; Schafer et al., 2004). Also, NO can react with O_2 and reactive oxygen species (ROS), exerting anti-oxidation properties (Wink et al., 2001). However, high concentration of NO exhibits cytotoxic effects. For instance, NO can inhibit cytochrome C oxidase and control oxygen consumption, leading to ATP depletion. Moreover, NO belongs to reactive nitrogen intermediates (RNIs), and can generate peroxynitrite ($ONOO^-$) and N_2O_3, through reacting with superoxide and O_2, separately. These molecules (NO, $ONOO^-$, and N_2O_3) can nitrosylate thiol groups and iron in proteins, nitrate protein tyrosines and DNA, and oxidize lipids, modifying their structures and function, and resulting in cytotoxicity (Oates, 2010; Forstermann and Sessa, 2012).

Nitric oxide is mainly synthesized by NO synthase (NOS) which transfers L-arginine to L-citrulline in the presence of molecular oxygen and cofactors. There are at least three isoforms of NOSs in mammals: the neuronal NOS (nNOS, *NOS1*) (Bredt et al., 1991), the inducible NOS (iNOS, *NOS2*) (Lyons et al., 1992), and the endothelial NOS (eNOS,

NOS3) (Lamas et al., 1992). For endothelial functions, we focus on eNOS and iNOS. Under physiological condition, eNOS is the dominant NOS isoform in vasculature, and the generated NO is among the picomolar to nanomolar range, which is associated with cytoprotective effects. iNOS is minimal in resting cells and highly expressed under inflammations. iNOS produces NO in the micromolar range, which usually associated with cytotoxic effects (Oates, 2010).

Endothelial NOS mainly contains an N-terminal oxygenase domain (where heme binds), and a C-terminal reductase domain [where the reduced form of NADPH (nicotinamide adenine dinucleotide phosphate), FMN (flavin mononucleotide), FAD (flavin adenine dinucleotide) and calmodulin can bind]. Endothelial NOS functions in dimer and requires the existence of its substrate L-arginine and the essential cofactor tetrahydrobiopterin (BH4). eNOS catalyzes the electron transfer from the C-terminal NADPH to the heme on the N-terminus. The transferred electrons are used to reduce O_2 and to oxidize arginine to generate citrulline and NO. Calmodulin can bind with eNOS and accelerate the electron transfer (Stuehr, 1997; Forstermann and Munzel, 2006). Endothelial NOS locates in a special domain of membrane called caveolae (Shaul et al., 1996). Caveolin-1 binds to the oxygenase domain of eNOS, preventing the calmodulin binding and inhibiting eNOS activity (Ju et al., 1997). When the substrate or the cofactor is depleted, the NOS switches from dimeric to monomeric and NOS “uncoupling” happens, which generates superoxide instead of NO, resulting in increased oxidative stress (Karbach et al., 2014).

Endothelial NOS can be phosphorylated on different serine, threonine, and tyrosine residues and then get regulated (Figure 1.3). Among these sites, the key active site is Ser1177 and the inhibitory site is Thr495. In unstimulated cultured ECs, Ser1177 is not phosphorylated. Several protein kinases, including Akt, PKA (protein kinase A), AMPK, and CaMKII (calmodulin-dependent kinase II), can regulate the Ser1177 phosphorylation on eNOS and thus the NO synthesis. Thr495 is constitutively phosphorylated in inactive ECs, most probably by PKC (protein kinase C) (Rafikov et al., 2011). Moreover, eNOS activities can be regulated by lipid modification, *O*-linked glycosylation, and *S*-nitrosylation (Fleming, 2010). Endothelial NOS expressions can also be regulated in response to numerous stimuli, such as shear stress, oxidized linoleic acid, hydrogen peroxide, 3-hydroxy-3-methylglutaryl coenzyme A reductase inhibitors, TGF-beta1, TNF-alpha, hypoxia, lipopolysaccharide, and thrombin, via transcriptional and posttranscriptional mechanisms (Searles, 2006).

Unlike the eNOS which is mainly constitutively expressed in endothelial cells, iNOS can be induced in various cell types in response to inflammations, such as pathogens invasion and pathological inflammatory diseases (Aktan, 2004). iNOS was first cloned and identified in murine macrophages, and then reported to be expressed in monocytes, neutrophils, hepatocytes, endothelial cells, vascular smooth muscle cells, astrocytes, fibroblasts, and osteoblasts (Feron and Michel, 2000). iNOS and eNOS share very similar genomic and protein structures (Fischmann et al., 1999; Alderton et al., 2001). However, their activities are differently regulated. iNOS is primarily regulated at the expression

level, while eNOS is mainly regulated at the posttranslational level (Kleinert et al., 2003). Among the complicated mechanisms regulating iNOS expression, the transcription factor NF-κB can bind to the iNOS promoter, and is important for iNOS induction (Pautz et al., 2010). Besides, iNOS expression can be regulated by NO itself (Katsuyama et al., 1998).

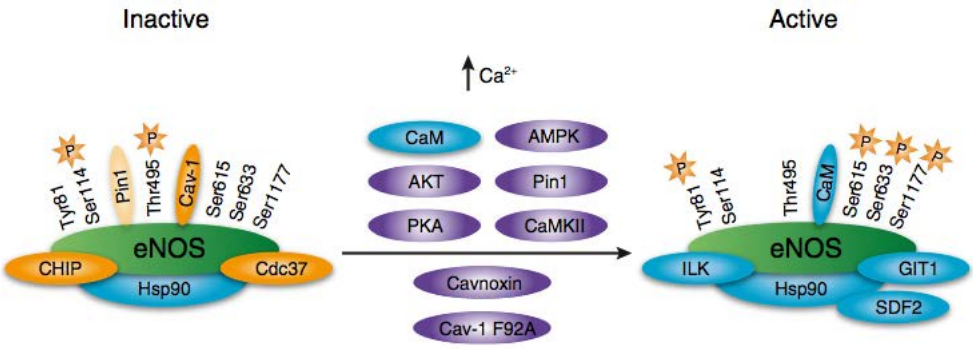

Figure 1.3 Diagram of the eNOS signalosome.

(Adapted from Siragusa and Fleming, 2016)

The activity of eNOS can be regulated by phosphorylation, intracellular calcium concentration, and protein-protein interactions. In unstimulated status, eNOS is phosphorylated on Thr495, Ser114, and bound with Caveolin-1 (Cav-1). Increased intracellular calcium concentration activates calmodulin (CaM). Then, CaM replaces Cav-1 to bind with eNOS, resulting in conformational changes and accelerated NO production. Several protein kinases, including Akt, PKA, AMPK, and CaMKII, phosphorylate eNOS on Ser1177, Tyr81, Ser615, and Ser633, leading to the eNOS activation.

1.3.3 Vascular lesions, endothelial dysfunctions and injuries are observed in lupus nephritis

The glomerulus is a well-developed capillary network. Kidney biopsy indicates that vascular lesions are common in LN (Tan et al., 2014). Wu's results revealed that renal vascular lesions were observed in 81.8% of the 341 LN patients. Renal vascular lesion with vascular IC deposits was the most common form. Patients with thrombotic microangiopathy presented with the most severe renal injury features and the worst renal outcome (Wu et al., 2013a). Vascular lesions indicate and are closely associated with EC injuries. In addition, loss of endothelial cells in glomerular capillaries was observed in renal biopsies from crescentic LN patients, associated with the formation of necrotizing and cellular crescentic lesions, and contributing to the development of glomerular sclerosis and collapse (Fujita et al., 2015).

For clinical researches and animal experiments, wide endothelial dysfunctions in LN have been reported. Increased expressions of endothelial adhesion molecules in glomeruli, including E-selectin and P-selectin, were detected in lupus-prone mice models and showed associations with severity of glomerular lesions (Nakatani et al., 2004). Soluble thrombomodulin, another marker for endothelial cell activation, was significantly increased in lupus patients compared with controls and had a strong association with a history of LN (Frijns et al., 2001), proven as a reliable marker of lupus activity (Boehme et al., 2000). Urine VCAM-1, an endothelial adhesion molecule, was elevated in LN patients and can be served as a marker of renal pathology activity index in LN (Singh et

al., 2012). Circulating endothelial cells, which were detached mature endothelial cells responding to microvascular injuries, were increased in peripheral blood in lupus patients compared with healthy controls, and had positively association with disease activity index scores. The number of circulating endothelial cells was also higher in lupus patients with renal symptoms than that in patients without (Elshal et al., 2009). Shedding of endothelial protein C receptor was observed in LN patients and contributed to vasculopathy and renal injury (Sesin et al., 2005). Besides, normal eNOS function is involved in LN development. Polymorphisms of intron 4 in *NOS3* gene (coding for eNOS) has been reported to associate with human LN development (Lee et al., 2004). Lupus nephritis mice which lacked eNOS developed more severe diseases, with more glomerular crescentic and necrotic lesions, elevated inflammatory infiltrates and vasculitis, and decreased survivals (Gilkeson et al., 2013). Transcriptional network analysis also revealed the importance of endothelial function in LN. Berthier and his colleague used transcriptional network approach to define the similarities and differences among human LN and three murine lupus models (NZB/W, NZM2410, and NZW/BXSB strains) in molecular terms and finally found 20 commonly shared network nodes which reflected the key pathologic processes in LN. Among the 20 key nodes, four nodes reflected injured endothelial cell functions, including adhesion (*VCAM-1*), fibrinolysis (*ANXA2*), coagulation (*F2R*, or thrombin receptor *RAP1*), and decreased angiogenesis (*VEGF-A*) (Berthier et al., 2012).

Data from *in vitro* studies have also demonstrated that ICs can bind to ECs via Fc receptors and other receptors and lead to endothelial activation and dysfunctions. There

are Fc receptors expressed in ECs (Tanigaki et al., 2015). The inhibitory receptor $Fc_{\gamma}R$ IIB is expressed in cultured human ECs (Pan et al., 1999; Mineo et al., 2005). In mice, low mRNA expressions of Fcgr2b, Fcgr3, Fcerg1, Fceb1, and Fcamr genes were detected in renal endothelial cells (Suwanichkul and Wenderfer, 2013). ICs induced tissue factor production in human ECs (Tannenbaum et al., 1986). ICs activated human umbilical vein endothelial cells (HUVECs), proven by upregulated expressions of ICAM-1 and VCAM-1, and increased secretions of interleukin-6, interleukin-8, TNF-alpha, and monocyte chemoattractant protein-1 (MCP-1), via the high-mobility group box 1 (HMGB1)-receptor for advanced glycation end products (RAGE) axis (Sun et al., 2013). Double strand-DNA could activate GECs, enhance albumin permeability and vascular permeability via TLR-independent pathways (Hagele et al., 2009). Interleukin-10 secreting B cells (B10 cells) ameliorated the progression of LN by attenuating GEC injuries (Yu et al., 2015b), further implying the role of GECs in the pathogenesis of LN.

1.4 Autophagy and cell injury

Autophagy (from the Greek, *auto*: oneself, *phagy*: to eat) is an evolutionarily conserved catabolic process to degrade cytoplasmic contents through lysosomes (Jain et al., 2013). Autophagy presents at basal level in most eukaryotic cells. It is typically a cytoprotective, pro-survival response in the beginning. However, if hyperactivated, it will ultimately kill the cell (known as type II programmed cell death). Depending on the ways delivering cytoplasmic materials to the lysosomes, at least three major types of autophagy have been identified: macroautophagy, microautophagy, and chaperone-mediated autophagy (CMA)

(Inguscio et al., 2012). **Macroautophagy** (hereafter called autophagy) describes a degradation process, through which unique double-membrane vesicles (autophagosomes) are formed to sequester a targeted portion of cytoplasm, then fuse with lysosomes to form autolysosomes and degrade the internal materials. **Microautophagy** involves direct engulfment of cytoplasmic cargo at the lysosomal surface (Mijaljica et al., 2011). Both macroautophagy and microautophagy have the abilities to engulf structures through non-selective and selective mechanisms (Mizushima et al., 2008). **CMA** involves direct translocation of unfolded proteins across the lysosome membrane with the help of chaperones. Particularly, cytosolic proteins containing a pentapeptide motif will be recognized by chaperone heat shock cognate 70 (Hsc70) and delivered to the surface of lysosomal membrane through the interaction between Hsc70 and the receptor lysosome-associated membrane protein 2A (LAMP-2A) (Bejarano and Cuervo, 2010).

Autophagy plays key roles in cell homeostasis. Autophagy is activated as an adaptive catabolic process in response to different forms of metabolic stresses, including starvation, growth factor depletion and hypoxia. Autophagy can also serve as a cellular housekeeper to remove damaged and dysfunctional organelles, misfolded proteins and intracellular pathogens (Levine and Kroemer, 2008). Autophagy is related to the pathogenesis of many diseases, including ischaemia, cardiovascular diseases, neuro-degeneration, obesity, cancer and aging (Levine and Kroemer, 2008; Nixon, 2013). In neuro-degenerative diseases, disease-related mutant proteins are prone to aggregate and lead to damage in neurons, such as expanded polyglutamine-containing proteins in Huntington’s disease,

mutant α-synucleins in familial Parkinson's disease, and different forms of tau in frontotemporal dementia. Clearance of these mutant proteins are highly depended on autophagy, and accumulation of autophagosomes are found in these patients as a sign of autophagy activation. Autophagy stimulatory agent can reduce the level and neurotoxicity of aggregated mutant proteins and present protection against neuro-degenetative disease. In Danon disease, resulting from a mutation in lysosomal protein LAMP-2, autophagy is inhibited from failure of lysosome-autophagosome fusion and patients are characterized by myopathy, cardiomyopathy, and variable mental retardation. For podocytes, they present a high level of basal autophagy. Our previous study also showed a cytoprotective role of autophagy in podocyte injury model, treated with puromycin aminonucleoside (Kang et al., 2014).

1.4.1 Autophagy process

The dynamic process of autophagy, is characterized by multiple signaling pathways in autophagosome formation and its fusion with lysosomes (Figure 1.4). Successful autophagy requires precise collaboration of Atg (autophagy-related) proteins. Till now, more than 37 Atg proteins have been identified in yeast. Half of them are shared by all organisms including mammals and regarded as the core proteins (Mizushima et al., 2011; Lamb et al., 2013; Ohsumi, 2014). The autophagy process can be divided into four steps: **initiation, nucleation, elongation and maturation** (reviewed in He and Klionsky, 2009; Periyasamy-Thandavan et al., 2009; Yang and Klionsky, 2010; Lamb et al., 2013). Briefly, **in the initiation**, the uncoordinated 51-like kinase 1 (ULK1) complex, including ULK1/2

(mammalian homologs of Atg1), Atg13, Atg101 and FAK family kinase-interacting protein of 200 kD (FIP200, aliases: RB1CC1, Atg17), moves into the autophagosomal formation site (AFS). Mammalian or mechanistic target of rapamycin (mTOR), a cellular energy/nutrient sensor, is the main inhibitor of this step. Repressive signals must be relieved by initiation signaling cascades and autophagy can be induced. **The nucleation step** results in the assembly of phagophore and involves the formation of class III phosphatidylinositol 3-Kinsase (PI3KC3)/vacuolar protein sorting 34 (Vps34) complex, which includes Vps34, Beclin1 (a homolog of Atg6), p150 (a homolog of Vps15), and Atg14L [also known as Beclin1-associated autophagy-related key regulator (Barkor), or Atg14]. The autophagophore is **elongated** during the third step via two ubiquitin-like conjugation systems, that is, formation of Atg12-Atg5-Atg16L complex and lipid conjugation of microtubule-associated protein 1 light chain 3 (MAP1LC3, or LC3) and its family members GATE16 and GABA receptor-associated protein (GABARAP) with phosphatidylethanolamine (PE). Atg7 and Atg10 are enzymes involved in Atg5-Atg12 conjugation. Atg4, Atg7, and Atg3 are involved in LC3-PE conjunction. LC3-PE (LC3-II) stays associated with the inner and outer membranes of the phagophore until the autophagosome formation and the level of LC3-II correlates with the steady-state number of autophagosomes. Thus, LC3-II becomes a widely-used marker of autophagosomes (Kabeya et al., 2000; Kabeya et al., 2004). **In the final maturation step,** the autophagosomes fuse with lysosomes to form autolysosomes, degrade the contents and export the remaining materials to the cytoplasm for recycling. p62 (SQSTM1, sequestosome 1) contains a ubiquitin-associated (UBA) domain, which binds ubiquitin

noncovalently) and a LC3-interacting region (LIR, which directly binds to LC3), thus serving as a linkage between the ubiquitinated protein substrates and the autophagy machinery. Then p62 and the p62-bound ubiquitinated proteins are incorporated and degraded in autophagosomes (Bjorkoy et al., 2005; Pankiv et al., 2007). p62 then becomes another widely-used marker for monitoring autophagy. The decreased level of p62 correlates with the activated autophagy.

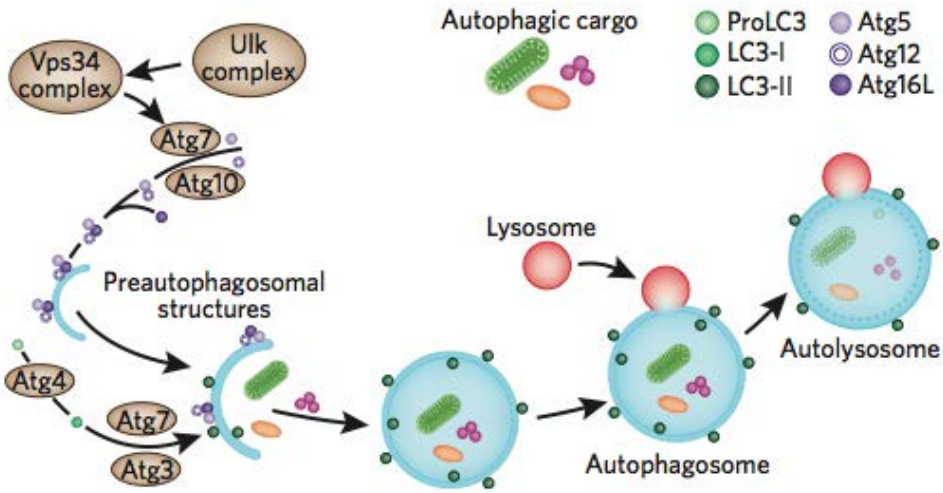

Figure 1.4 Diagram of the autophagy process.

(Adapted from Fleming et al., 2011)

The autophagy process can be divided into four steps: initiation, nucleation, elongation and maturation. In the initiation, the ULK1 complex (ULK1/2-Atg13-Atg101-FIP200) moves into the autophagosomal formation site. The nucleation step results in the assembly of phagophore and the PI3KC3/Vps34 complex (Vps34-Beclin1-p150-Atg14L) is required. Then, the autophagophore is elongated via Atg12-Atg5-Atg16L complex and LC3-II system. Atg7 and Atg10 are enzymes involved in Atg5-Atg12 conjugation. Atg4, Atg7, and Atg3 are involved in LC3-II formation. The membranes grow and form autophagosomes. In the maturation step, the autophagosomes fuse with lysosomes to form autolysosomes, degrade the contents and export the remaining materials to the cytoplasm for recycling.

1.4.2 Autophagy regulation

Autophagy is precisely regulated by many signals sensing the environment, as a response to both extracellular and intracellular stresses (reviewed in Periyasamy-Thandavan et al., 2009; Lavallard et al., 2012; Sarkar, 2013).

1.4.2.1 mTOR-dependent pathways

mTOR, a conserved serine/threonine protein kinase, can sense and integrate various stimuli and coordinate metabolism pathways and cell growth. The mTOR forms two distinct complexes, mTORC1 and mTORC2. mLST8 (mammalian lethal with SEC thirteen 8), DEPTOR (DEP domain containing mTOR-interacting protein), and the Tti1/Tel2 complex co-exist in both mTORC1 and mTORC2. RAPTOR (regulatory-associated protein of mTOR) and PRAS40 (proline-rich Akt substrate of 40 kD) are specific to mTORC1, whereas RICTOR (rapamycin-insensitive companion of mTOR), mSin1 (SAPK-interacting 1, or MAPKAP1, mitogen-activated protein kinase associated protein 1), and PROCTOR1/2 (protein observed with Ricto) are specific to mTORC2 (reviewed in Kim and Guan, 2015).

Unlike mTORC1, the effects of mTORC2 and the mechanisms for mTORC2 regulation are largely unknown. It has been reported that mTORC2 can regulate actin cytoskeleton organization.

1.4.2.1.1 Upstream regulators for mTORC1

mTORC1 is a core negative regulator of autophagy (Kim and Guan, 2015). Different

signals and upstream proteins control mTORC1 activity (Figure 1.5). **Rag** proteins (Rag A/B/C/D), the sixth subfamily of Ras-related GTPases, regulate mTORC1 activity responding to amino acid levels (Kim and Kim, 2016) (Figure 1.5, b). Rag A and B are functional redundant and Rag C and D are functional redundant. Rag proteins form heterodimers and are tethered to lysosome by a pentameric lysosomal complex Ragulator, which acts as amino acid-stimulated guanine nucleotide exchange factor (GEF). When amino acids are sufficient, Rag GTPases heterodimmers are activated by Ragulator and then recruit mTORC1 to the lysosome surface, where it encounters Rheb and gets activated (Bar-Peled et al., 2012).

Rheb (Ras-homolog enriched in brain), another small GTPase, when bound with GTP, can directly bind and activate mTORC1 (Groenewoud and Zwartkruis, 2013). The trimeric tuberous sclerosis complex (TSC), which is comprised by TSC1, TSC2, and TBC1D7 (TBC 1 domain family, member 7), negatively regulate Rheb activity, as TSC2 contains a GAP (GTPase-activating protein) domain (Dibble et al., 2012). The TSC-Rheb axis is central for regulating mTORC1 activity, in response to various stimuli, including growth factors, cellular energy, and endoplasmic reticulum (ER) stress.

(1) Insulin and insulin-like growth factors activate mTOR activity through a PI3K-Akt-TSC-Rheb pathway. After binding with insulin, insulin receptor (a kind of receptor tyrosine kinase) autophosphorylates on its tyrosine residues and recruits insulin receptor substrate 1 (IRS1), which facilitates binding SH2-containing adaptor proteins, including class I PI3K. This helps to convert phosphatidylinositol 3,4-bisphosphate (PIP2) to

phosphatidylinositol 3,4,5-bisphosphate (PIP3). PIP3 increases recruitment of Akt to plasma membrane where it gets activated by phosphorylation. Activated Akt phosphorylates and inhibits TSC2 and blocks its interaction with TSC1, which promotes Rheb-mTORC1 activation and leads to suppressed autophagy (Inoki et al., 2002). In addition, activated Akt can phosphorylate PRAS40 and mediate the disassociation of PRAS40 from mTOR, resulting in mTOR activation and suppressed autophagy (Vander Haar et al., 2007).

(2) Reduced cellular energy level suppresses mTORC1 through AMPK-TSC-Rheb pathway. AMPK is activated by decreased ATP/AMP ratio in the cytosol through the LKB1 (liver kinase B1, STK11). Phosphorylation on Thr172 is required for AMPK activation. Activated AMPK phosphorylates and activates the TSC complex and thus inhibits mTOR activity, leading autophagy stimulation (Inoki et al., 2003; Mihaylova and Shaw, 2011). Besides, AMPK can also directly inhibit mTORC1 activity by phosphorylating RAPTOR on Ser722 and Ser792 (Gwinn et al., 2008).

(3) WNT signaling activates mTORC1 activity via GSK3β (glycogen synthase kinase 3β)-TSC pathways. GSK3β can phosphorylate TSC2 and activate TSC complex formation (Inoki et al., 2006). Once WNT ligands bind to the Frizzled family receptor and the co-receptor LRP 5/6 (low-density lipoprotein receptor-related protein), the WNT pathway is activated and inhibits GSK3β, leading to activated mTORC1 activity.

(4) Endoplasmic reticulum (ER) stress in mammalian cells also affect the Rheb-mTOR axis (Rashid et al., 2015). ER expansion and autophagosome formation are observed under ER stress. At least three pathways are involved in ER stress signaling, that is,

IRE1α (inositol-requiring protein 1α)-JNK (c-Jun N-terminal kinases) pathway, ATF6α (activating transcription factor 6α) pathway, and PERK (protein kinase RNA-like ER kinase)-eIF2α pathways. ER stress can downregulate Akt, which could in turn suppress mTORC1 activity and induce autophagy. Besides, ER stress also induces the release of calcium from ER to cytosol, which stimulates CaMKK2 and then activates AMPK.

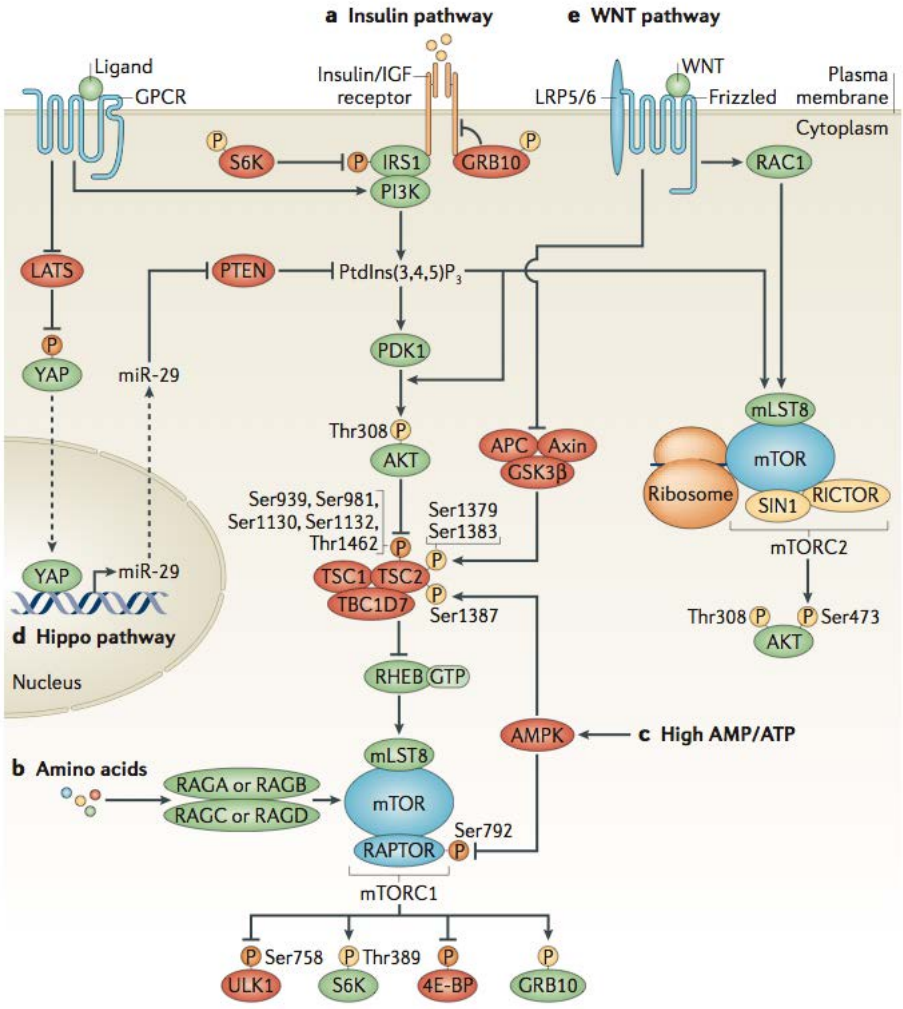

Figure 1.5 Regulation of autophagy through mTOR-dependent pathways.

(Adapted from Shimobayashi and Hall, 2014)

mTORC1 is a core negative regulator of autophagy. Different signals and upstream proteins regulate mTOR activity. a) Insulin and insulin-like growth factors activate mTORC1 activity through a PI3K-Akt-TSC-Rheb pathway. b) Sufficient amino acids activate Rag heterodimmers and recruit mTORC1 to the lysosome surface, where it encounters Rheb and becomes activated. c) Reduced cellular energy level (high AMP/ATP ratio) suppresses mTORC1 through AMPK-TSC-Rheb pathway. d) Inhibited Hippo signaling activates mTORC1 and mTORC2 through LATS-YAP-miR-29-PIP3 pathway. e) WNT signaling activates mTORC1 activity via GSK3β-TSC pathways.

Akt is an important upstream regulator for mTORC1 and autophagy. Akt contains a pleckstrin homology (PH) domain, a central kinase domain, and a carboxy terminal regulatory domain (Figure 1.6). In unstimulated cells, Akt exists in cytoplasm, with two key phosphorylation sites Thr308 and Ser473 unphosphorylated. Under growth factors stimulations, Akt binds with the product of PI3K (PIP3), through its PH domain, and translocates to plasma membrane. Then, Akt is phosphorylated by its upstream regulator, 3-phosphoinositide-dependent protein kinase 1 (PDK1, or PDPK1), which also translocates to cell membrane through its PH domain), on Thr308 (Alessi et al., 1997). Ser473 can be phosphorylated by mTORC2 (Sarbassov et al., 2005) or by DNA-dependent protein kinase (DNA-PK) (Feng et al., 2004). Fully activated Akt phosphorylates its downstream substrates and transduces different signals. Activated Akt is dephosphorylated by protein phosphatases, such as PP2A (protein phosphatase 2A), PTEN (phosphatase and tensin homolog), PHLPP1/2 (PH-domain leucine-rich-repeat-containing protein phosphatases), and becomes inactivated (Hemmings and Restuccia, 2012).

Akt is a versatile serine/threonine protein kinase for cell functions. Beyond suppressing autophagy and protein synthesis, activated Akt can regulate cell survival, migration, proliferation, glucose metabolism, angiogenesis, and other cell functions (Manning and Cantley, 2007). Especially, activated Akt phosphorylates eNOS (on Ser1177 in human, Ser1176 in mouse, Ser1179 in bovine and pig), leading to increase eNOS activity and NO production in endothelial cells (Dimmeler et al., 1999).

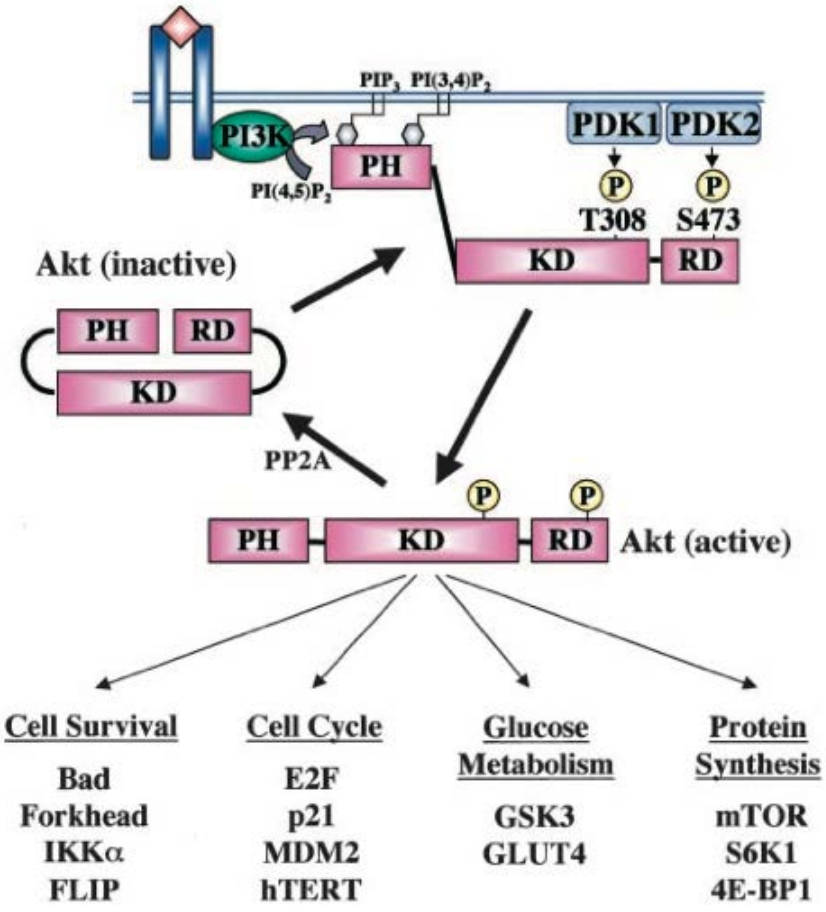

Figure 1.6 Diagram of Akt structure, activation and functions.

(Adapted from Shiojima and Walsh, 2002)

Akt contains an amino terminal pleckstrin homology (PH) domain, a central kinase domain (KD), and a carboxy terminal regulatory domain (RD). The PH domain can bind with membrane lipid products, such as PIP2 and PIP3. Full activation of Akt need phosphorylation on Thr308 and Ser473. Activated Akt is dephosphorylated by protein phosphatases, such as PP2A, and becomes inactive again.

Downstream substrates of mTORC1

After activation, mTORC1 target on its main downstream substrates, **4E-BP-1** (eIF4E-binding protein 1) and **S6K** (40S ribosomal S6 kinase), which mediate the cap-dependent protein translation initiation (Ma and Blenis, 2009). In addition, mTORC1 can phosphorylate **ULK1** and regulate autophagy.

Protein translation initiation requires assembly of eIF4F (eukaryotic translation initiation factor 4F) complex on the 5'cap structure of mRNA. The eIF4F complex contains eIF4E, eIF4G, and eIF4A. eIF4E binds to the 5' cap structure and then recruits eIF4G and eIF4A binding. The 4**E-BP-1** binds with eIF4E and inhibits eIF4G binding to eIF4E. Activated mTORC1 phosphorylates 4E-BP-1 and results in its dissociation from eIF4E, thus initiating the protein translation.

Another substrate of mTORC1 is **S6K**, including S6K1 and S6K2. Two phosphorylation sizes are essential for S6K activation: Thr229 and Thr389. mTORC1 phosphorylates S6K on Thr389, forming a docking site for PDK1, which subsequently phosphorylates S6K on Thr229 and activates it. eIF4A is an RNA helicase and its activity can be greatly enhanced when associates with eIF4B. Activated S6K phosphorylates eIF4B on Ser422 and increases its association with eIF4A, thus promoting the helicase activity of eIF4A (Raught et al., 2004). Moreover, PDCD4 (programmed cell death 4) binds and inhibits eIF4A activity. Activated S6K mediates phosphorylation and degradation of PDCD4, promoting protein translation (Dorrello et al., 2006).

Besides translation initiation machinery, mTORC1 targets on **ULK1** and regulate autophagy. ULK1, identified as the mammalian homologue of yeast Atg1, is a

serine/threonine kinase that can receive the upstream signals related to nutrition and energy (Dunlop and Tee, 2013). In human, there are 5 proteins orthologous to Atg1 in yeast: ULK1-4 and STK36 (serine/threonine kinase 36). ULK1 and ULK2 are the mostly closely related to yeast Atg1. They share 55% identical sequences and process redundant functions in autophagy (Wirth et al., 2013; Wong et al., 2013). ULK1 contains an N-terminal kinase domain, a serine-proline-rich central region, and a conserved C-terminal domain (Figure 1.7). ULK1 functions in a complex with Atg13, FIP200, and Atg101, and acts as an initiator of the autophagy process. ULK1 complex can phosphorylate Beclin1 (on Ser15 in human, Ser14 in mouse) and enhance the activity of Vps34 complex (Russell et al., 2013). Besides, the ULK1 complex controls the trafficking of Atg9, a critical transmembrane protein of the phagophore (Mack et al., 2012).

Phosphorylation is an important step to regulate ULK1 activities. More than 30 phosphorylation sites have been identified in ULK1. mTORC1 and AMPK are important upstream regulators for ULK1 complex. Activated mTORC1 kinase can phosphorylate ULK1 (on Ser757 in mouse, Ser758 in human) and Atg13, leading to suppression of the ULK1 kinase activity (Jung et al., 2009; Kim et al., 2011; Shang et al., 2011; Kang et al., 2013). Ser757 is also required for AMPK binding (Figure 1.7). Phosphorylation on Ser757 by mTORC1 disrupts the interaction between AMPK and ULK1, contributing to the suppressed ULK1 activity. AMPK can activate ULK1 by phosphorylating it on Ser638 (Shang et al., 2011; Mack et al., 2012). Moreover, mTORC1 phosphorylates AMBRA1 on Ser52 and regulates ULK1 stability (Nazio et al., 2013).

Figure 1.7 Diagram of ULK1 structure.

(Adapted from Wong et al., 2013)

ULK1 contains an N-terminal kinase domain, a serine-proline-rich central region, and a conserved C-terminal domain (CTD). ULK1/2, together with Atg13, RB1CC1 (FIP200), and Atg101, forms the ULK1 complex and acts as an initiator of the autophagy. ULK1 has a LC3-interacting region (LIR) in its serine-proline-rich central region and can interact with LC3 family proteins.

1.4.2.2 mTOR-independent pathways

In addition to mTOR-dependent pathways, there exist mTOR-independent pathways to regulate autophagy (Figure 1.8).

(1) Phosphoinositol pathways

Inositol 1,4,5-trisphosphate (IP3) is a negative regulator for autophagy. Lithium inhibits inositol monophosphoatase (IMPase) and leads to free inositol depletion, which in turn decreases IP3 level (Williams et al., 2002), and induces autophagy (Sarkar et al., 2005). IP3 binds with its receptor IP3R on the ER, leading to release of Ca^{2+} from ER. siRNA and pharmacological blockades of IP3R can also induce autophagy (Criollo et al., 2007).

(2) Cyclic model through cAMP-Epac-PLC-IP3 pathway and Ca^{2+}-calpain-G-protein α pathway

Autophagy can be regulated by intracellular Ca^{2+} level. L-type Ca^{2+} channel antagonists (such as verapamil, nimodipine, nitrendipine), which decrease the cytosolic Ca^{2+}, enhance autophagy (Williams et al., 2008). Increased cytosolic Ca^{2+} activates calpains, a kind of Ca^{2+}-dependent cysteine protease. Calpains can activate G-protein, which increases adenylate cyclase activity and then generates cAMP. Increased cytosolic cAMP level inhibits autophagy (Williams et al., 2008). Moreover, increased cAMP activates Epac (exchange protein directly activated by cAMP level, a GEF for a small G-protein Rap) and Rap2B. Rap2B then activates PLC (phospholipase C). PLC catalyzes PIP2 to generate IP3, then inhibit autophagy as described previously.

(3) JNK1-Beclin1-PI3KC3 pathway

Besides inhibiting mTORC1, starvation can activate JNK1, which phosphorylates Bcl-2

on Thr69, Ser70 and Ser87. Phosphorylated Bcl-2 detaches from Beclin1, encouraging the formation of Beclin1-Vps34 complex and inductin of autophagy (Wei et al., 2008). NO generated by NOS can inhibit JNK1 phosphorylation and then inhibit autophagosome synthesis through this pathway (Sarkar et al., 2011).

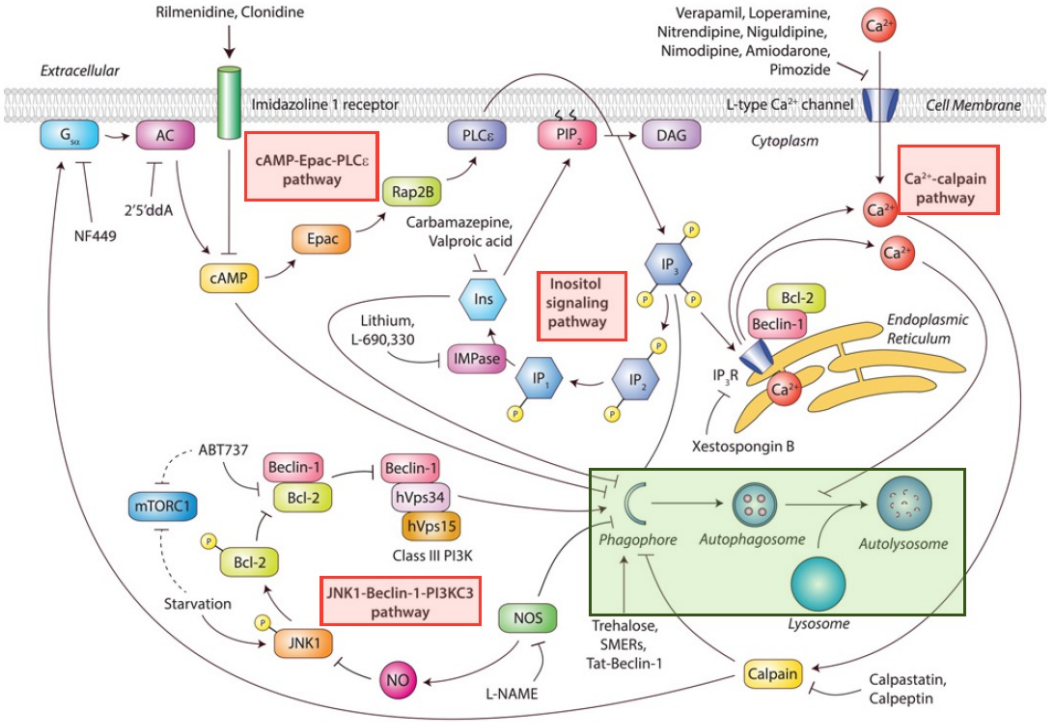

Figure 1.8 Regulation of autophagy through mTOR-independent pathways.

(Adapted from Sarkar, 2013)

Various signals regulate autophagy through mTOR-independent pathways. IP3 is a negative regulator of autophagy. Increased intracellular Ca^{2+} concentration inhibits autophagy through the cyclic Ca^{2+}-calpain-G-protein α -cAMP-Epac-PLC-IP3 pathway. NO can inhibit autophagy through JNK1-Beclin1-PI3KC3 pathway.

1.4.3 Drugs and genetic methods for autophagy regulation

Beside the extracellular and intracellular stimuli, chemical drugs are also found to enhance or block autophagy (Yang et al., 2013b; Li et al., 2015). Some of the chemical autophagy inhibitors (Table 1.4) and activators (Table 1.5) are listed below. There are also genetic methods to regulate autophagy, including gene deletions/inactivations [e.g. generating Atg-deficient embryonic stem cells (Mizushima et al., 2001), or in vivo using transgenic knockout model animals, especially using conditional knockout models (Hara et al., 2006)] and functional knockdowns (e.g. using RNAi against *Atg* genes). MicroRNAs are also demonstrated to be involved in autophagy regulation (Xu et al., 2012).

These autophagy regulation methods help us to understand the mechanisms of autophagy in different stresses and diseases and new tools to interfere autophagy are continuing to emerge. However, most current chemical inhibitors are not entirely specific. Genetic modifications may have systemic effects. Then long-term sequences of genetic modifications may be more complex. Therefore, the side-effects of autophagy regulators must be carefully considered.

Table 1.4 Autophagy inhibitors

Reagents	Mechanisms
MHY1485 (Choi et al., 2012)	mTOR activator
3-mehtyladenine (3MA) (Seglen and Gordon, 1982)	PI3K inhibitor
Wortmannin (Blommaart et al., 1997)	
Cycloheximide (Watanabe-Asano et al., 2014)	protein synthesis inhibitor
Vinblastine (Xie et al., 2010)	microtubule disturber
Chloroquine (CQ) (Seglen et al., 1979)	pH regulator
Hydroxychloroquine (HCQ) (Ramser et al., 2009)	
Bafilomycin A1 (Mauvezin and Neufeld, 2015)	prevent autophagosome-lysosome fusion
Leupeptin (Seglen et al., 1979)	lysosomal protease inhibitor
E-64d (Tanida et al., 2005)	
Pepstain A (Tanida et al., 2005)	

Table 1.5 Autophagy activators

Reagents	Mechanisms
mTOR-dependent activators of autophagy	
Rapamycin (sirolimus) (Choi et al., 1996)	mTOR inhibitors
Temsirolimus (CCI-779) (Yazbeck et al., 2006)	
Everolimus (RAD001) (Crazzolara et al., 2009)	
Ku-0063794 (Garcia-Martinez et al., 2009)	ATP-competitive catalytic site mTOR inhibitors
AZD8055 (Chresta et al., 2010)	
CC214 (Mortensen et al., 2013)	
Torin 2 (Liu et al., 2013)	
PP242 (Feldman et al., 2009)	
NVP-BEZ235 (Liu et al., 2009)	PI3K/mTOR dual-specificity inhibitors
PI-103 (Fan et al., 2010)	
Metformin (Shi et al., 2012b)	AMPK activators
Resveratrol (Park et al., 2016)	Natural product, through mTOR-ULK1 pathway
mTOR-independent activators of autophagy	
Tunicamycin (Carpenter et al., 2011)	ER stressing inducer
Thehalose (Sarkar et al., 2007)	mTOR-independent activators
Lithium chloride (Sarkar et al., 2005)	IMPase inhibitors
Verapamil (Williams et al., 2008)	Ca^{2+} channel blocker
Calpastatin (Williams et al., 2008)	calpain inhibitor
Xestospongin B (Vicencio et al., 2009)	IP3R blocker
Vitamin D3 (Yuk et al., 2009)	Up-regulate Beclin1 and Atg5
L-NAME (Sarkar et al., 2011)	NOS inhibitor

1.5 Autophagy in immunity and lupus nephritis

Autophagy participates in nearly all aspects of immunity, affecting both innate and adaptive immunity processes (reviewed in Levine et al., 2011; Deretic et al., 2015; Shibutani et al., 2015). First of all, autophagy can directly eliminate intracellular pathogens (Gomes and Dikic, 2014; Huang and Brumell, 2014). Secondly, autophagy participates in inflammation (Deretic et al., 2013). It can regulate type I interferons production, although conflict results were reported (Jounai et al., 2007; Lee et al., 2007b; Henault et al., 2012; Kunanopparat et al., 2016). Meanwhile, type I interferons can also induce autophagy (Schmeisser et al., 2013; Schmeisser et al., 2014). Inflammasomes are molecular platforms activated under infection or stresses which trigger the maturation of proinflammatory cytokines and play critical roles in inflammation. Autophagy can negatively regulate inflammasome activation (Saitoh et al., 2008). Assembled inflammasomes recruit autophagic adaptor p62 to assist their delivery to autophagosomes and the degradation within them (Shi et al., 2012a). Thirdly, autophagy regulates major histocompatibility complex (MHC) class II presentation of intercellular and extracellular antigens (Dengjel et al., 2005; Munz, 2012). Besides, autophagy is vital for T cell and B cell homeostasis (McLeod et al., 2012).

Moreover, autophagy is involved in autoimmunity (Bhattacharya and Eissa, 2013; Gianchecchi et al., 2014; Yang et al., 2015). GWAS have linked polymorphisms in *Atg* genes to some autoinflammatory and autoimmune diseases, such as that a coding variant in *Atg16L1* is strongly associated with Crohn disease, a kind of inflammatory bowel disease (IBD) (Rioux et al., 2007; Xavier and Rioux, 2008).

As SLE and LN result from impairments in immune system and losing tolerance of autoantigens, there exist evidences implicating linkage between autophagy and pathogenesis of SLE and LN (Pierdominici et al., 2012):

1.5.1 Lupus susceptibility genes are related to autophagy.

The rapid development of GWAS reveals more than 60 genes associated with SLE (Teruel and Alarcon-Riquelme, 2016). Among them, some genes are proven highly related to autophagy, including *ATG5* (Gateva et al., 2009; Zhou et al., 2011), *ATG7* (Zhou et al., 2011), *IRGM* (immunity-related GTPase family M) (Zhou et al., 2011), *DRAM1* (DNA damage regulated autophagy modulator) (Yang et al., 2013a), *CDKN1B* (cyclin-dependent kinase inhibitor 1 B) (Yang et al., 2013a), and *PTPN22* (protein tyrosine phosphatase non-receptor type 22) (Kyogoku et al., 2004).

Especially, SNPs in *APOL1* (apolipoprotein L1, a BH3-only protein, which can induce autophagic cell death when it is overexpressed) shows associations with SLE-ESRD in African American (odds ratia: 2.57) (Freedman et al., 2014). *MTMR3* (Myotubularin-related phosphatase 3), which can regulate the intracellular PtdIns3P level and is involved in constitutive autophagy initiation and autophagosome size (Taguchi-Atarashi et al., 2010), shows association with LN in northern Han Chinese population (Zhou et al., 2014).

1.5.2 Activated PI3K-Akt-mTOR signaling pathways have been detected in murine lupus nephritis.

Highly increased expressions of phosphorylated (Thr308 and Ser473) and total Akt, together with phosphorylated and total mTOR, were observed in kidney specimens from untreated LN mice compared with normal control. Especially, increased phosphorylated mTOR was detected in GECs from untreated LN mice by double-immunofluorescent staining. Treatment with rapamycin could reverse these increase and prolonged mice survival, decrease autoantibody titers and improve renal functions (Stylianou et al., 2011). Winkler and his colleague demonstrated that oral administration of PI3KC1 inhibitor IPI-145 for 20 weeks significantly suppressed lupus activity in NZB/W mice compared with lupus mice with vehicle control (Winkler et al., 2013). This result also highlighted the abnormal activated PI3K pathways in LN. As PI3K-Akt-mTOR signaling is an important pathway to regulate autophagy process, these observations implied the potential roles of autophagy in LN and further investigations are needed to evaluate the autophagy process.

1.5.3 Abnormal autophagy is detected in cells participating in LN pathogenesis.

Lupus nephritis is a complex and systemic diseases. Various cells contribute to the pathogenesis of disease, especially including the T cells, B cells, phagocytes, and the renal parenchyma cells. Abnormal autophagy is detected in these cells. For instance, peripheral T cells from lupus-prone mice (MRL/lpr and NZB/W mice) exhibited increased autophagy activity when compared with CBA/J and BALB/c control mice. Increased number of autophagic vacuoles were also observed in peripheral T cells from

lupus patients than controls (Gros et al., 2012). Autophagy in splenic B cells from NZB/W lupus mice was increased compared with C57BL/6 control mice. Increased autophagy was also detected in B cells from lupus patients (Clarke et al., 2015). Neutrophils can release NETs (neutrophil extracellular traps) when facing infections. NETs which are not removed timely become a source to be presented as self-antigens and stimulate autoantibodies production. Rapamycin or WYE-354 activated autophagy and accelerated NET release (Itakura and McCarty, 2013). Macrophages are important participants for LN development. Deficient phagocytic capacity of macrophage is observed in lupus patients, leading to accumulation of cell materials and providing sources for self-antigens (Li et al., 2010). Li and colleagues detected significantly increased LC3-II expression in spleen and kidney macrophages from activated lymphocytes-derived DNA (ALD-DNA) induced lupus mice when compared with those in control mice. When transferring Beclin1-knockdown macrophages into lupus mice which were previously depleted of the original macrophages, the authors observed alleviated symptoms in lupus mice receiving these autophagy-suppressed macrophages. These results implied that increased autophagy in macrophages may play an important role in murine LN pathogenesis (Li et al., 2014).

Podocytes are crucial parenchyma cells for renal functions. A German research group reported that podocytes could uptake SLE autoantibodies and aggregate these antibodies in cytosolic speckles. These aggregates impaired podocytes survivals and could be degraded by autophagy. Inhibition of autophagy with Bafilomycin A or MG132 led to significantly accumulated cytoplasmic aggregates (Hillmann et al., 2012). Cheng and her

colleagues also reported that stimulation by complement-inactivated SLE serum increased the LC3-II expressions in podocytes (Cheng, 2013).

1.5.4 Autophagy regulators can be used as therapeutic drugs for LN.

Glucocorticoid has been a classical drug for lupus for decades and has wide suppressant effects of the whole immune system. Recent evidences show that corticosteroid can inhibit cytoplasmic calcium signaling and induce autophagy in WEHI 7.2 cells (a CD4/CD8 double positive T cell lines) (Harr et al., 2010). Chloroquine (CQ) or hydroxychloroquine (HCQ), the first line-treatment for lupus, raises the lysosomal pH value and impairs the last step of autophagy and autophagic protein degradation, acting as autophagy inhibitors (Lee et al., 2011). Besides regulating autophagy, CQ/HCQ can reduce proinflammatory cytokines production, inhibit B cell receptor (BCR)/T cell receptor (TCR)-mediated calcium signaling, absorb and block UV reaction, and inhibit TLR signaling, all of which may contribute to their beneficial effects in lupus patients (Ben-Zvi et al., 2012). The autophagy inducer rapamycin and its analogues have displayed protective and beneficial effects on murine LN models and LN patients (Lui et al., 2008a; Lui et al., 2008b; Yap et al., 2012a). In addition, rapamycin can act as immunosuppressant and the effects of rapamycin on LN are complex. Rapamycin nephrotoxicity has also been observed (Marti and Frey, 2005).

Lupuzor ^{TM} (Rigerimod, IPP-201101 or P140), is a 21-mer linear peptide (sequence 131-151 derived from the small nuclear ribonucleoprotein U1-70K) phosphorylated at Ser140. In the phase IIb clinical trial, Lupuzor improved Systemic Lupus Erythematosus Disease

Activity Index (SLEDAI) score in lupus patients (Schall and Muller, 2015). Administration of Lupuzor in saline to MRL/lpr lupus-prone mice before they presented symptoms could prolong mice survival, reduce proteinuria, and decrease the titer of anti-dsDNA antibodies (Monneaux et al., 2003). Lupuzor treatment could also alleviate renal vasculitis, glomerulonephritis and dermatitis in MRL/lpr mice. Currently, Lupuzor entered its phase III trial at the end of 2015. Mechanisms of Lupuzor action involve autophagy. Lupuzor could bind with chaperone Hsc70 protein (which played a vital role in CMA), decrease its expression in MRL/lpr splenic B cells and impaired the refolding properties of this chaperone. Lupuzor suppressed the autophagic flux, with increased accumulation of p62 and LC3-II in B cells from MRL/lpr mice (Page et al., 2011). The effects of Lupuzor on LN indicated the potential role of autophagy on this disease.

1.6 Research gap and hypothesis

As described above, GEC injury is a key step in the development of LN and kidney damage. Meanwhile, evidences showed that autophagy is involved in SLE and LN. As autophagy has been proved to play protective roles in various kinds of cells under different stresses, including endothelial cells, this leads us to question whether autophagy participates in GEC injury and protection, especially in LN.

It has been noticed for a long time that IC is a key factor for lupus pathogenesis and GEC injuries. However, the underlying mechanisms for GEC injury directly induced by IC are not very clear. As reported, autoantibodies typically developed many years before the clinical onset and diagnosis of SLE (Arbuckle et al., 2003). Renal immune deposits are

found in nearly all patients with SLE, yet a considerable proportion of them present normal histology under microscopy (Borchers et al., 2012). These “delayed” or “silent” phenomena indicate the progression from immune deposits to function alternation, and implicate the potential complicated mechanisms. GECs injury induced by IC are associated with intracellular energy state changes, altered profile of protein synthesis and endoplasmic reticulum pressures, which are important signals for autophagy regulation and may affect the autophagy process.

Since the mechanisms of GEC injury induced by ICs have not been clearly answered, our research question is to investigate whether IC alters autophagy in GECs and is associated with GECs activation and injury. The objectives of this project include:

1. To investigate the effects of ICs on GECs autophagy.
2. To investigate the effects of ICs on GECs injury.
3. To investigate the relationships between autophagy and GECs injury.

Chapter 2 Materials and Methods

In the previous chapter, we have reviewed the background of the project and hypothesised the important role of GECs in LN. There are plenty of researches on endothelial cells but the researches on GECs were scanty due to the difficulties in isolation, purification and maintenance. In this project, we used a commercially available human GECs and verified the identity by specific markers. There are also studies using patient serum as sources of ICs and autoantibodies. Patient samples collected at different stages of SLE contain a big variation of antibodies and inflammatory cytokines. To keep the variable to the minimum, we used human heat-aggregated gamma globulin (HAGG). For autophagy, we followed the latest guidelines and the methodologies are summarised below. The reagents used in this project are listed in the Appendix.

2.1 Cell culture

Primary human GECs were purchased from Cell Systems (Certificate # ACBRI 128, Kirkland, WA, USA) and cultured in CSC complete medium (containing 10% fetal bovine serum) activated with CultureBoost^{TM} (50 μg/mL, containing bovine growth factor, Cell Systems, USA), at 37 ℃ in a humidified atmosphere of 5% CO_2-95% air. Culture surfaces were pre-coated with Attachment Factor^{TM} (an extracellular matrix product, Cell Systems, USA), and cells were seeded at a density of 1×10^5 cells/mL. Cells were passaged at a ratio of 1:3 every four to five days. Experiments were performed in

cells that reached 80% confluence. To minimize the effects of senescence, cells at passage 5-11 were used.

2.2 Heat-aggregated gamma globulin preparation

Heat-aggregated gamma globulin (HAGG) was prepared as an artificial substitute of ICs. Purified human monomeric IgG (10 mg/mL, Sigma-Aldrich Corporation, USA) was heated at 62 °C for 30 minutes, as described (Cines et al., 1984), and diluted in phosphate buffer saline (PBS) to the desired concentration for experiments.

The large aggregated proteins were precipitated from mixture solutions by polyethylene glycol (PEG) precipitation method. HAGG solution was added with equal volume of 7% PEG 6000 (Sigma-Aldrich Corporation, USA) and then precipitated at 4°C overnight. The next day, the precipitated aggregates were pelleted by centrifugation at 13,000 rpm for 10 minutes. The supernatant was collected and the pellet was dissolved in PBS for further examination.

The presence of large-size covalent aggregates of gamma globulins was identified by SDS-PAGE (sodium dodecyl sulfate-polyacrylamide gel electrophoresis) and Coomassie blue staining (Figure 2.1). Monomeric IgG (mIgG), HAGG (heated), supernatant (S/N) and precipitates after PEG treatment (PEG) were mixed with loading buffers which contains reductive substance (reducing condition) or not (non-reducing condition) separately and added to the top of the gel. Under non-reducing condition, all samples

showed a prominent band around 150 kD, which represented the gamma globulin monomers. Especially, for heated samples in labeled lane 1 (Heated) and lane 2 (PEG), there was a clear band at the top of the stacking gel, which represented the aggregates that could not enter the gel matrix because of their large size and deposit on top of the gel. Under reducing condition, covalent bonds among and within gamma globulin aggregates were broken, and two bands around 25 kD and 50 kD appeared, representing the light and heavy chains of gamma globulin. Meanwhile, absence of bands on top of the corresponding lane 3 and 4 substantiated the covalent bond-mediated characteristic of the large aggregates.

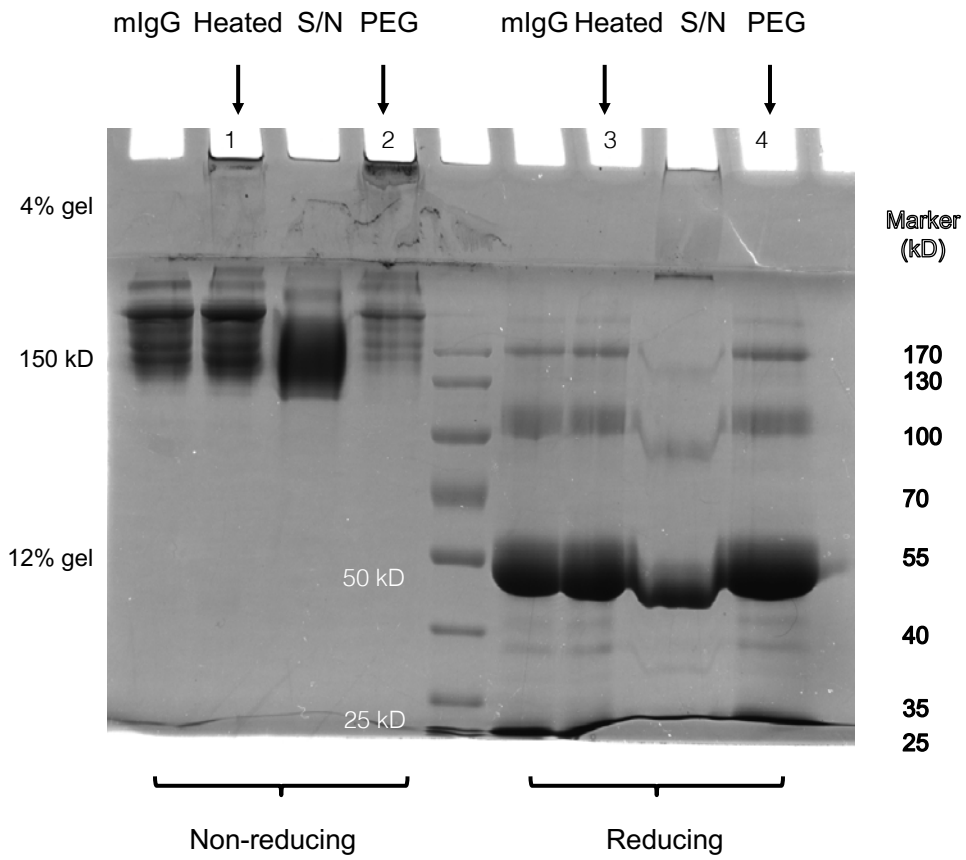

Figure 2.1 SDS-PAGE image of monomeric IgG (mIgG), HAGG (heated), supernatant (S/N) and precipitates after PEG treatment (PEG), under non-reducing and reducing conditions.

Left four lanes: samples mixed with loading buffer containing no reducing agent; Middle lane: protein molecular weight markers; Right four lanes: samples mixed with loading buffer containing β-mercaptoethanol.

2.3 Western blotting

2.3.1 Protein extraction

After incubation with different reagents for desired periods, human GECs were rinsed with PBS and detached by EDTA-trypsin solution. The detached cells were collected and centrifuged at 1,000 rpm for 5 minutes. The cell pellets were washed with ice-cold PBS by centrifugation at 1,000 rpm for 5 minutes. Then cell pellets were lysed in RIPA buffer (50 mM Tris, pH 8.0, 150 mM NaCl, 1% Triton X-100, 0.5% sodium deoxycholate, and 0.1% SDS), supplemented with complete protease inhibitor cocktail (Roche Applied Science, Germany) and phosphatase inhibitors (Calbiochem, Merck Millipore, Germany). Cells were mixed with the buffer by pipetting up and down and the mixture was then maintained in constant agitation for 40 minutes at 4°C. The cell lysate was clarified by centrifugation at 13,000 rpm for 20 minutes at 4°C. The clarified supernatant was carefully collected and stored at -70°C for further analysis.

2.3.2 Measurement of protein concentration

Protein concentrations were determined by Pierce^{TM} BCA Protein Assay Kit (Thermo Fisher Scientific Inc., USA). This BCA (bicinchoninic acid) assay is mainly based on the mechanism that Cu^{2+} will be reduced into Cu^{+} by proteins in an alkaline medium and each Cu^{+} ion can chelate with two BCA molecules, forming a colored complex which exhibits a strong absorbance at 562 nm. The absorbance at 562 nm is nearly linear with the protein concentration (within the range of 20-2,000 mg/mL).

The BCA working reagent was prepared by mixing Reagent A (an alkaline medium containing bicinchoninic acid) and Reagent B (a cupric sulfate solution) in a ratio of 50:1. Protein samples were diluted 15 times in RIPA buffer. A set of diluted BSA standards were also prepared according to the recipe in Table 2.1. Then, 25 μL of each diluted sample or BSA standard was added to the 96-well plate. 200 μL of prepared BCA working reagent was added into each well and the plate was mixed thoroughly. Then the plate was covered and incubated at 37°C for 30 minutes. After the plate was cooled at room temperature for 10 minutes, the absorbance at 562 nm was measured by Benchmark Plus™ Microplate Reader (Bio-Rad, USA). The protein concentration of each sample was calculated using the standard curve.

Table 2.1 Preparation of diluted BSA standards

Vial	Volume of RIPA buffer (μL)	Volume and source of BSA (μL)	Final BSA concentration (μg/mL)
A	30	30 of 2 mg/ml BSA stock	1000
B	25	15 of 2 mg/ml BSA stock	750
C	30	30 of Vial A dilution	500
D	30	30 of Vial C dilution	250
E	30	30 of Vial D dilution	125
F	40	10 of Vial E dilution	25
G	30	0	0

2.3.3 Electrophoresis and blotting

Samples were mixed with an equal volume of 2×Laemmli sample buffer (125 mM Tris pH 6.8, 4% SDS, 0.004% bromophenol blue, 20% glycerol, and 10% β-mercaptoethanol). Then the samples were boiled at 98°C for 5 minutes for denaturation. Equal amounts of proteins (20-40 μg) were loaded and separated by 8-12% SDS-PAGE and transferred to a polyvinylidene difluoride (PVDF) membrane (Bio-rad, USA). The membrane was blocked for 2 hours by 5% non-fat dry milk in Tris-buffered saline with 0.1% Tween-20 (TBST, pH7.4), and incubated with primary antibodies overnight with gentle agitation at 4 °C. After incubation, the membrane was washes with TBST four times for 5 minutes each. Subsequently, the membrane was incubated with horseradish peroxidase (HRP)-conjugated secondary antibodies for one hour at room temperature, with gentle agitation. The membrane was washed with TBST four times for 5 minutes each. Bands were visualized by using chemiluminescence substrates Western Lightning (Perkin Elmer, USA) and captured by the ChemiDoc MP system (Bio-Rad, USA). The images were quantified with ImageJ software (version 1.50i, NIH, USA). Primary antibodies, including anti microtubule-associated proteins 1A/1B light chain 3 (MAP1LC3, or LC3), sequestosome 1 (SQSTM1 or p62), p-mTOR (Ser2448), mTOR, p-p70s6k (Thr389), p70s6k, p-4E-BP-1 (Thr37/46), 4E-BP-1, p-Akt (Thr308), Akt, p-ULK1 (Ser758), ULK1, p-eNOS (Ser1177), eNOS, iNOS, ICAM-1, VCAM-1, and GAPDH, were purchased from Cell Signaling Technology (Beverly, MA, USA) and used at a recommended dilution of 1:1000. The secondary antibody was use at a dilution of 1:3000-5000.

2.4 Immunofluorescence staining

GECs were grown on sterile glass coverslips coated with Attachment Factor™ (Cell Systems, USA) in 24-well plates (30,000 cells per well). After treated with stimulations, cells were fixed in 4% paraformaldehyde for 15 minutes and permeabilized by 0.2% Triton X-100 for 10 minutes at room temperature. Then cells were blocked in 5% bovine serum albumin (BSA) in PBS for one hour. **Endothelial features** were identified by incubating coverslips with mouse anti-CD31 (1:50 dilution, R&D Systems, Minneapolis, MN, USA), and anti-vWF (1:50 dilution, DakoCytomation, Ely, Cams, UK) primary antibodies for 4 hours at room temperature. Then the coverslips were washed three times with PBS for 5 minutes each. Subsequently, the coverslips were incubated in Alexa Fluor 647-conjugated secondary anti-mouse IgG antibodies (1:1000 dilution, Cell Signaling Technology, USA) for 2 hours at room temperature in the dark. **LC3 puncta** were detected by using rabbit anti-LC3 primary antibody (1:400 dilution, 4°C, overnight, Cell Signaling Technology, USA) and the corresponding Alexa Fluor 488-conjugated anti-rabbit IgG antibody (1:1000 dilution, room temperature, 2 hours, Cell Signaling Technology, USA). Then coverslips were mounted in ProLong® Gold Antifade Reagent with DAPI (Thermo Fisher Scientific Inc., USA) and kept overnight in the dark at room temperature. Cells were observed using a Leica DMi8 microscope (Leica Microsystems, Germany). 25-40 cells under each condition were counted and the mean fluorescence intensity of LC3 puncta per cell was analyzed with ImageJ software.

2.5 Cell morphological analysis

GECs were seeded in 6-well plates, at a density of 0.3 million cells per well. When cells reached 70%-80% confluency, stimulations were added. After 8 hours, cells were observed and photographed using an inverted phase contrast microscope (Eclipse TS100, Nikon, Japan), at 100 times magnification. Cell morphology was assessed by multiply quantitative measurements, all of which were performed by ImageJ software. Outlines of individual GECs were traced manually using Polygon selection tool. Cell area, perimeter, circularity, and aspect ratio, were measured. ***Perimeter*** is the length of the outside boundary of the selection. ***Circularity*** was defined as $4\pi\times\frac{[Area]}{[Perimeter]^2}$, with a value ranging from 0 to 1. The value of 1 indicates a perfect circle, while when the value approaches 0, indicating an increasingly elongated shape. ***Aspect Ratio*** **(AR)** was defined as $\frac{[Major\ Axis]}{[Minor\ Axis]}$, which can also reflect the degree of cell elongation. At least 30 cells were chosen under each condition, at random. Results were from three independent experiments.

2.6 Apoptosis assay by flow cytometry

Apoptosis was measured using Dead Cell Apoptosis Kit with YO-PRO-1 and PI (Invitrogen, Thermo Fisher Scientific Inc, USA) and PE Active Caspase 3 Apoptosis Kit (BD Biosciences, USA), according to the manufacturers' instructions by flow cytometry (BD FACS Aria III, BD Biosciences, USA).

YO-PRO-1/PI assay: After incubation with different stimuli, GECs were harvested, washed and re-suspended in cold PBS, at a concentration of 1 million cells per 1 mL PBS. Each 1mL cell suspension was incubated with 1 µL YO-PRO-1stock solution and 0.5 µL propidium iodide (PI) stock solution for 20 minutes on ice. Then cells were distinguished and analyzed by flow cytometry. Green fluorescent YO-PRO-1 dye can enter apoptotic or dead cells and be detected using the 530/30 nm channel, while red fluorescent dye PI cannot enter apoptotic cells but can enter dead cells, detected using the 610/20 nm channel. Cells stained with single dye were used to perform standard compensation. Then, live cells exhibit a low level of green fluorescence, apoptotic cells showed higher level of green fluorescence, and dead cells display both red and green fluorescence. A representative result was shown in Figure 2.2, A.

Active caspase 3 assay: Harvested GECs were re-suspended and fixed in BD Cytofix/Cytoperm^{TM} solution (1 million cells/0.5 mL) for 20 minutes on ice. Then, cells were washed twice with BD Perm/Wash^{TM} solution at a volume of 0.5 mL buffer/1 million cells at room temperature and incubated with the active caspase 3 antibody solution for 30 minutes at room temperature. Eventually cells were washed and re-suspended in 250 µl BD Perm/Wash^{TM} solution and analyzed by flow cytometry. A representative result was shown in Figure 2.2, B.

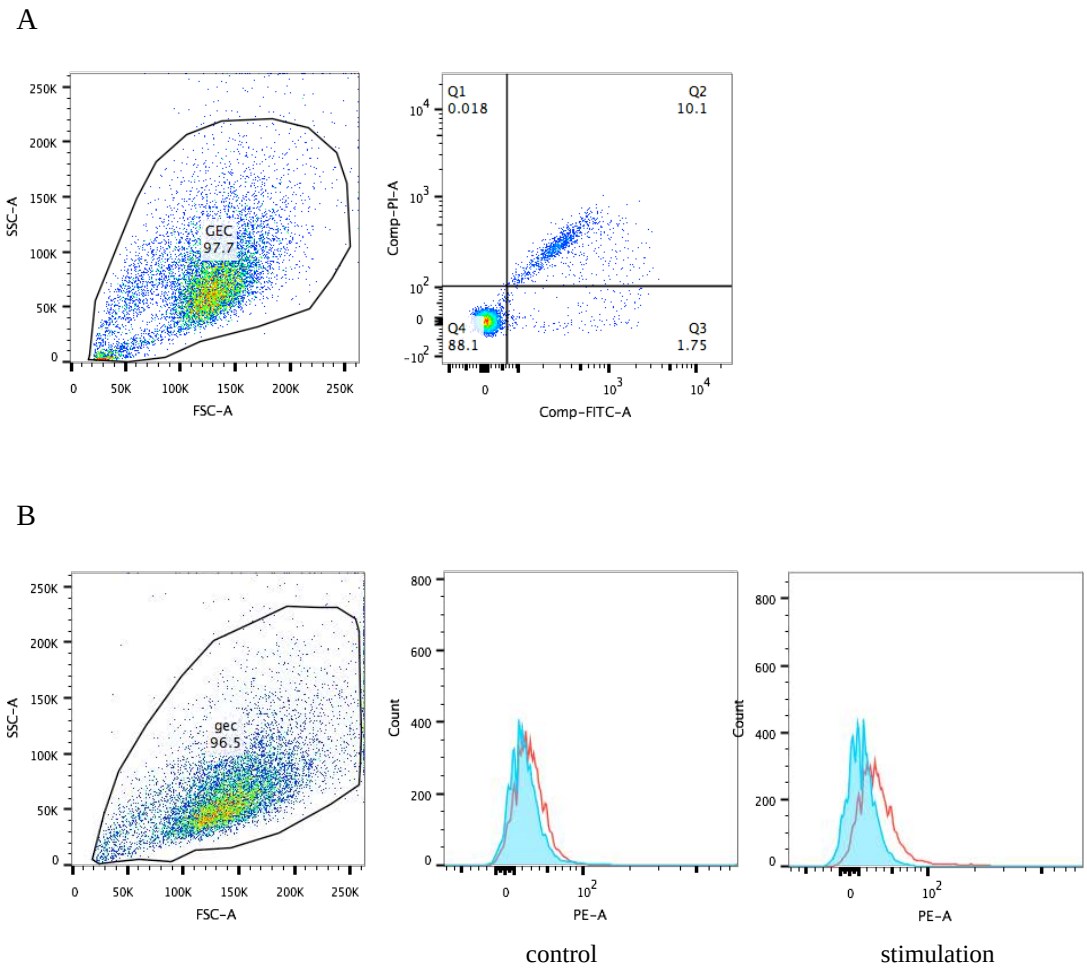

Figure 2.2 Representative results of apoptosis assays by flow cytometry.

(A) YO-PRO-1/PI assay. Apoptotic cells are defined as FITC (YO-PRO-1) positive and PI negative subsets in Q3.

(B) Active caspase 3 assay. Open histograms represent fluorescent labeling with the active caspase 3 antibody. Shaded histograms show the background fluorescent signal in the same cells without active caspase 3 antibody labeling. The changed mean fluorescence intensity (ΔMFI) indicates the expression of active caspase 3.

2.7 Cell viability assay

Cell viability was measured using the Cell Counting Kit-8 (Dojindo, Kumamoto, Japan), according to the manufacturer's instructions. Briefly, GECs were seeded in pre-coated 96-well plates and incubated for 48 hours. Then, cells were treated with HAGG, rapamycin, TNF-alpha, or 3MA, jointly or separately, for 48 hours. 10 μL CCK-8 reagent was added to each well and the absorbance at 450 nm was measured by Benchmark Plus™ Microplate Reader (Bio-Rad, USA) after incubation at 37 ℃ for 3 hours. Cell viability is proportional to the absorbance at 450 nm. Experiments were carried out in triplicate.

The cell seeding density was investigated. A set of GEC suspensions were seeded in 96-well plate, with the seeding density from 2,000-10,000 cells per well. Then cells were incubated in complete culture medium for 4 days and A450 was measured after adding CCK-8 reagent (Figure 2.3). Based on the O.D. value, seeding cells at the density of 7000-8000 cells per well in 96-well plate was chosen for the subsequent experiments.

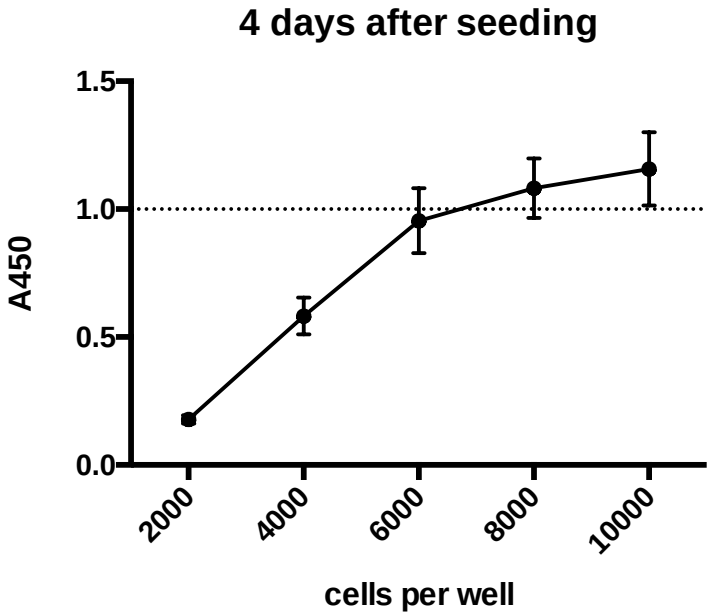

Figure 2.3 CCK-8 results for different cell seeding density conditions.

2,000-10,000 cells were seeded into wells in 96-well plate. A450 was measured after incubation in complete medium for 4 days. Data was expressed as mean ± SEM (n=3).

2.8 Necrosis measurement

Necrosis associated with different treatments in GECs was evaluated by measuring the released lactate dehydrogenase (LDH) in the cell medium, using the CytoTox 96® Non-radioactive Cytotoxicity Assay (Promega, USA), following the modified protocols (Smith et al., 2011). Two sets of replicates for each condition were used. Wells with medium alone without cells were used as blank control. At the end of treatment period, 2 μL (2% of total volume) of Triton X-100 (Sigma-Aldrich Corporation, USA) was added to one set of the wells to thoroughly degrade the cell membranes and release the total LDH. The plate was then centrifuged for 5 minutes at 1,000 rpm. 50 μL of the supernatants from the two set of wells (with and without Triton X-100) were transferred

to a new clean 96-well plate, and mixed with 50 μL CytoTox 96 Reagent. The CytoTox 96 Reagent was pre-prepared by mixing 12 mL room-temperature Assay Buffer to a bottle of Substrate Mix. Then the plate was incubated at room temperature for 20 minutes in the dark. The absorbance at 490 nm was measured by Benchmark Plus Microplate Reader (Bio-Rad, USA).

2.9 Intracellular nitric oxide measurement

Intracellular NO production was detected by fluorescence microscopy using the NO-specific probe 4-amino-5-methylamino-2,7- difluorofluorescein diacetate (DAF-FM-DA, Thermo Fisher Scientific Inc., USA), according to the manufacturer's instructions. DAF-FM-DA is cell-permeant and non-fluorescent. Once it diffuses into cells, DAF-FM-DA is de-acetylated by intracellular esterases and becomes DAF-FM, which has a weak fluorescence. After interacting with NO, DAF-FM is oxidized to a triazole product and the fluorescence quantum yield increases greatly about 160~ fold.

For experiments, GECs were grown on glass coverslips in 24-well plates (30,000 cells per well) and stimulated. After stimulations, cells were washed with pre-warmed PBS (with Mg^{2+} and Ca^{2+}) and treated with diluted DAF-FM-DA (5 μM, in PBS with Mg^{2+} and Ca^{2+}) for 20 minutes at 37 ℃. Cells were then washed to remove the excess probes and incubated in fresh CSC complete medium for 30 minutes, allowing complete de-esterification of the intercellular diacetates. Cells were fixed in 4% paraformaldehyde and visualized using a fluorescence microscope (Eclipse 600, Nikon), equipped with a 495

nm excitation and 515 nm emission filter. Mean fluorescence intensity per cell was analyzed using ImageJ software.

2.10 Tube formation assay

The tube or vascular-like structure formation by endothelial cells was assessed on Corning® Matrigel® Standard (Product # 356237) and Growth Factor-Reduced (GFR) (Product # 356231) Basement Membrane Matrix (Corning, Bedford, MA, USA), as previously described (Arnaoutova and Kleinman, 2010). Matrigel is a solubilized basement membrane preparation extracted from the Engelbreth-Holm-Swarm (EHS) mouse sarcoma, mainly containing laminin, collagen IV, heparin sulfate proteoglycans, entactin, and growth factors.

Briefly, the Matrigel was thawed overnight at 4°C and 300 µL of Matrigel was added to each well of 24-well plate. Then the plate was incubated at 37°C for 30 minutes, to ensure complete gelation of the matrix. GECs were seeded on top of the solidified Matrigel layer in 200 µL of culture medium, with different stimulations, and incubated at 37°C. Subsequently, the tube network was observed using an inverted phase contrast microscope (Eclipse TS100, Nikon, Japan), at 40 times magnification. Five randomly selected non-overlapping fields were photographed for each treatment. Each experimental treatment condition was tested in triplicate. The images were analysed using Angiogenesis Analyzer in ImageJ software and checked by manual counting. The degree of tube formation was quantified by measuring the number of junctions, the number of meshes, and the total tube length.

Some parameters, including the type of Matrigel, cell seeding density, and time intervals for measurement, are essential for experiments. Hence, we optimized these crucial parameters for tube formation assay as follow.

2.10.1 Types of Matrigel

GECs were seeded on two types of Matrigel, Standard or GFR Basement Membrane Matrix, separately. The differences between these two matrixes were listed in Table 2.2. Three hours after seeding, untreated cells already organized into clusters and began to form networks. On GFR Matrigel, more junctions and tubes were formed (Figure 2.4). Thus, GFR Matrigel was used in the following experiments.

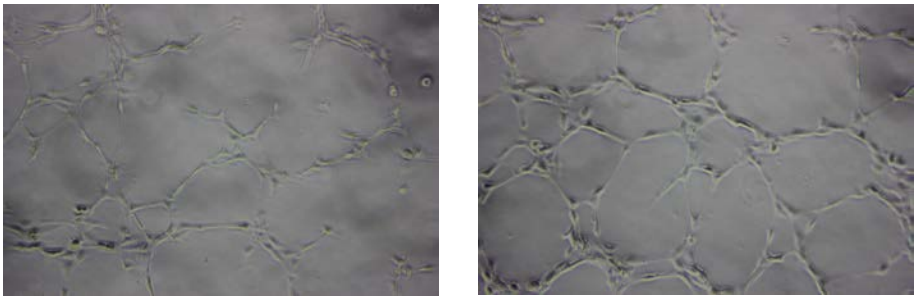

Figure 2.4 Types of Matrigel affect tube formation.

GECs were seeded on standard Matrigel (A) or GFR (growth factor-reduced) Matrigel (B), at the seeding density of 100,000 cells per well in 24-well plate. Images were observed 3 hours after seeding. 40 times magnification.

Table 2.2 Comparison of growth factors in Standard and Growth Factor Reduced (GFR) Matrigel Matrix

(Corning, 2017)

Growth factor (GF)	GF concentration in Standard Matrigel	GF concentration in GFR Matrigel
Basic fibroblast growth factor (bFGF) (pg/mL)	<0.1-0.2	Not determined
Epidermal growth factor (EGF) (ng/mL)	0.5-1.3	<0.5
Insulin-like growth factor 1 (IGF-1) (ng/mL)	11-24	5
Platelet derived growth factor (PDGF) (pg/mL)	5-48	<5
Nerve growth factor (NGF) (ng/mL)	<0.2	<0.2
Transforming growth factor β (TGF- β) (ng/mL)	1.7-4.7	1.7

2.10.2 Seeding density of cells

Effects of cell seeding density were investigated. Five hours after seeding, in the wells seeded with 50,000 cells, large areas of clustered, undifferentiated cells covered the surface of Matrigels, not forming the tube-like network structures (Figure 2.5), which indicated too high seeding density. Thus, 30,000 cells per well was chosen to be seeded in 24-well plate in the following experiments.

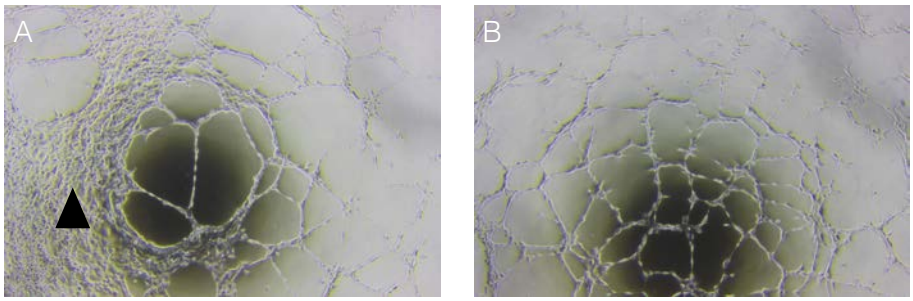

Figure 2.5 Seeding density affects tube formation.

GECs were seeded on growth factor reduced (GFR) Matrigel, at the seeding density of 50,000 cells per well (A) or 30,000 cells per well (B) in 24-well plate. Images were observed 5 hours after seeding. 40 times magnification. Dark triangle: areas of clustered, undifferentiated cells, not forming tube-like structures.

2.10.3 Time intervals for measurement

The optimal time points for measurement were also investigated. GECs were seeded on GFR Matrigel, at the seeding density of 30,000 cells per well, and imaged at 4 hours, 8 hours, 12 hours, and 20 hours. Figure 2.6 showed a clear progression of tube formation from preliminary organization to an elaborate network. Within 4 hours after seeding, tube-like network already appeared. There were cells left undifferentiated and clustered (Figure 2.6, A, arrow). Till 8 hours after seeding, the proportion of undifferentiated cells continued to decrease and the tube-like structures became more distinct and elaborate. Then the complexity of the tube-like network declined slightly, as the size of the network meshes increased and the tube length of the network decreased. Thus, images were recorded at 12 hours and 20 hours after seeding for the following experiments.

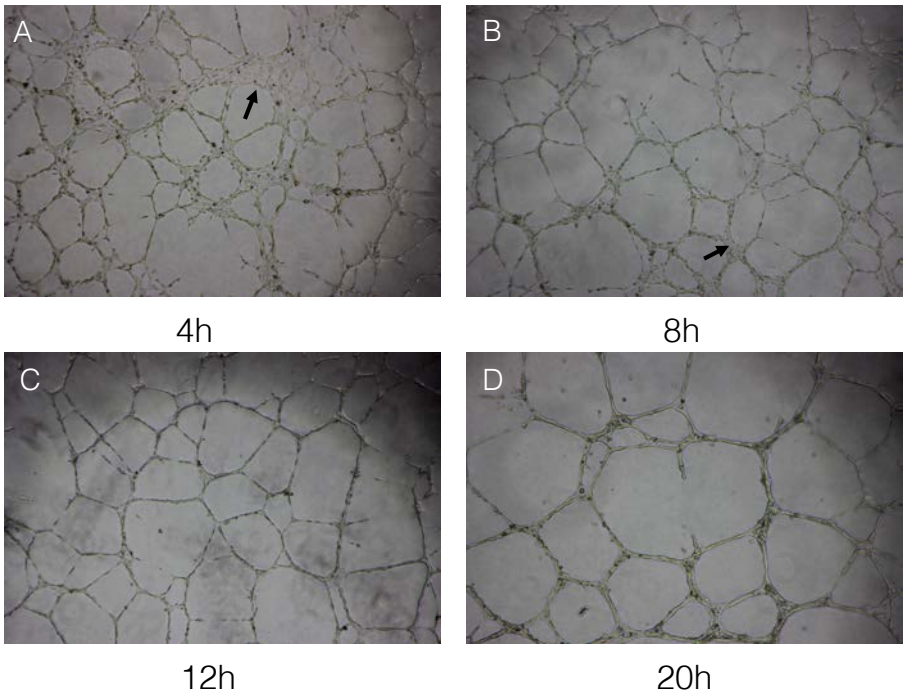

Figure 2.6 Tube formation time course assay.

GECs were seeded on growth factor reduced (GFR) Matrigel, at the seeding density of 30,000 cells per well. Images were taken at 4 hours (A), 8 hours (B), 12 hours (C), and 20 hours (D) after seeding, respectively. 40 times magnification. Arrow: clustered, undifferentiated cells.

2.11 Statistical analysis

Mean fluorescence intensity of LC3 puncta per cell, A450 for indicating cell viability, and results for tube formation assay were presented as mean ± SEM. Other data were expressed as mean ± SD (indicated in the legends). Comparisons between two groups were examined by non-parametric Wilcoxon matched-pairs signed rank test or paired t-test. Comparisons among multiple groups were analysed by One-way ANOVA or Kruskal-Wallis test with post hoc procedures. Data were plotted and analysed by Prism

5.0 Software (GraphPad, San Diego, CA, USA). P value <0.05 was regarded as statistically significant.

Chapter 3 Immune Complexes Suppressed Autophagy in Glomerular Endothelial Cells

3.1 Introduction

In this chapter, we followed the objectives and investigated whether ICs could affect autophagy. We hypothesized that ICs play an important role in the development of LN. Since the kidney receives approximately 20% of the resting cardiac output (~1 L blood /minute), the endothelial cells in the glomerular will constantly be exposed to ICs in the circulation. Besides, ICs can deposit on subendothelial area in the kidney. Autophagy may be triggered when cells are under stress or as a cytoprotective response, hence, it may also be induced or suppressed by ICs depositing on the GECs.

In this chapter, heat-aggregated gamma globulin (HAGG), as prepared by the method outlined in Chapter 2 (2.2), was used to substitute ICs. Glomerular endothelial cells (GECs) were incubated with HAGG and autophagy related markers were measured by western blotting (Chapter 2, 2.3) and immunofluorescence staining (Chapter 2, 2.4). The direct effects of HAGG on GECs autophagy, especially under inflammatory microenvironment, were investigated.

3.2 Results

3.2.1 Characterizations of cultured GECs

Cell line authentication improves confidence and reliability in research results and required by more publishers (Yu et al., 2015a; Almeida et al., 2016). Since May 2015, the Nature publishing group required all authors to provide cell line authentication. Thus, we first verified the endothelial origin of the cultured cells. Commercially available human GECs displayed typical endothelial morphology under light microscopy, forming confluent monolayers with polygonal cells (Figure 3.1, A). Immunofluorescence staining revealed that GECs were positive for endothelial-specific markers CD31 and vWF. CD31 localized over the cell surface (Figure 3.1, B), whereas vWF staining was cytoplasmic, perinuclear, granular, and discrete (Figure 3.1, C).

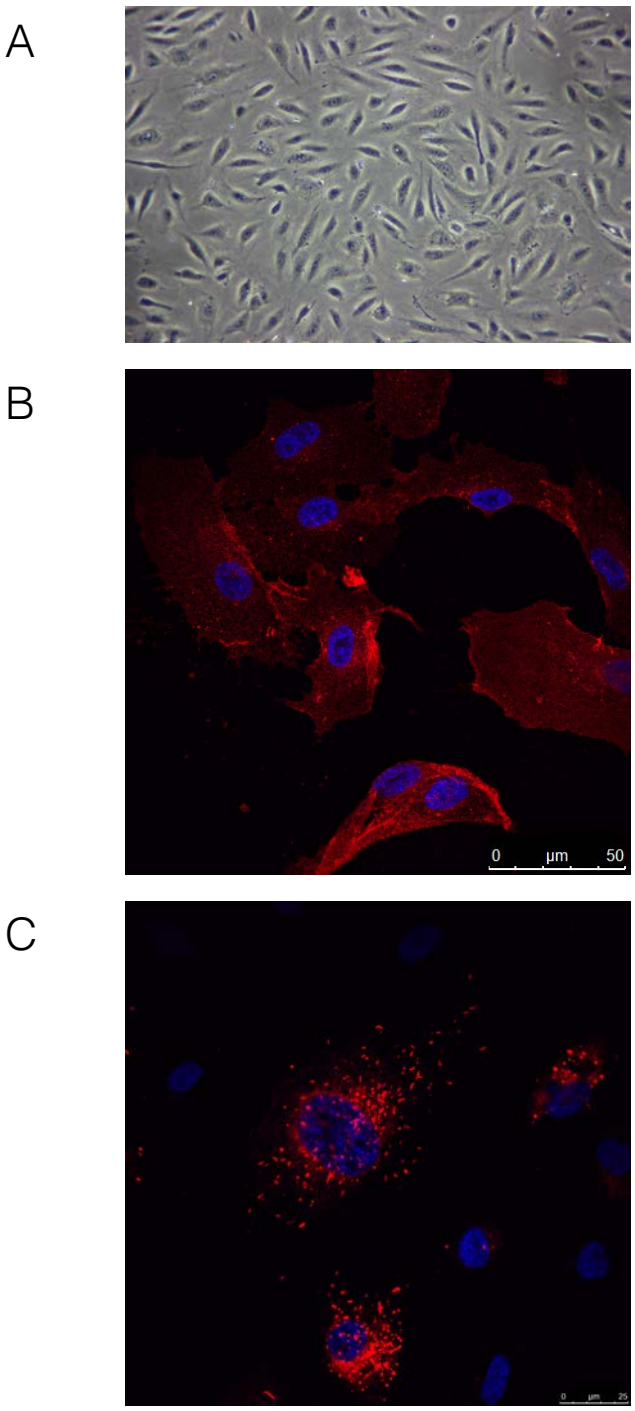

Figure 3.1 Characterizations of cultured human GECs.

(A) Representative phase contrast micrograph of normal cultured human GECs. Magnification: 100×.

(B, C) Immunofluorescence images of GECs stained by anti-CD31 (red) and anti-vWF (red) antibodies, respectively. Nuclei were stained with DAPI (blue).
Magnification: 400×.

3.2.2 HAGG suppressed autophagy in GECs

Microtubule-associated proteins 1A/1B light chain 3 (MAP1LC3, or LC3) and p62, are the two widely accepted protein markers for monitoring autophagy (Klionsky et al., 2016). The lipid phatidylethanolamine-conjugated form LC3-II is required for phagophore elongation and is reliably associated with the number of completed autophagosomes. The conversion from LC3-I to LC3-II can be used to evaluate autophagy. p62 and p62-bound polyubiquitinated protein can interact with LC3 and be degraded in the autolysosomes. Therefore, p62 can serve as an index for autophagic degradation.

We evaluated the ratio of LC3 conversion and p62 expressions in GECs (Figure 3.2). As highly differentiated cells, normal GECs exhibited a high level of basal autophagy (Figure 3.2, “control”). After being treated with HAGG at 400 μg/mL for 24 hours, GECs displayed significantly decreased ratio of LC3-II/I (0.85 fold of control, p=0.031). Corresponding to the decrease in LC3 conversion, there was a significant increase in p62 expression after incubating with HAGG (1.49 fold of control, p=0.031). Rapamycin (100 ng/mL, 24 hours) was used as a positive control and enhanced autophagy in GECs. Further addition with HAGG suppressed the increase of autophagy induced by rapamycin (ratio of LC3 conversion: 1.40 *vs* 1.64, p=0.031; p62: 0.79 *vs* 0.62, p=0.031).

Immunofluorescence staining also revealed decreased mean fluorescence intensity of LC3 puncta in HAGG-treated GECs (0.93 fold of control group, p=0.049, Figure 3.3). Rapamycin stimulation led to a higher mean fluorescence intensity of LC3 puncta (1.21 fold of control group, p=0.011, Figure 3.3). This value decreased in GECs under rapamycin and HAGG co-stimulation significantly (1.01 *vs* 1.21, p=0.042, Figure 3.3).

Then, we treated GECs with HAGG in series of concentrations and durations. Incubation with HAGG for 8-36 hours at 400 μg/mL (Figure 3.4, A), and incubation with HAGG at 100-800 μg/mL for 24 hours (Figure 3.4, B), resulted in decreased trends of LC3 conversion, respectively.

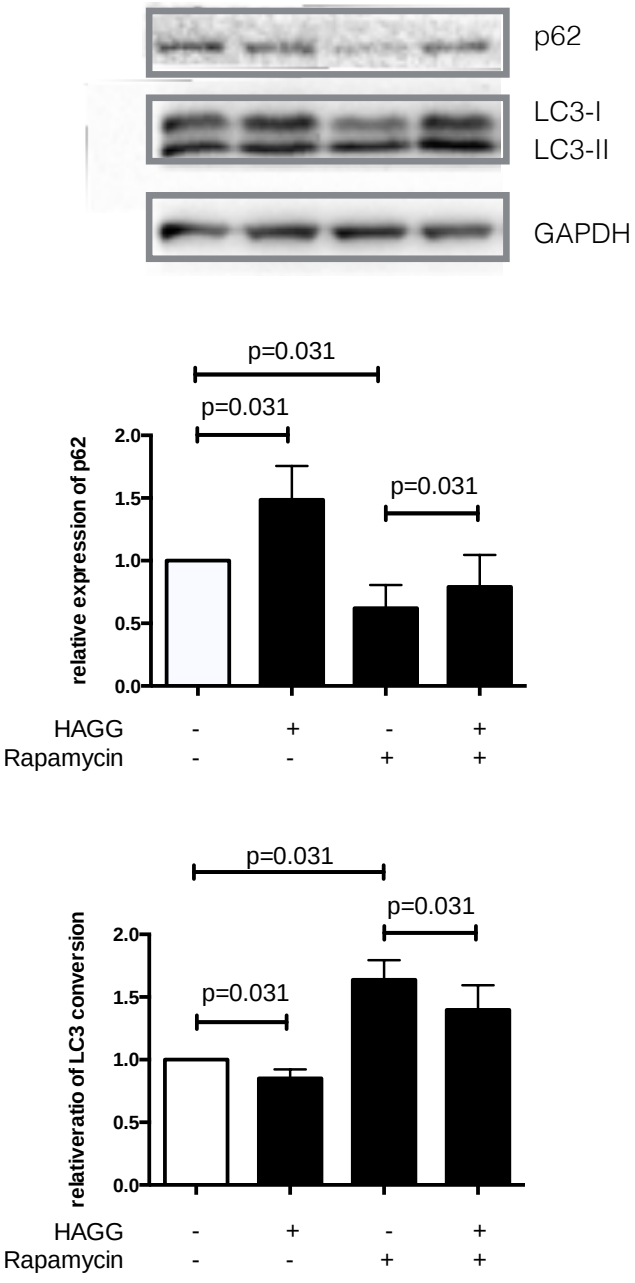

Figure 3.2 HAGG suppressed autophagy in GECs.

GECs were treated with complete medium (control), HAGG (400 μg/mL), rapamycin (100 ng/mL), or rapamycin plus HAGG, for 24 hours. Protein expressions of LC3 and p62 were measured by western blotting. The relative ratio of LC3 II/I and p62 expression were presented as mean ± SD (n=6).

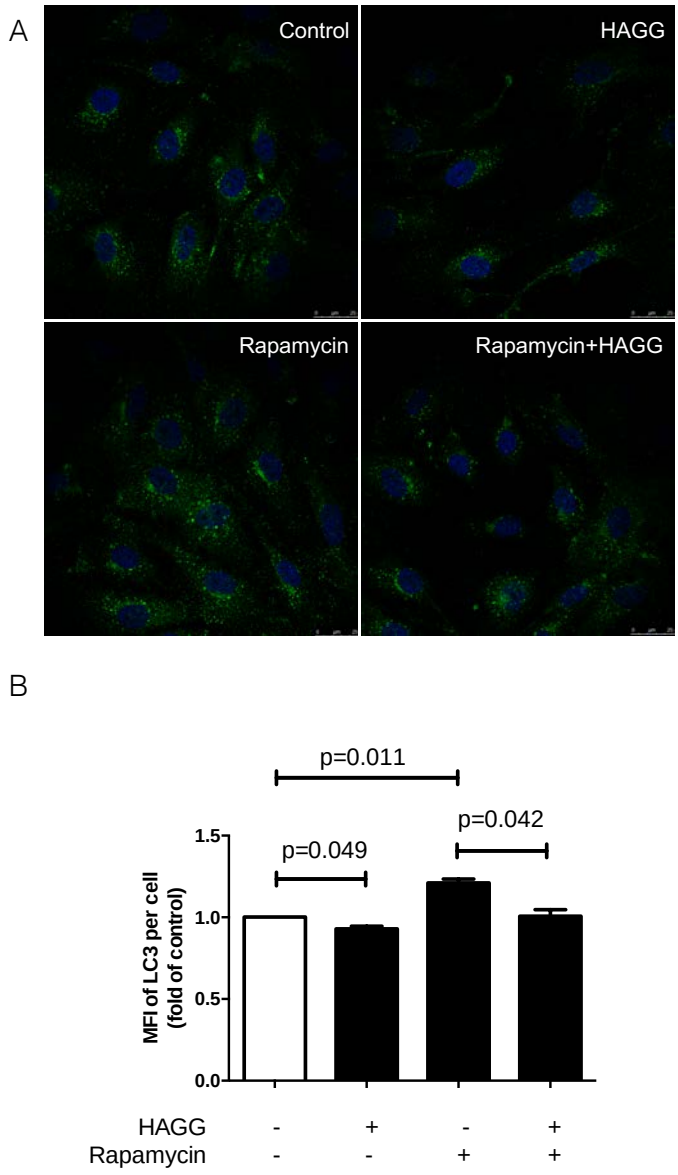

Figure 3.3 LC3 immunostaining in HAGG-treated GECs.

(A) Representative confocal microscopy images of LC3 immunostaining. GECs were treated with complete medium (control), HAGG (400 μg/mL), rapamycin (100 ng/ml), or rapamycin plus HAGG, separately. After 24 hours, cells were fixed, permeabilized and stained with anti-LC3 antibody (green). The nuclei were stained with DAPI (blue). Images were taken by Leica DMi8 microscope.

(B) Quantification analysis of LC3 immunostaining. 25-40 cells under each condition were counted and the mean fluorescence intensity (MFI) of LC3 puncta per cell was analyzed with ImageJ. Data were from 3 independent experiments and presented as mean ± SEM. Magnification: 400×.

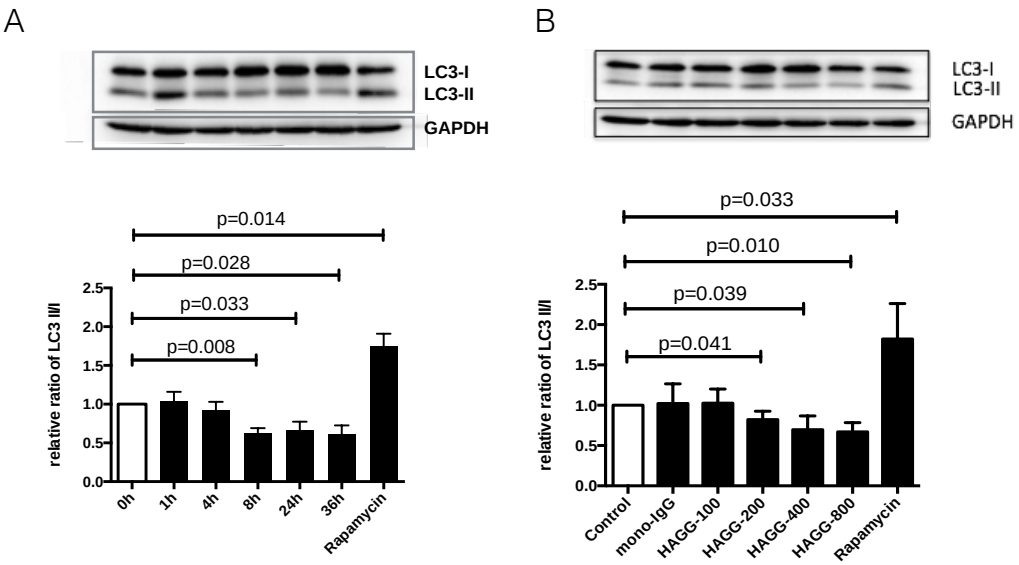

Figure 3.4 Time and dosage dependent effects of HAGG on autophagy in GECs.

(A) GECs were treated with HAGG at 400 μg/mL for 0-36 hours. Rapamycin (100 ng/mL, 24 hours) was used as a positive control. Protein expression of LC3 was measured by western blotting. Relative ratio of LC3 conversion was presented as mean ± SD (n=3). (B) GECs were treated with HAGG at a series of concentrations from 100-800 μg/mL for 24 hours. Besides complete medium (control), monomer human immunoglobulin (400 μg/mL) was used as a negative control. Protein expression of LC3 was measured by western blotting (mean ± SD, n=4).

3.2.3 HAGG suppressed autophagy through Akt-mTOR-dependent pathways

The serine/threonine kinase mTOR is a core regulator of autophagy. The mTOR forms two distinct complexes, mTORC1 and mTORC2. Phosphorylated and activated mTORC1 can phosphorylate the mRNA translation repressor 4E-binding proteins, and ribosomal S6 kinase, and inhibit the autophagy. The role of mTORC2 in autophagy is not very clear, although mTORC2 can phosphorylate a subset of AGC family kinases (protein kinase PKA, PKG, and PKC) and regulate cell survival and cytoskeletal organization (Bhaskar and Hay, 2007). There are also other mTOR-independent pathways regulating autophagy. Thus, to investigate whether the suppressed autophagy in HAGG-treated GECs went through an mTOR-dependent pathway or not, we evaluated the expressions of phosphorylated mTOR (p-mTOR), p70S6K (p- p70S6K), and 4E-BP-1 (p-4E-BP-1). As shown in Figure 3.5, HAGG treatment for 8 hours significantly increased the expressions of p-mTOR (1.59 fold of control, p=0.008), and the corresponding downstream proteins p-p70S6K (1.3 fold of control, p=0.008) and p-4E-BP-1 (1.58 fold of control, p=0.045). However, the expression of total mTOR was not changed after HAGG treatment. Rapamycin, an inhibitor of mTOR kinase, significantly suppressed the expressions of the above three phosphorylated proteins. Addition of HAGG increased the expressions of p-mTOR (0.85 *vs* 0.57, p=0.004), p-p70S6K (1.00 *vs* 0.65, p=0.016), and p-4E-BP-1 (1.34 *vs* 0.76, p=0.017), which were suppressed by rapamycin.

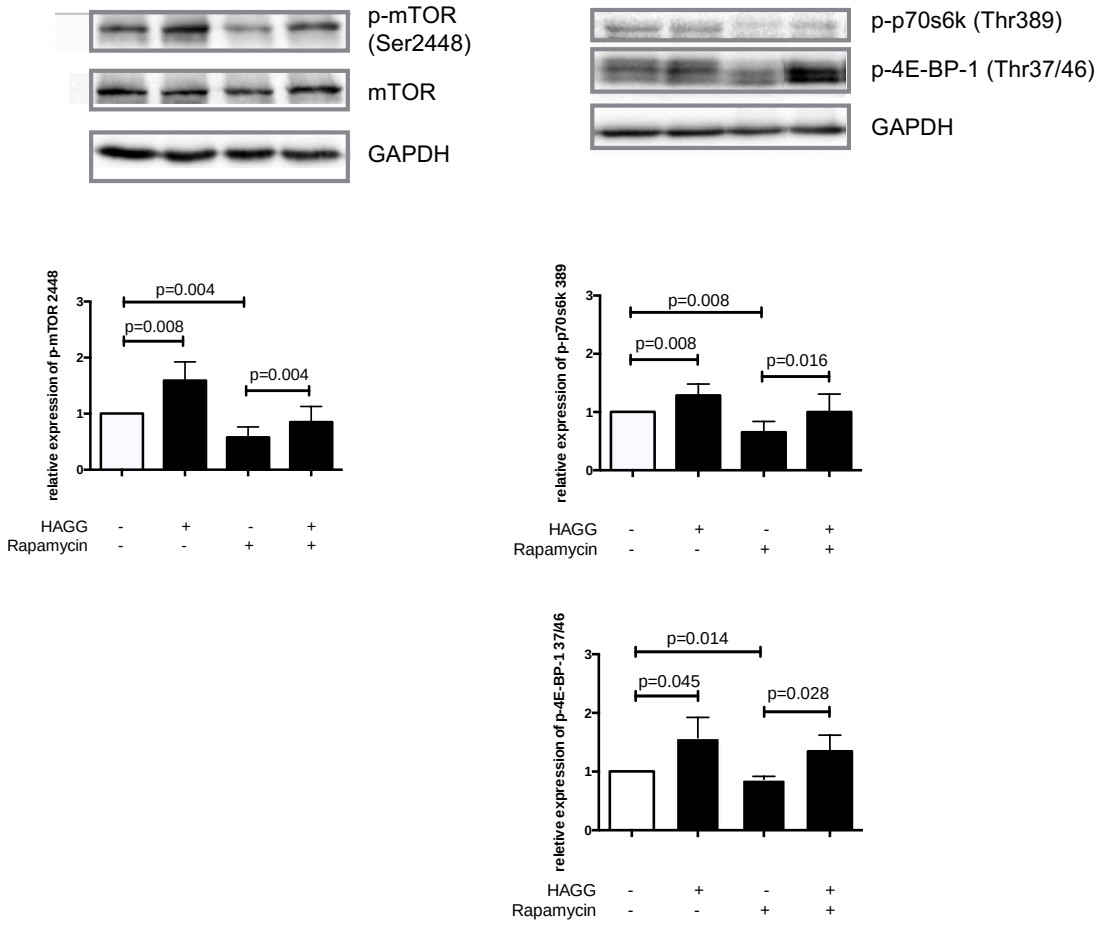

Figure 3.5 HAGG suppressed autophagy in GECs through mTOR-dependent pathways.

GECs were treated with complete medium (control), HAGG (400 μg/mL), rapamycin (100 ng/mL), or rapamycin plus HAGG, for 8 hours. Protein expressions of p-mTOR (n=8), p-p70s6k (n=6), and p-4E-BP-1 (n=4) were measured by western blotting (mean ± SD).

We also investigated the upstream regulator of mTORC1 activity, the Akt protein. Activated Akt phosphorylates TSC2 and promotes mTORC1 activity, thus leading to suppressed autophagy. Akt activation is mainly regulated by phosphorylation on two sites, the Thr308 and Ser473. The phosphorylation on each site is independent on one another. Thr308 is exclusively phosphorylated by PDK1, which is activated in insulin-receptor tyrosine kinase-PI3K signaling pathway, while Ser473 is phosphorylated by mTORC2. Furthermore, evidences show that phosphorylated Akt on Thr308, not Ser473, is essential for activation of mTORC1 (Jacinto et al., 2006; Rodrik-Outmezguine et al., 2011). Thus, in this project, we only measured the phosphorylated Akt on Thr308.

As shown in Figure 3.6, C, the expression of p-Akt (Thr308) was significantly increased after HAGG treatment for 8 hours (2.19 fold of control, p=0.008, Figure 3.6, C). As expected, rapamycin led to suppressed p-Akt expression (0.84 fold of control, p=0.03), while rapamycin plus HAGG reverted the suppression of rapamycin alone on p-Akt expression (0.84 *vs* 2.03, p=0.004, Figure 3.6, C).

3.2.4 HAGG plus TNF-alpha suppressed autophagy in GECs

Disturbed cytokine profiles are detected in LN. In the urinary sediment of patients with active LN, expression of IFN-gamma was significantly elevated (Chan et al., 2003). The glomerular mRNA expressions of IL-2, IL-18, IL-4, and MCP-1 were significantly decreased in patients with LN (Chan et al., 2007). IL-1 beta and IL-17 were detected in the kidney of patients with LN (Iwata et al., 2011). Besides, the serum concentrations of IL-6, IL-10, IFN-gamma, and soluble VCAM-1, were elevated in patients with LN (Mok,

2010; Davis et al., 2011). These abnormally expressed cytokines play essential roles in the development of lupus nephritis. Among these disturbed cytokines, TNF-alpha is elevated in patient serum and closely associated with disease activities (Weckerle et al., 2012). TNF-alpha is highly expressed in glomerulus (Gigante et al., 2011). TNF-alpha is an important cytokine for LN development, assessment, and therapy. Thus, we used TNF-alpha to simulate the chronic inflammatory microenvironment in LN glomerulus and investigated the roles of ICs together with pro-inflammatory cytokines on autophagy in GECs.

After incubation with TNF-alpha (10 ng/mL) for 24 hours, p62 expression was highly elevated in GECs (3.40 fold of control, p=0.031, Figure 3.6, A). The expression of p-mTOR was also increased (1.64 fold of control, p=0.016, Figure 3.6, B). However, the ratio of LC3 II/I was slightly increased under TNF-alpha treatment (1.21 fold of control, p=0.09, Figure 3.6, A). Co-stimulation with TNF-alpha and HAGG led to further upregulated p-mTOR expression (1.94 *vs* 1.64, p=0.047, Figure 3.6, B) and decreased ratio of LC3 II/I (1.13 *vs* 1.21, p=0.03, Figure 3.6, A), while the p62 expression showed no significant difference, when compared with TNF-alpha stimulation alone.

Similarly, we also evaluated the phosphorylation of Akt, the upstream regulator of mTOR activity. The expression of p-Akt (Thr308) was significantly increased after incubation with TNF-alpha (10 ng/mL) for 8 hours (1.28 fold of control, p=0.016, Figure 3.6, C). Combination of TNF-alpha and HAGG further increased the phosphorylation of Akt (2.07 *vs* 1.28, p=0.002, Figure 3.6, C). The expressions of total Akt were not changed under these conditions (Figure 3.6, C).

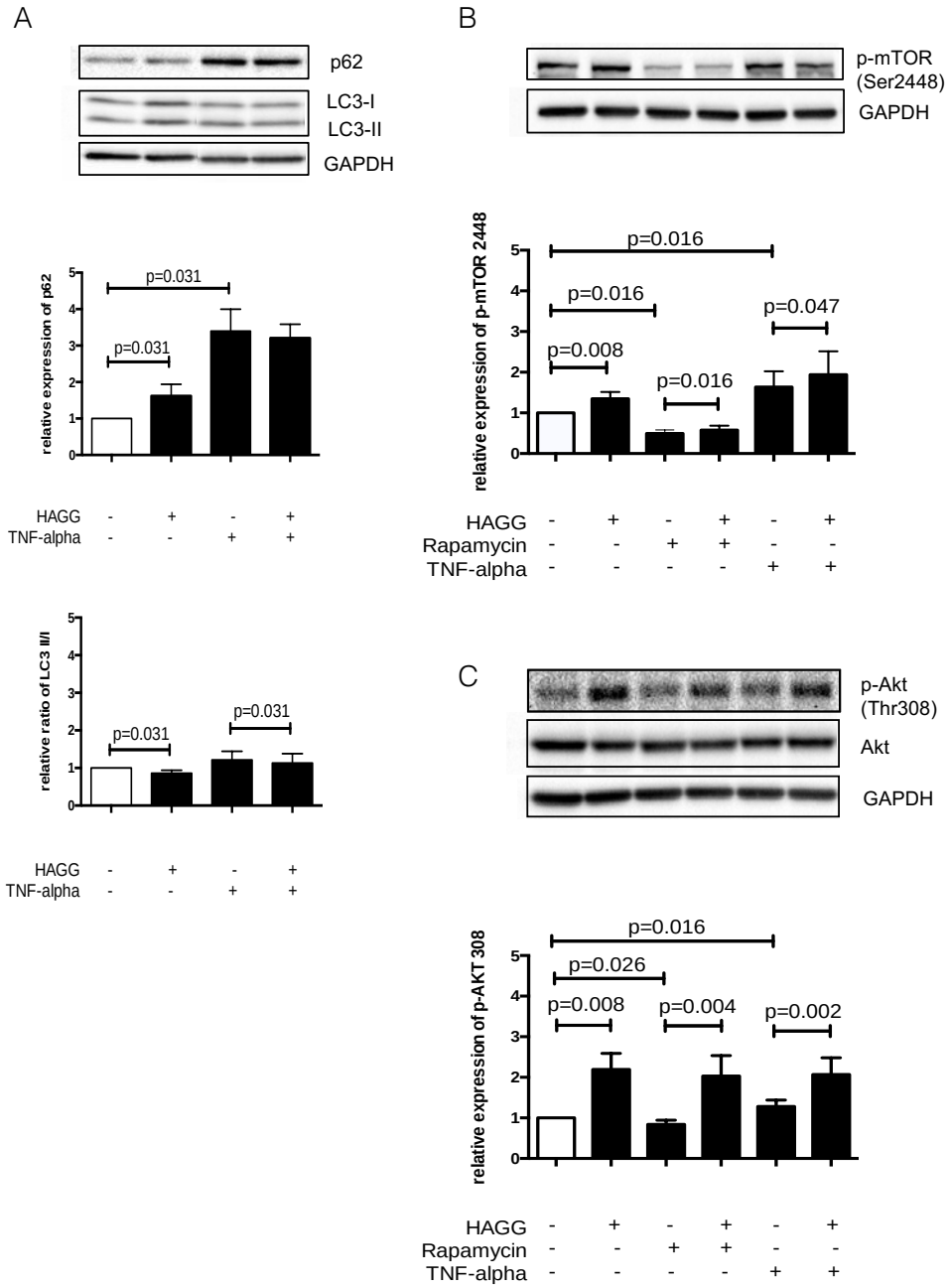

Figure 3.6 HAGG plus TNF-alpha suppressed autophagy in GECs, through Akt-mTOR pathway.

(A)(B) GECs were treated with complete medium (control), HAGG (400 μg/mL), TNF-alpha (10 ng/mL), TNF-alpha plus HAGG, rapamycin (100 ng/mL), or rapamycin plus HAGG, for 24 hours. Protein expressions of LC3, p62, and p-mTOR (Ser2448) were measured by western blotting (mean ± SD, n=6). (C) p-Akt (Thr308) expressions in GECs were measured after stimulations for 8 hours by western blotting (mean ± SD, n=5).

3.3 Discussions

Lupus nephritis is the most severe complication of lupus patients, which pathogenesis is still not thoroughly understood. Although GECs are important for glomerular structure and functions, few attentions have been paid on this kind of cells, compared with other resident and migrating cells in the glomerulus. Understanding the risk factors for GEC damage, especially how ICs interact with GECs, and finding out the protective methods for GECs, are crucial for understanding the pathogenesis of LN. Autophagy is a highly conserved catabolic process. Autophagy is important for cell protection and used as a therapeutic method in many diseases. We have previously shown that autophagy is cytoprotective in podocytes, the important cell of the tripartite of the filtration barrier (Kang et al., 2014). Therefore, we investigated the direct effects of ICs on GEC autophagy.

Our results indicated that autophagy was suppressed in GECs under HAGG treatment, through Akt-mTOR pathways. Previous reports provided clues for the linkages between ICs and endothelial cell autophagy. Fujii and colleagues reported that self-aggregated antibodies could be internalized by endothelial cells via actin polymerization induced by fibronectin-integrin interaction (Fujii et al., 2003). Autophagy requires membrane remodeling and vesicle transportation and actin polymerization and depolymerisation could potentially participate in every step of autophagy (Aguilera et al., 2012). Besides, activated mTOR pathway has been detected in renal endothelial cells in patients with anti-phospholipid syndrome (APS) nephropathy, which often occurs secondary to lupus and characterized by presence of circulating anti-phospholipid antibodies. After incubation

with anti-phospholipid antibodies isolated from APS patients, cultured human microvascular endothelial cells exhibited increased S6RP and Akt phosphorylations, implying the activated mTOR pathways (Canaud et al., 2014). In transplant vasculopathy model, anti-HLA antibodies ligation to HLA class I molecules expressed in human aortic endothelial cells, activated mTOR pathways, demonstrated by increased phosphorylations of S6K and Akt (Jindra et al., 2008). Activation of Akt-mTOR pathway was also illustrated in GECs in NZB/W female lupus-prone mice, as over-expressed phosphorylated Akt and mTOR were detected and visualized in renal endothelial cells by double-immunofluorescence staining (Stylianou et al., 2011). These results implied activated mTOR pathways in endothelial cells in IC-mediated diseases. However, the authors did not evaluate the autophagy status. Together with the changed expressions of autophagic markers LC3 and p62, our results showed the suppressed autophagy in GECs under HAGG treatment, by activating Akt-mTOR pathways.

For the effects of TNF-alpha on autophagy, Lee and colleagues demonstrated that TNF-alpha activated mTOR signaling, through inactivation of TSC1 by activating IKK-beta activity in breast cancers (Lee et al., 2007a). p62 was reported upregulated under TNF-alpha treatment. Kojima and colleagues reported that p62 was upregulated in rat optic nerve after intravitreal injection of TNF-alpha (Kojima et al., 2014). Opperman et al also observed accumulated p62 and increased LC3 II/I ratio in rat cardiomyoblasts under TNF-alpha stimulation (Opperman and Sishi, 2015). Here, our results showed that TNF-alpha upregulated expressions of p-mTOR and p62, together with slightly increased LC3 II/I

ratio in GECs (Figure 3.6). These results suggested that the clearance step in autophagy may be inhibited. Moreover, Mostowy et al reported not only significantly increased p62 and LC3-II levels in HeLa cells treated with TNF-alpha, but also the increased p62 mRNA expression under TNF-alpha stimulation (Mostowy et al., 2011). Their results implied that, besides the inhibited clearance step in autophagy, TNF-alpha may regulate p62 at transcriptional level and then the autophagy process.

We also investigated the interaction between ICs and TNF-alpha on endothelial cell functions. HAGG and TNF-alpha co-incubation led to reduced ratio of LC3 conversion and increased expression of p-mTOR, compared to the effects of TNF-alpha alone, implying aggravated suppression of autophagy in GECs. Actually, there are evidences implying the interactive effects of ICs and TNF-alpha on endothelial cell functions. In TNF $^{-/-}$ mice, ICs-induced inflammation and microvascular dysfunctions were attenuated (Norman et al., 2005). TNF-alpha increased the expressions of FcγRII and FcγRIII on aortic endothelial cells, which may facilitate circulating ICs localization on ECs (Pan et al., 1998). Further investigation on Fc receptor expressions is needed for GECs.

Nowadays, people have paid more attentions on the roles of autophagy in lupus and tried autophagy regulators for therapy. Rapamycin could prevent the development of nephritis (Lui et al., 2008b) and attenuate the established nephritis (Lui et al., 2008a) in lupus-prone NZB/W mice. Rapamycin also reduced disease activities in lupus patients (Fernandez et al., 2006). Glucocorticoid, the current first-line medicine for lupus therapy,

is demonstrated to induce autophagy in different cell kinds, including osteocytes (Xia et al., 2010) and lymphocytes (Harr et al., 2010), through mTOR-dependent pathways. Our results showed suppressed autophagy in GECs under HAGG stimulation. The altered autophagy in LN may be part of the reasons for organ damage and may provide new targets for therapy.

In conclusion, we demonstrated that HAGG alone suppressed autophagy in GECs, through mTOR-dependent pathways. Additional TNF-alpha also suppressed autophagy in GECs. The direct effects of HAGG on GECs autophagy, especially under inflammatory microenvironment, provided new views for mechanisms of GEC dysfunctions.

Chapter 4 Immune Complexes Hampered Glomerular Endothelial Cells Functions

4.1 Introduction

Endothelial cells are not static cells just lining the inner surfaces of vessels and serving as a passive barrier. Normal endothelial cells are metabolically active and participate in multitudes of physiological processes, including regulating vasomotor tone, vascular permeability, thrombosis, redox balance, immune responses, and angiogenesis (Gimbrone and Garcia-Cardena, 2016). When challenged by stresses, such as pro-inflammatory cytokines, invading pathogens, abnormal metabolic products, or various pathological conditions, endothelial cells become activated and dysfunctional.

Endothelial dysfunctions or injuries represent a shift from normal to a vasoconstrictive, pro-inflammatory, and pro-thrombotic status. The dysfunctions are characterized by abnormal cell morphology and mechanics, imbalanced cell proliferation and death, disturbed nitric oxide synthesis and bioavailability, increased expressions of adhesion molecules, the shedding components of the glycocalyx, and other molecular and biochemical changes (Rajendran et al., 2013). Thus, various methods are needed for assessing different aspects of endothelial cell functions and injuries.

There are many clues indicating that endothelial cells are injured in LN (Mak and Kow, 2014; Skeoch et al., 2014). In this chapter, we investigated the effects of ICs, a major pathogenic factor for LN, on GEC functions and injuries. Functional characteristics of GECs, including cell morphology, viability, necrosis, apoptosis, tube formation ability,

intracellular NO production, eNOS expression, and adhesion molecules, were measured. HAGG was used as an artificial substitute of ICs. TNF-alpha was used to simulate the inflammatory microenvironment. Autophagy regulators (rapamycin, 3MA, and chloroquine) were also used, to investigate the relationships between autophagy and endothelial dysfunctions.

4.2 Results

4.2.1 HAGG induced GEC morphology changes

Cell morphology is a large-scale synthetic result of a global precisely-regulated biological processes of cells, controlled by the interactions among cytoskeletons, membrane, membrane-bound proteins, and the extracellular environment. Changed cell morphology reflects changed cell physiology and functions. Cell morphology is commonly used as a measurement of the outcomes of various stimulations (Pincus and Theriot, 2007).

In our experiments, GECs were cultured in 8 conditions with complete medium, HAGG (400 μg/mL), TNF-alpha (10 ng/mL), TNF-alpha plus HAGG, rapamycin (100 ng/mL), rapamycin plus HAGG, 3MA (5mM), or 3MA plus HAGG, respectively. After 8 hours of treatment, phase-contrast images were taken and randomly-reselected single cells were outlined. Cell morphology parameters, including cell area (unit: square pixel, or pixel^2), perimeter (unit: pixel), circularity (defined as $4\pi\times\frac{[Area]}{[Perimeter]^2}$), and aspect ratio (defined as $\frac{[Major\ Axis]}{[Minor\ Axis]}$), were measured and calculated by ImageJ software.

As shown in Figure 4.1, HAGG treatment led to a significant increase in cell area (4979 pixel^2 *vs* 4358 pixel^2, p=0.014) and no significant difference in cell perimeter, in comparison with the control cells. In geometry, the circle shape encloses the largest area for a given arc length (for plane curves). Therefore, these results indicated a rounder cell shape induced by HAGG. The significantly increased circularity (0.60 *vs* 0.57, p=0.008) and decreased aspect ratio (2.88 *vs* 3.04, p=0.017) also supported the same conclusion.

TNF-alpha led to larger and more elongated GECs. Cells treated with TNF-alpha exhibited larger cell area (5001 pixel^2 *vs* 4358 pixel^2, p=0.035) and perimeter (364.7 pixel *vs* 314.5 pixel, p=0.002), lower circularity (0.48 *vs* 0.57, p=0.002), and higher aspect ratio (4.10 *vs* 3.04, p=0.047), compared with control cells. Cells treated with TNF-alpha plus HAGG displayed a rounder shape than cells treated with TNF-alpha alone, demonstrated by the increased cell area (5495 pixel^2 *vs* 5001 pixel^2, p=0.007) under same perimeter, increased circularity (0.52 *vs* 0.48, p=0.001) and decreased aspect ratio (3.77 *vs* 4.10, p=0.023).

The autophagy inducer (Rapamycin) and inhibitor (3MA) used also significantly changed cell morphology. Both the rapamycin and 3MA led to increased cell areas (rapamycin: 5149 pixel^2, p=0.025; 3MA: 4973 pixel^2, p=0.007; control: 4358 pixel^2) and perimeters (rapamycin: 353.8 pixel, p=0.016; 3MA: 403.2 pixel, p=0.014; control: 314.5 pixel). Rapamycin induced mild cell elongation, with decreased cell circularity (0.54 $\pm$ 0.037, p=0.021) and increased aspect ratio (3.26 $\pm$ 0.15, p=0.010). 3MA led to extremely extended slim cells, with greatly decreased circularity (0.40 *vs* 0.57, p=0.014, minimum: 0.14) and elevated aspect ratio (5.15 *vs* 3.04, p=0.046, maximum: 13.15).

In Figure 4.1 A, we also noticed that after eight hours of incubation with different stimulations, GECs exhibited different cell densities per visual field, although the same number of cells were seeded in the 6 well plate at the beginning. This observation prompted us to investigate cell proliferations and viabilities under different stimulations.

A

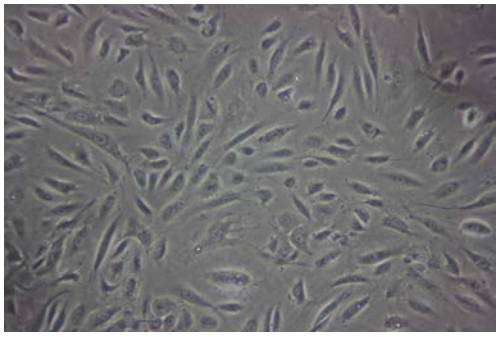

Control

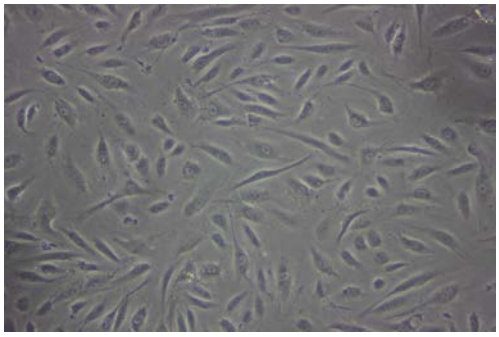

HAGG

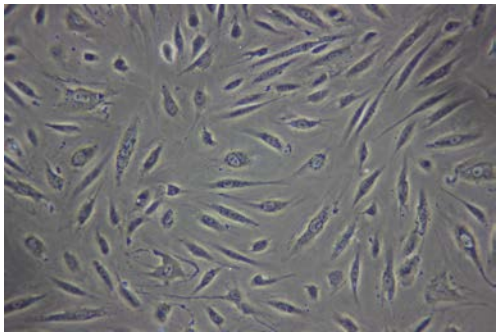

TNF

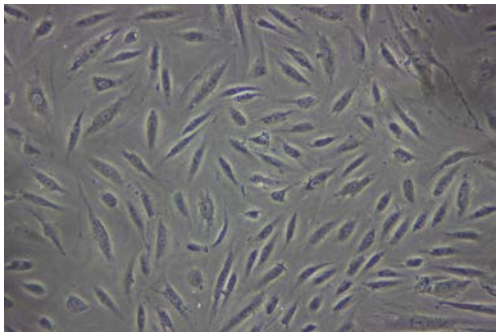

TNF+HAGG

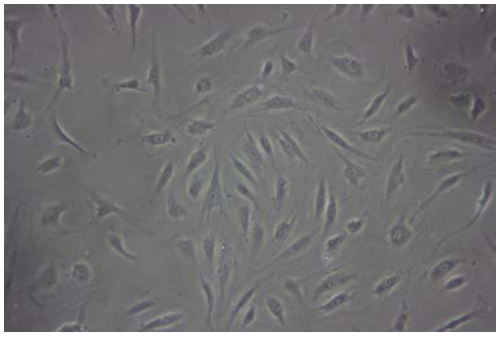

Rapamycin

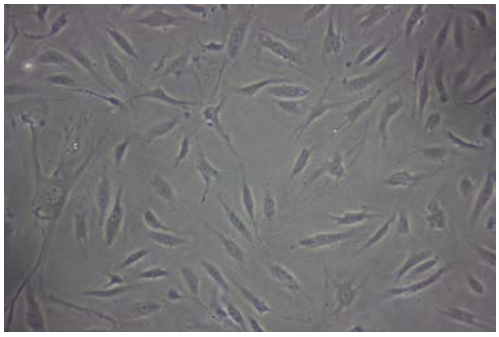

Rapamycin+HAGG

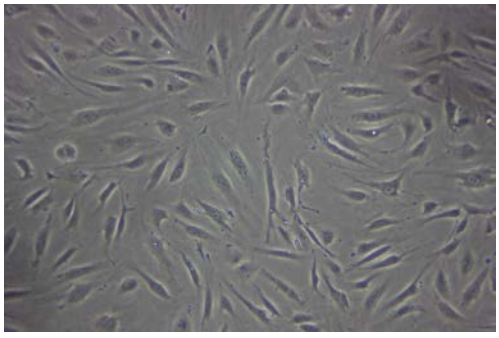

3MA

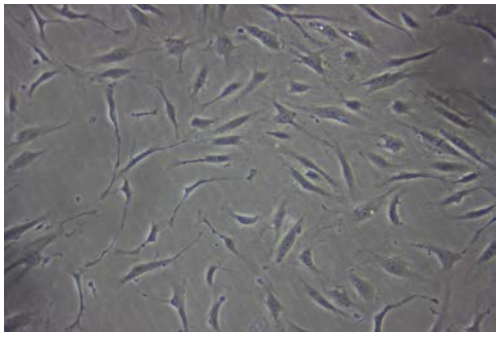

3MA+HAGG

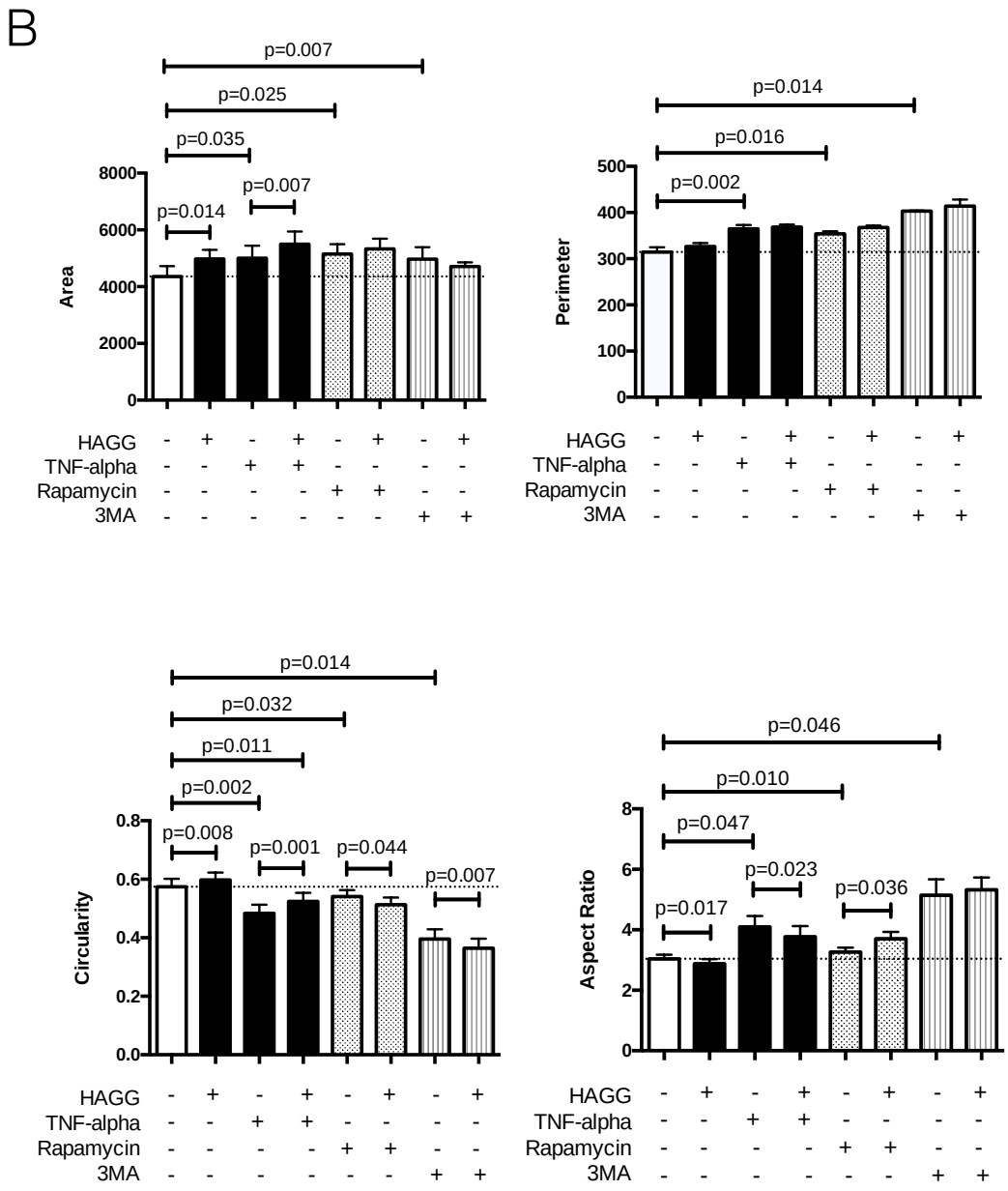

Figure 4.1 Cell morphology was changed after HAGG treatment.

GECs were treated with complete medium (Control), HAGG (400 μg/mL), TNF-alpha (10 ng/mL), TNF-alpha plus HAGG, rapamycin (100 ng/mL), rapamycin plus HAGG, 3MA (5mM), or 3MA plus HAGG, respectively, for 8 hours. (A) Representative photographs of cells after 8-hour incubation with different stimuli. Magnification: 100 times. (B) Statistical analysis of cell morphology parameters. Cell area, perimeter, circularity, and aspect ratio, were qualified by ImageJ software and plotted by Prism 5.0 Software. Dotted lines indicated the mean values of the variables under Control condition. Data was presented as mean ± SEM (n=3).

4.2.2 HAGG decreased cell viabilities in GECs

Cell viability was measured by CCK-8 reagent (Chapter 2, Method 2.7). Two days after seeding, GECs were stimulated with HAGG (400 μg/mL) and TNF-alpha (10 ng/mL), alone or in combination, for 48 hours. We also investigated the effects of autophagy by incubating GECs with autophagy regulators (rapamycin: autophagy inducer, 100 ng/mL; 3MA: autophagy inhibitor, 5mM), for 48 hours.

As shown in Figure 4.2, HAGG led to 4% decrease of cell viability in GECs (p=0.008). TNF-alpha significantly decreased cell viability (0.84 fold of control, p=0.016). While the combination of HAGG and TNF-alpha further decreased cell viability (0.79 *vs* 0.84, p=0.016). Both autophagy regulators led to significantly decreased cell viabilities (rapamycin: 0.53 fold of control, p=0.008; 3MA: 0.42 fold of control, p=0.008). Cell viabilities further decreased under co-stimulation with HAGG (rapamycin+ HAGG *vs* rapamycin: 0.49 *vs* 0.53, p=0.008; 3MA+HAGG *vs* 3MA: 0.38 *vs* 0,42, p=0.039).

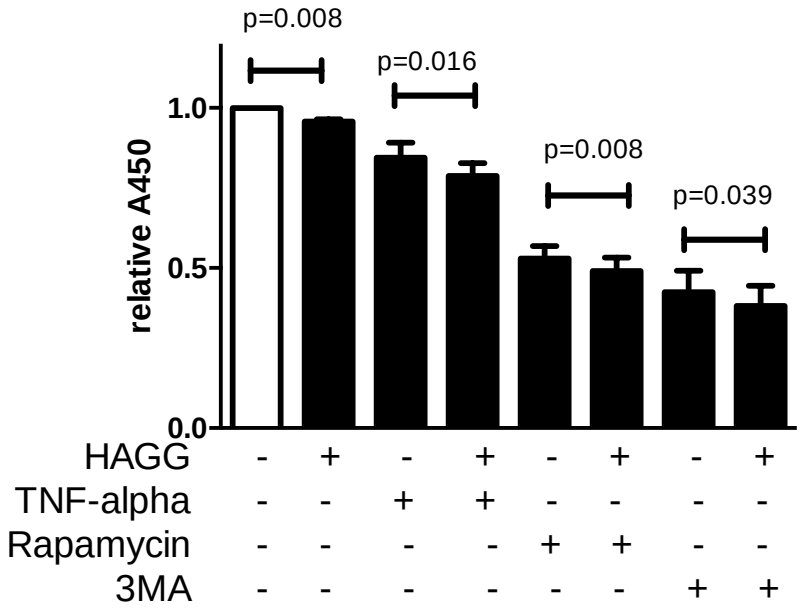

Figure 4.2 HAGG decreased cell viabilities in GECs.

GECs were treated with complete medium (Control), HAGG (400 μg/mL), TNF-alpha (10 ng/mL), TNF-alpha plus HAGG, rapamycin (100 ng/mL), rapamycin plus HAGG, 3MA (5mM), or 3MA plus HAGG, for 48 hours. Cell viabilities were measured using CCK-8 methods in 8 independent experiments with triplicates and the data was presented as mean ± SEM.

4.2.3 HAGG did not induce necrosis in GECs

To investigate the mechanism of the decreased viability, cell necrosis was measured by LDH release assay (Chapter 2, Method 2.8). LDH is a soluble and stable cytoplasmic enzyme existing in every living cells which will be released into surrounding microenvironment through impaired plasma membrane in necrotic cells (Chan et al., 2013).

In our experiments, GECs were cultured with complete medium, or treated with HAGG (400 μg/mL), TNF-alpha (10 ng/mL), TNF-alpha plus HAGG, rapamycin (100 ng/mL), rapamycin plus HAGG, 3MA (5mM), or 3MA plus HAGG, respectively, for 48 hours. Then released LDH activity in culture medium was measured. Results showed that HAGG treatment for 48 hours did not increase LDH release (Figure 4.3). TNF-alpha nor TNF-alpha plus HAGG did not alter the LDH release. Both autophagy regulators induced necrosis significantly in GECs (rapamycin: 1.42 fold of control, $p=0.008$; 3MA: 2.33 fold of control, $p=0.008$, Figure 4.3).

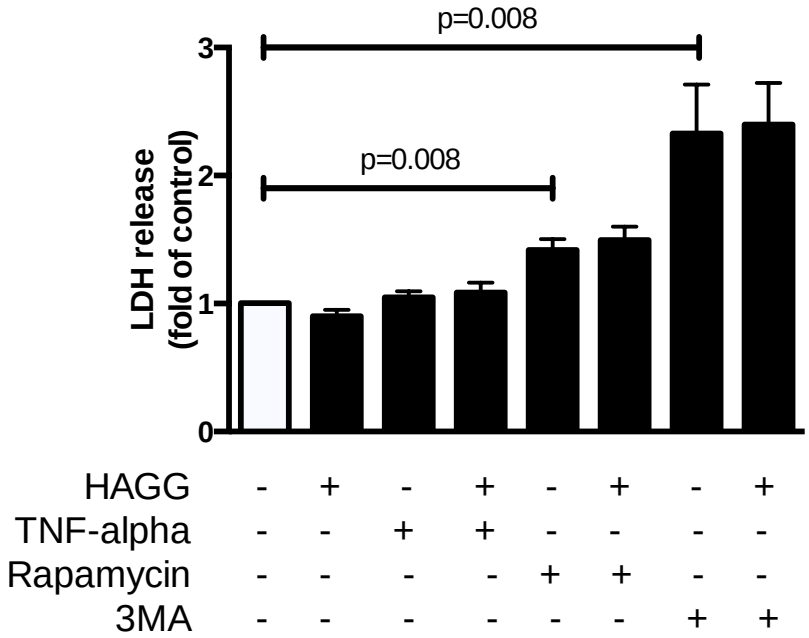

Figure 4.3 Effects of HAGG on GEC necrosis.

GECs were treated with complete medium (control), HAGG (400 μg/mL), TNF-alpha (10 ng/mL), TNF-alpha plus HAGG, rapamycin (100 ng/mL), rapamycin plus HAGG, 3MA (5mM), or 3MA plus HAGG, for 48 hours. Necrosis was measured using LDH release assay. Data was presented as mean ± SEM. n=8.

4.2.4 HAGG upregulated intracellular level of active caspase 3 in GECs

Further to the investigation on necrosis, apoptosis was measured by YO-PRO-1/PI assay and Active Caspase 3 assay (Chapter 2, Method 2.6) using flow cytometry. Apoptotic cells display a series of characteristic morphological and biochemical changes, including externalization of phosphatidylserine (PS), slightly permeable membranes, and activation of caspases (Henry et al., 2013). Apoptotic cells are permeable to YO-PRO-1 dye, but not permeant to PI dye. Thus, after staining, apoptotic cells can be defined as YO-PRO-1 positive and PI negative cells. Meanwhile, caspase 3 belongs to effector/executioner caspases in mammalian cell apoptosis. After cleavage, the active caspase 3 cleaves a wide spectrum of substrates, and serves as a crucial component in apoptosis pathways (McIlwain et al., 2013). Therefore, the intracellular level of active caspase 3 is an important marker for evaluating apoptosis.

In our experiment, HAGG treatment for 48 hours resulted in increased intracellular level of active caspase 3 (represented by increased ΔMFI of active caspase 3, 2.25 fold of control, p=0.017, Figure 4.4, A). Although the percentage of apoptotic cells (YO-PRO-1 positive and PI negative subsets) in HAGG-treated GECs showed no significant difference from the percentage in control cells, the mean percentage of apoptotic cells increased (1.30 fold of control, Figure 4.4, B).

TNF-alpha is a typical inducer of apoptosis in endothelial cells by binding with its receptors and it is often used as a positive control. TNF-alpha (10 ng/mL) treatment for 48 hours led to increased ΔMFI of active caspase 3 (5.55 fold of control, p=0.001) and

percentage of apoptotic cells (1.65 fold of control, p=0.018). There is no significant difference between the effects of TNF-alpha alone and TNF-alpha plus HAGG.

ΔMFI of active caspase 3 in GECs increased after rapamycin treatment (2.94 fold of control, p=0.044), while the percentage of apoptotic cells showed a mild increase (1.22 fold of control, p=0.007). 3MA induced apoptosis, with significantly increased ΔMFI of active caspase 3 (4.81 fold of control, p=0.009) and increased percentage of apoptotic cells (3.45 fold of control, p=0.011).

A

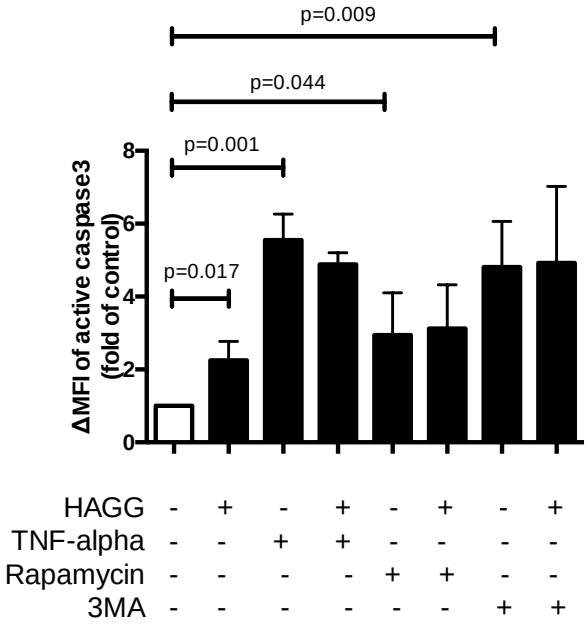

B

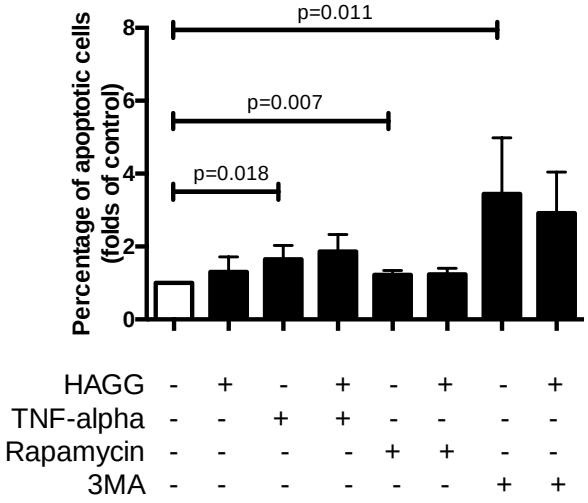

Figure 4.4 Effects of HAGG on GECs apoptosis.

GECs were treated with complete medium (control), HAGG (400 μg/mL), TNF-alpha (10 ng/mL), TNF-alpha plus HAGG, rapamycin (100 ng/mL), rapamycin plus HAGG, 3MA (5mM), or 3MA plus HAGG, for 48 hours. (A) ΔMFI of active caspase 3 in GECs. n=4. (B) Percentages of apoptotic cells measured by YO-PRP-1/PI assay. n=6.

4.2.5 HAGG suppressed GEC Tube formation

A variety of endothelial cells, endothelial progenitor cells, and transformed endothelial cells, have demonstrated to form tube-like structures rapidly *in vitro* when seeded on top of a reconstituted basement membrane extracellular matrix, such as Matrigel (Yamamoto et al., 2003; Arnaoutova et al., 2009). The formation of tube-like structures on basement membrane is specific to endothelial cells (other cells form other structures) (Kleinman and Martin, 2005), and simulates multiple steps in angiogenesis process, including endothelial cell adhesion, degradation of basement membrane, endothelial cell proliferation, migration, alignment, and tube formation. Therefore, this tube formation assay is widely used for assessing angiogenesis properties of endothelial cells.

In our results, tube-like structures began to form within 3 hours after seeding GECs on the growth factor-reduced Matrigel-coated multi-well plates. Similar to previous literatures, we used two parameters, the number of junctions and the number of meshes, to describe the complexity of the tube-like structures (Lin et al., 2015; Marquez-Curtis et al., 2016). As shown in Figure 4.5 A and C, after 12-hours incubation, HAGG-treated GECs formed less junctions (73 *vs* 85, p=0.046) and less meshes (40 *vs* 46, p=0.030) than control cells, suggesting suppressed tube formation ability. TNF-alpha also inhibited tube formation, with decreased number of junctions (62 *vs* 85, p=0.033) and meshes (36 *vs* 46, p=0.018), when compared with control cells. Combined stimulation with TNF-alpha and HAGG further suppressed the tube formation, when compared with the effects of TNF-alpha alone (number of junction: 58 *vs* 62, p=0.035; number of meshes: 30 *vs* 36,

p=0.048). Autophagy inducer rapamycin and autophagy inhibitor CQ (10 μM), which is used for LN treatment, suppressed tube formations, demonstrated by decreased number of junctions (rapamycin: 72, p=0.025; CQ: 73, p=0.048; control: 85) and decreased number of meshes (rapamycin: 42, p=0.025; CQ: 42, p=0.048; control: 46). Tube formations were further suppressed by the combination of HAGG and autophagy regulators (rapamycin plus HAGG *vs* rapamycin: number of junctions: 67 *vs* 72, p=0.028; number of meshes: 38 *vs* 42, p=0.020. CQ plus HAGG *vs* CQ: number of junctions: 65 *vs* 73, p=0.004; number of meshes: 36 *vs* 42, p=0.002).

For tube formation assay observed at 20 hours, the network structure became sparse, with less meshes (control: 46 *vs* 28, p=0.003) and less junctions (control: 85 *vs* 58, p=0.007, Figure 4.5, C and D). Results at 20 hours revealed a similar response to the individual stimulation as shown at 12 hours. That is, HAGG treatment for 20 hours suppressed GEC tube formation (number of junctions: 48 *vs* 58, p=0.002; number of meshes: 23 *vs* 28, p=0.016; compared with control cells). GEC tube formations were also suppressed by TNF-alpha (number of junctions: 45, p=0.041; number of meshes: 23, p=0.023), rapamycin (number of junctions: 54, p=0.024; number of meshes: 26, p=0.013), and CQ (number of junctions: 53, p=0.029; number of meshes: 24, p=0.041), respectively, compared with control cells. Additional HAGG with these above drugs led to further suppressions on tube formations (TNF-alpha plus HAGG *vs* TNF-alpha: number of junctions: 40 *vs* 45, p=0.004; number of meshes: 19 *vs* 23, p=0.031. Rapamycin plus HAGG *vs* rapamycin: number of junctions: 49 *vs* 54, p=0.039; number of meshes: 23 *vs*

26, p=0.020. CQ plus HAGG *vs* CQ: number of junctions: 49 *vs* 53, p=0.020; number of meshes: 21 *vs* 24, p=0.025) (Figure 4.5, B and D).

A 12h

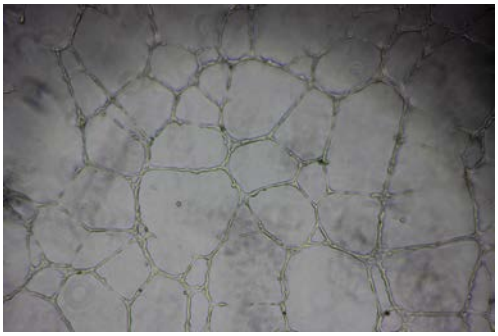

Control

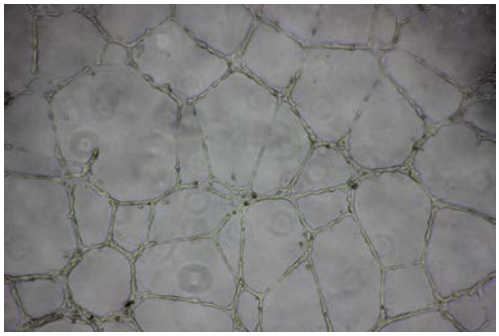

HAGG

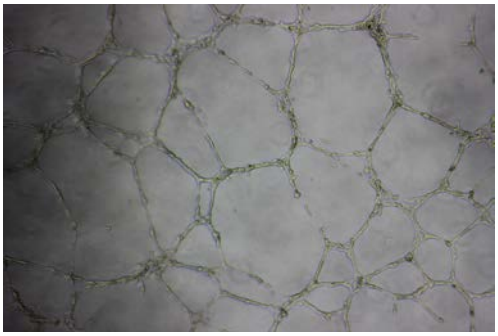

TNF

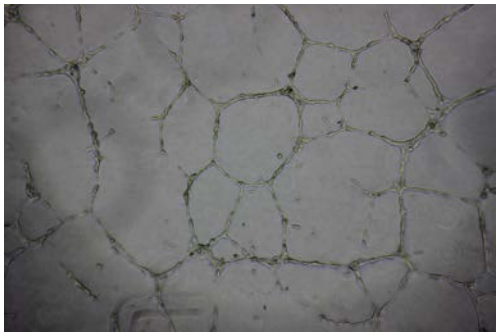

TNF+HAGG

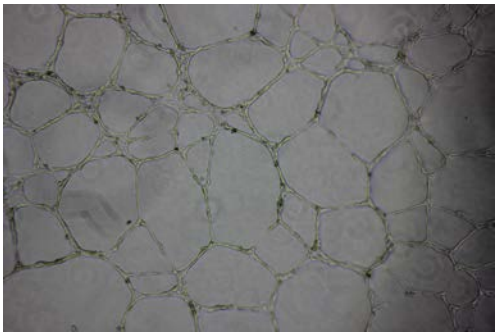

Rapamycin

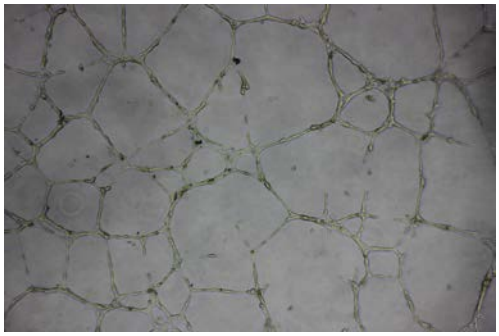

Rapamycin+HAGG

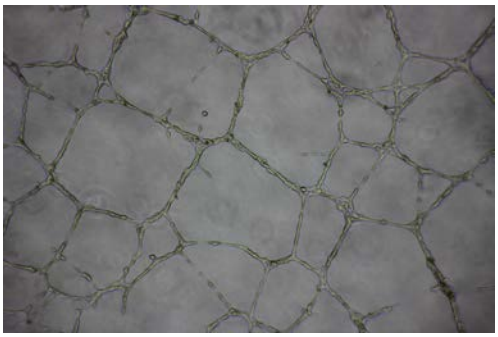

CQ

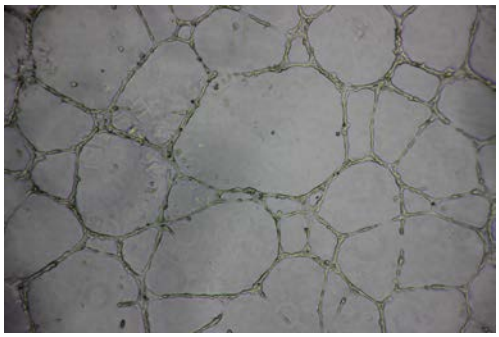

CQ+HAGG

B 20h

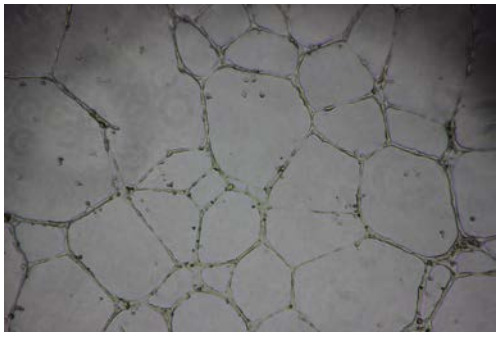

Control

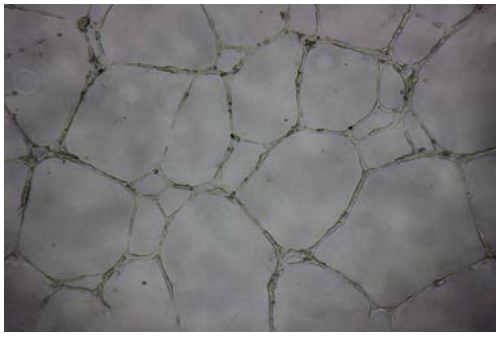

HAGG

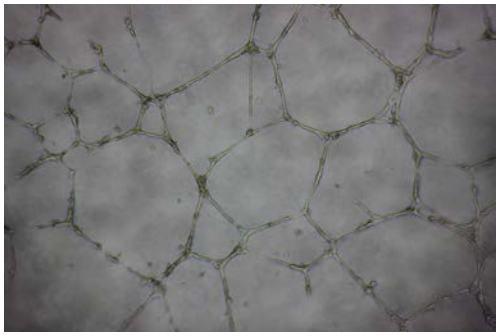

TNF

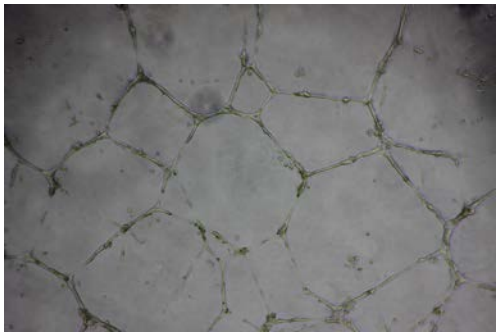

TNF+HAGG

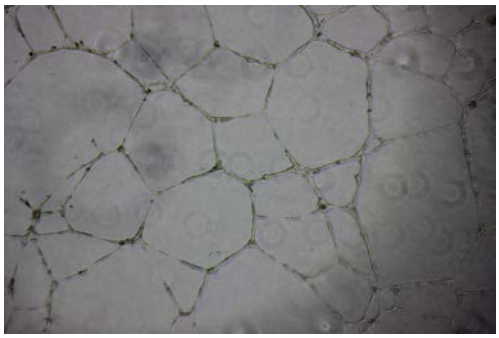

Rapamycin

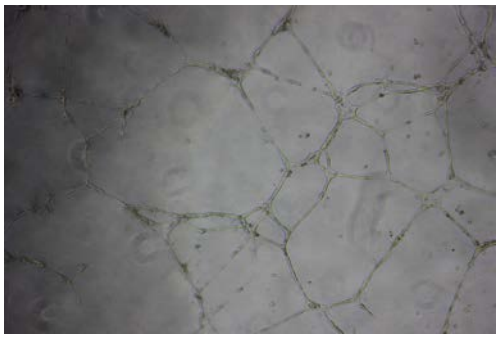

Rapamycin+HAGG

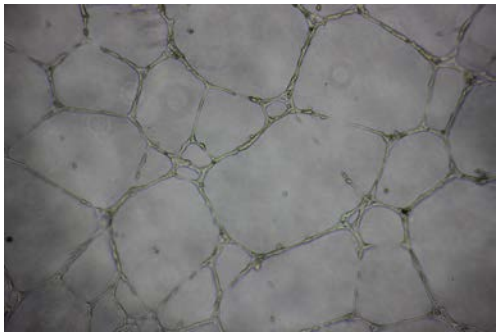

CQ

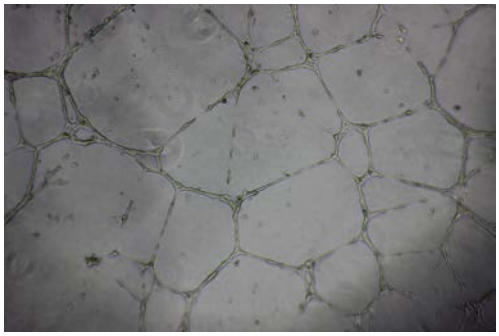

CQ+HAGG

C

12h

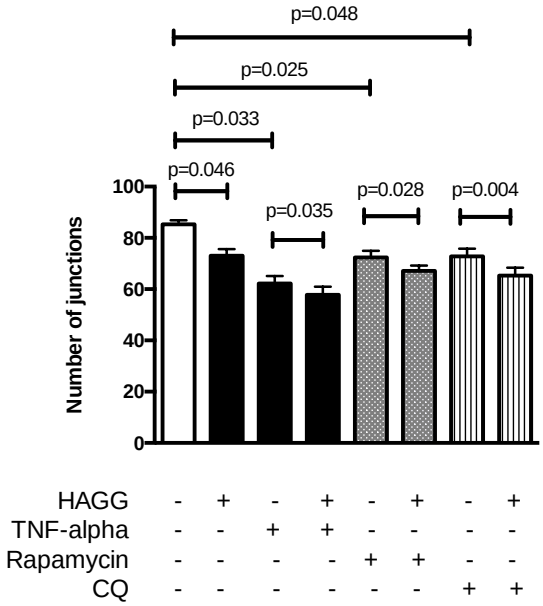
p=0.048
p=0.025
p=0.033
p=0.046
p=0.035
p=0.028
p=0.004
Number of junctions
100
80
60
40
20
0
HAGG - + - + - + - +
TNF-alpha - - + + - - - -
Rapamycin - - - - + + - -
CQ - - - - - - + +

12h

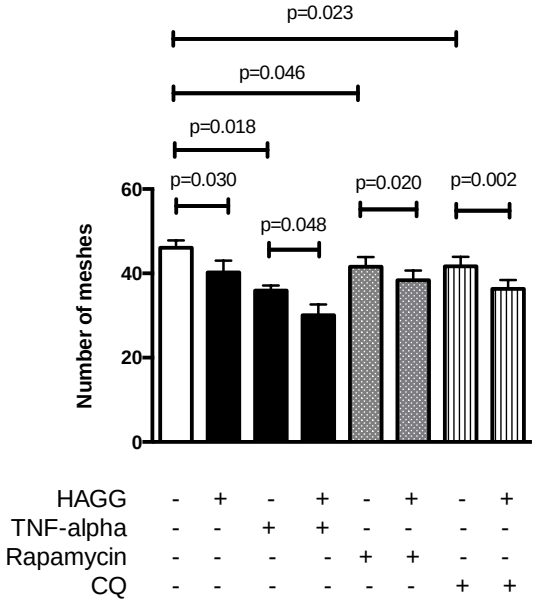
p=0.023
p=0.046
p=0.018
p=0.030
p=0.048
p=0.020
p=0.002
Number of meshes
60
40
20
0
HAGG - + - + - + - +
TNF-alpha - - + + - - - -
Rapamycin - - - - + + - -
CQ - - - - - - + +

D

20h

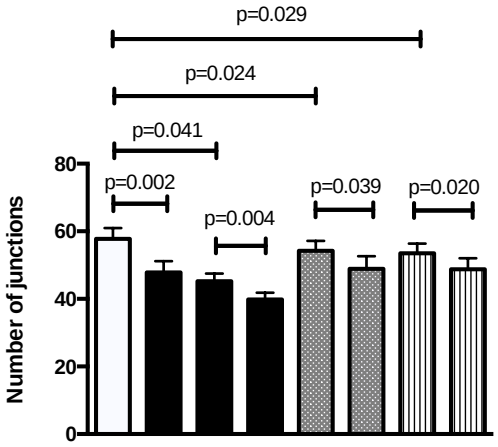

HAGG	-	+	-	+	-	+	-	+
TNF-alpha	-	-	+	+	-	-	-	-
Rapamycin	-	-	-	-	+	+	-	-
CQ	-	-	-	-	-	-	+	+

20h

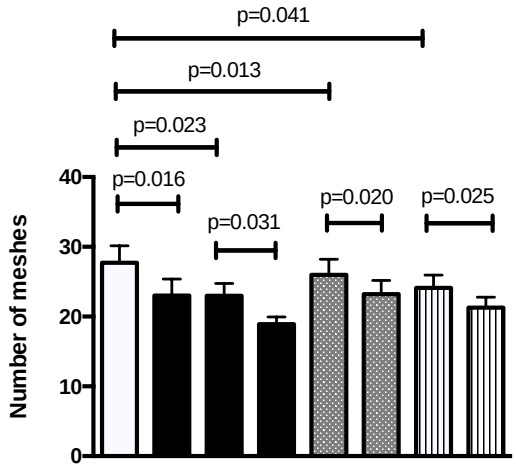

HAGG	-	+	-	+	-	+	-	+
TNF-alpha	-	-	+	+	-	-	-	-
Rapamycin	-	-	-	-	+	+	-	-
CQ	-	-	-	-	-	-	+	+

Figure 4.5 HAGG suppressed GEC tube formation on Matrigel.

GECs were seeded on growth factor-reduced Matrigel and cultured with complete medium (control), HAGG (400 μg/mL), TNF-alpha (10 ng/mL), TNF-alpha plus HAGG, rapamycin (100 ng/mL), rapamycin plus HAGG, chloroquine (CQ, 10 μM), or CQ plus HAGG, respectively. Representative images of tube formation assay were captured after incubation for 12 hours (A) and 20 hours (B), using an inverted phase contrast microscope (magnification: 40 times). Quantifications of tube formation assays at 12 hours (C) and 20 hours (D), including the number of junctions and the number of meshes, were evaluated by ImageJ software and plotted in column diagrams. Data were presented as mean ± SEM. n=3.

4.2.6 HAGG induced intracellular nitric oxide production in GECs

Nitric oxide (NO) is a membrane-permeable signaling molecule which is mainly synthesized by NOS. NO is involved in a variety of biological processes and is essential for endothelial cell functions and vascular homeostasis, including regulation of blood tone, inhibition of plate aggregation and leukocyte adhesion, and suppression of cell proliferation. However, overproduction of NO exhibits deleterious effects. NO can inhibit cytochrome C oxidase, leading to ATP depletion. NO also belongs to reactive nitrogen intermediates (RNIs). NO and its relevant productions peroxynitrite ($ONOO^-$) and N_2O_3, can nitrosylate, nitrate, and oxidize proteins, DNA, and lipids, resulting in cytotoxicity (Oates, 2010). Thus, in this section, intracellular NO production in GECs was measured using a NO-specific probe 4-amino-5-methylamino-2,7-difluorofluorescein diacetate (DAF-FM-DA).

DAF-FM-DA is cell-permeant and non-fluorescent. Once it diffuses into cells, DAF-FM-DA is de-acetylated by intracellular esterases and becomes DAF-FM, which is weak fluorescent. After interacting with intracellular NO, DAF-FM is oxidized to a triazole product and emits strong fluorescence signals. Thus, the intensity of the fluorescent probe reflects the level of intracellular produced NO. In our experiments, GECs were incubated with complete medium, or treated with HAGG (400 μg/mL), TNF-alpha (10 ng/mL), TNF-alpha plus HAGG, rapamycin (100 ng/mL), rapamycin plus HAGG, 3MA (5mM), or 3MA plus HAGG, respectively, for 24 hours. After staining with DAF-FM-DA probe for 20 minutes, images were captured by the camera attached to the fluorescence

microscope and the mean fluorescence intensity (MFI) of DAF-FM probe per cell was measured by the ImageJ software (Chapter2, Method 2.9).

As summarised in Figure 4.6, incubation with HAGG for 24 hours increased the intracellular NO production (the MFI of NO probe was 1.12 fold of control, p=0.006). TNF-alpha led to significant increase of NO production (1.68 fold of control, p=0.003). However, combination of TNF-alpha and HAGG alleviated the effect of TNF-alpha alone (TNF-alpha+HAGG *vs* TNF-alpha: 9.02 *vs* 14.01, p=0.003), while the NO production stimulated by this combined stimulation was still slightly higher than the control (1.10 fold of control, p=0.046).

We also investigated the effects of autophagy regulators. Rapamycin inhibited NO production (0.73 fold of control, p=0.019). Additional HAGG elevated intracellular NO levels (rapamycin+HAGG *vs* rapamycin: 8.18 *vs* 6.01, p=0.010). 3MA also suppressed NO production (0.85 fold of control, p=0.037). However, addition of HAGG further suppressed NO production, when compared with 3MA alone (5.77 *vs* 7.00, p=0.040).

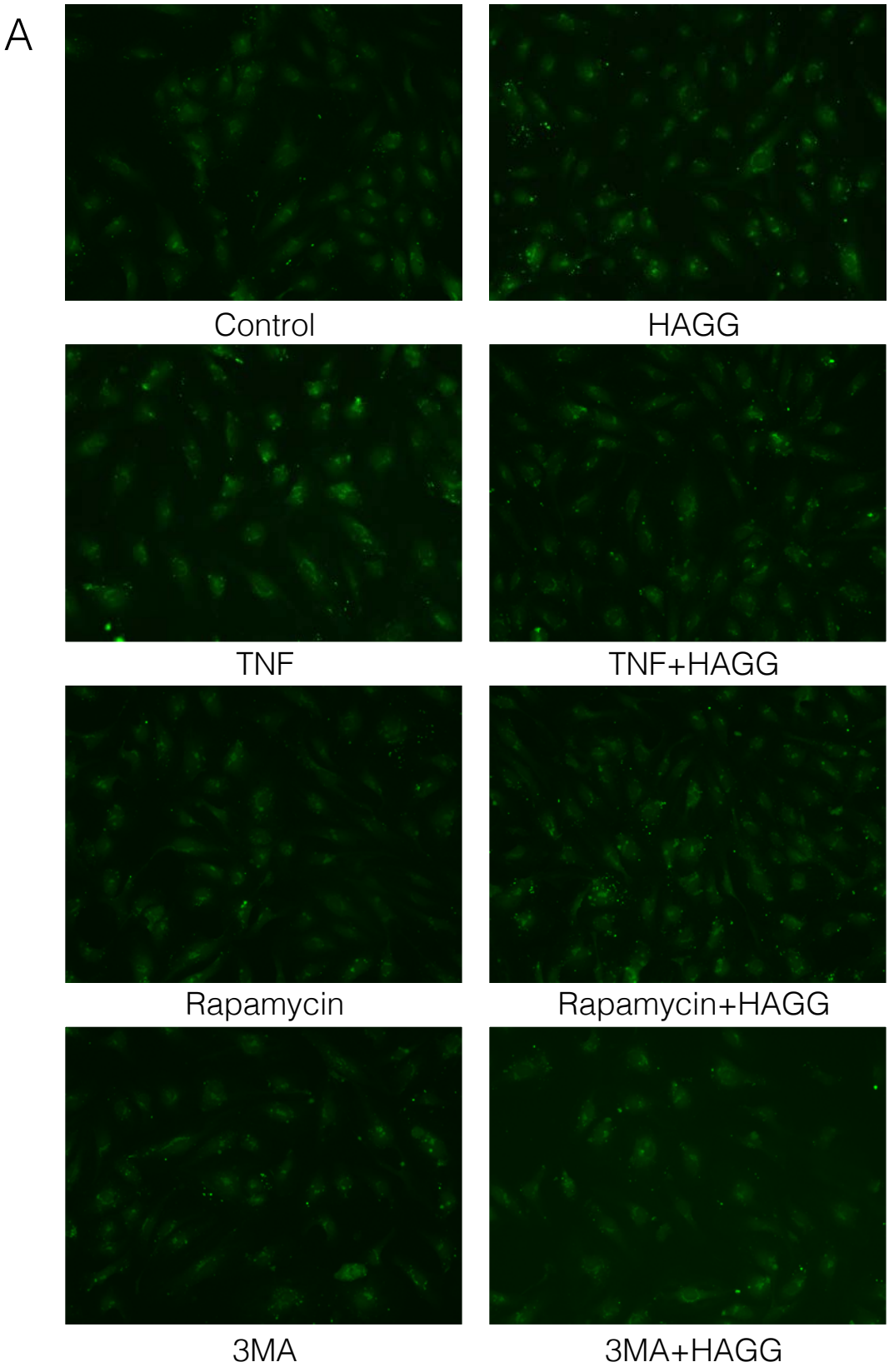
A
Control
HAGG
TNF
TNF+HAGG
Rapamycin
Rapamycin+HAGG
3MA
3MA+HAGG

B

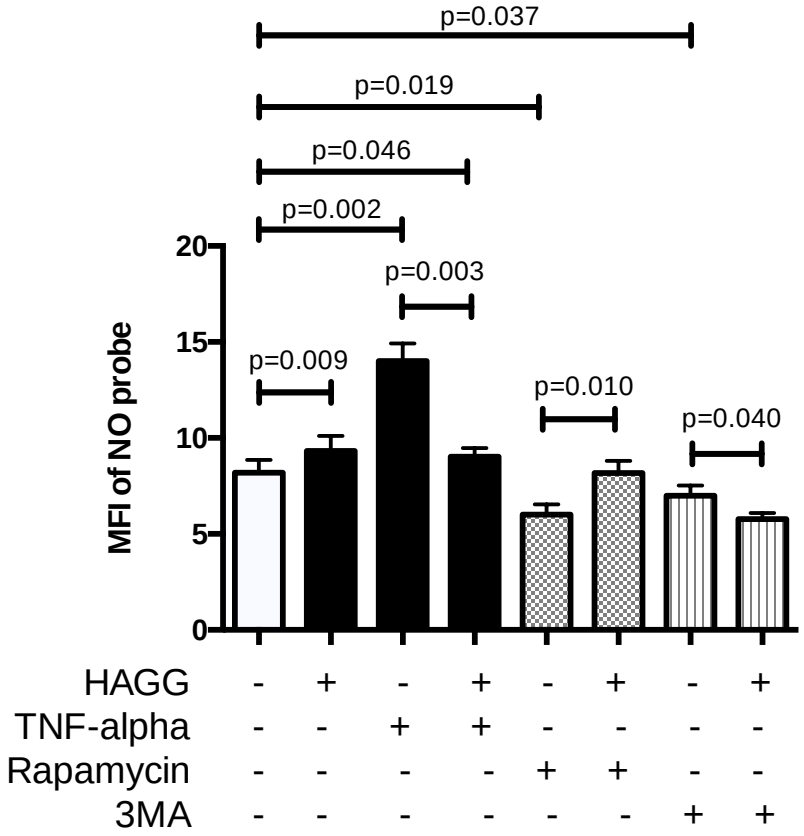

Figure 4.6 HAGG induced intracellular nitric oxide (NO) production in GECs.

GECs were cultured with complete medium (Control), HAGG (400 μg/mL), TNF-alpha (10 ng/mL), TNF-alpha plus HAGG, rapamycin (100 ng/mL), rapamycin plus HAGG, 3MA (5mM), or 3MA plus HAGG, for 24 hours. (A) Representative fluorescent images of GECs stained with DAF-FM probe, indicating intracellular NO production (magnification: 200 times). (B) Statistical analysis of the mean fluorescence intensity (MFI) of DAF-FM probe per cells. Data were presented as mean ± SEM. n=4.

Next, we measured the expressions of phosphorylated eNOS on Ser1177 (p-eNOS), which was an indicator for eNOS activation. As shown in Figure 4.7, HAGG incubation led to 1.22 times increase of p-eNOS expression (p=0.004). TNF-alpha inhibited eNOS phosphorylation (0.73 fold of control, p=0.003). Combination of HAGG and TNF-alpha further inhibited eNOS phosphorylation (HAGG+TNF-alpha *vs* TNF-alpha: 0.73 *vs* 0.52, p=0.003). As for the effects of autophagy regulators, rapamycin decreased p-eNOS expression (0.75 fold of control, p=0.017) while combination with HAGG attenuated the inhibition caused by rapamycin alone (0.91 *vs* 0.75, p=0.004). 3MA also inhibited eNOS activation (0.80 fold of control, p=0.035). 3MA plus HAGG further decreased expression of p-eNOS (0.59 *vs* 0.80, p=0.001).

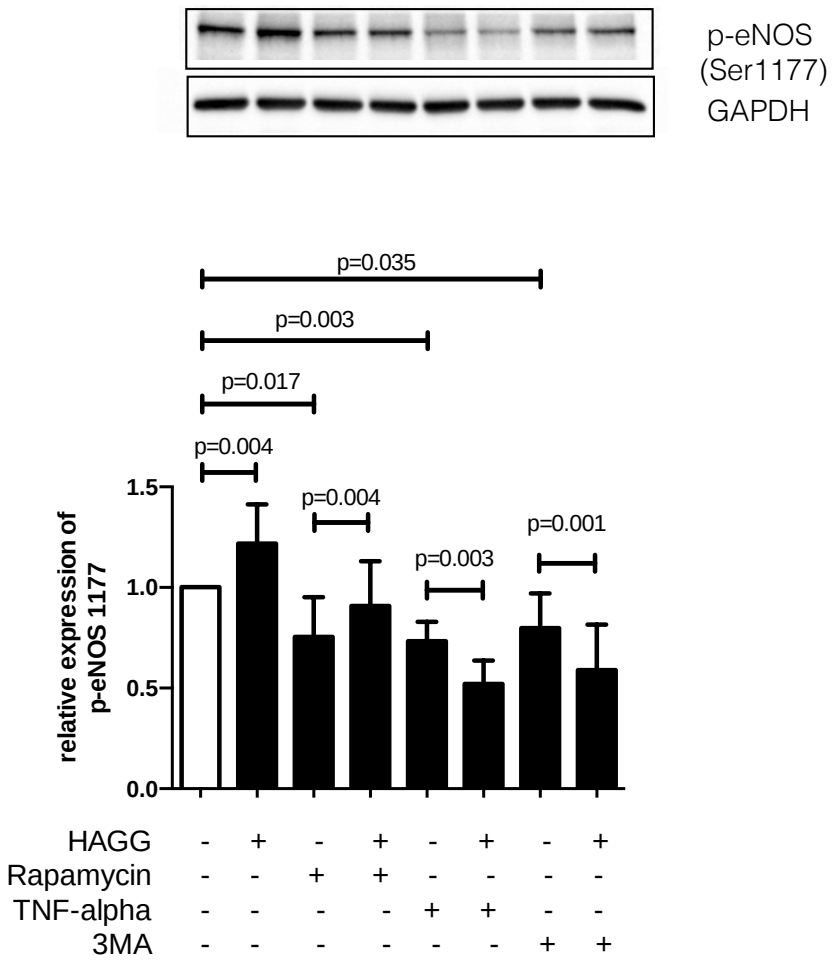

Figure 4.7 HAGG induced the expression of phosphorylated eNOS (Ser1177) in GECs.

GECs were cultured with complete medium (Control), HAGG (400 μg/mL), rapamycin (100 ng/mL), rapamycin plus HAGG, TNF-alpha (10 ng/mL), TNF-alpha plus HAGG, 3MA (5mM), or 3MA plus HAGG, for 24 hours. Expressions of phosphorylated eNOS (Ser1177) were measured by western blotting. Data were presented as mean ± SD. n=5.

4.3 Discussions

Endothelial cells are metabolically active, rapidly responsive, and versatile cells which are crucial in multitudes of physiological and pathological processes. There are various evidences indicating impaired endothelial cell functions in LN. Especially, GEC is one type of the resident parenchymal cells in the kidney and participate in the formation of glomerular filtration barrier, which is the structural and functional foundation for the kidney. GEC function evaluations are important for understanding LN pathogenesis, and clinical diagnosis. Thus, in this chapter, we incubated GECs with HAGG and inflammatory cytokines, and analysed cell morphology, viability, cell death (including necrosis, apoptosis), tube formation, and intracellular NO production, which reflected several important aspects of endothelial cell functions.

4.3.1 Cell morphology and cell function

Normal cell morphology is fundamental for cell functions. Changed cell morphology reflected changed cell functions. In this chapter, our results revealed that GECs displayed a rounder cell shape after HAGG treatment, demonstrated by increased cell area, unchanged perimeter, increased circularity and decreased aspect ratio. GECs became larger and elongated after TNF-alpha stimulation. Combination of TNF-alpha and HAGG resulted in a rounder shape than GECs treated with TNF-alpha alone. There are published papers investigating the relationships among cell morphology, biomechanics, cytoskeletal dynamics, and other cell functions. Stroka and colleagues observed that HUVECs became larger and elongated after TNF-alpha treatment for 8 hours, supported

by the increased cell area and aspect ratio, which was consistent with our results. Meanwhile, TNF-alpha-treated extended endothelial cells displayed increased contraction forces (measured by traction-force microscopy), and reduced migration speed, corresponding to the increased aspect ratio. Endothelial cells became softer after TNF-alpha treatment (Stroka et al., 2012). Szczygiel et al also stimulated human dermal microvascular endothelial cells with TNF-alpha for 1-24 hours. Changed cell shapes from spherical to longitudinal were observed. Meanwhile, longer stimulation with TNF-alpha (more than 6 hours) resulted in progressive decrease in cell stiffness, F-actin depolymerization, and increased NO production (Szczygiel et al., 2012). Roca-Cusachs and colleagues reported that cell elongation decreased cell stiffness (measured by atomic force microscopy) (Roca-Cusachs et al., 2008). These results remind us that, the rounder cells caused by HAGG incubation in our experiments may indicate increased stiffness. Cell attachment, migration, even NO production properties, may be affected corresponding to the changed morphology and cytoskeleton arrangement.

4.3.2 Cell viability and cell death

Our results revealed that, HAGG, inflammatory cytokines (TNF-alpha), and autophagy regulators (rapamycin, 3MA), all of them suppressed cell viabilities, but they may go through different mechanisms. Normally, decreased cell viabilities mainly result from two reasons: cell death (including necrosis and apoptosis) and cell growth inhibition. When combining the results presented in Figure 4.2-4.4, we inferred that cell apoptosis may mainly contribute to the slightly decreased cell viability caused by HAGG (4%

decrease of cell viability compared with the control cells). TNF-alpha predominantly induced GEC apoptosis, not inducing necrosis. On the other hand, 3MA was cytotoxic and induced significant necrosis and apoptosis, accounting for the 58% decrease of viabilities in GECs, in comparison with control cells. Rapamycin also induced mild necrosis and apoptosis. However, taking account of the great decrease of cell viability (0.53 fold of control) caused by rapamycin, its effects on cell growth inhibition should also be considered. There were evidences showing that rapamycin impaired endothelial proliferation. Rapamycin increased the percentage of endothelial cells in G0/G1 phase and decreased the percentage of cells in S and G2/M phases, indicating suppressed cell proliferation (Parry et al., 2005). Rapamycin increased the expression of a cyclin-dependent kinase inhibitor p27 (Kip) and inhibited endothelial cell proliferation and migration (Hayashi et al., 2009; Moss et al., 2010). Rapamycin can also upregulate the expression of MicroRNA-21 (miR-21) in endothelial cells (Jin et al., 2013). Overexpression of miR-21 reduced the expression of RhoB, and inhibited endothelial cell proliferation, migration and the tube formation ability (Sabatel et al., 2011).

4.3.3 Tube formation assay or angiogenesis

Angiogenesis is commonly defined as a process of generating new blood vessels from the pre-existing vasculature. Angiogenesis contains multiple steps, including endothelial cell degradation of the local basement membrane, cell migration toward stimulus (sprouting), cell proliferation, and cell reorganization for tubular structure and lumen formation

(Potente et al., 2011). Tube formation assay simulates most of these steps in angiogenesis and thus is widely used to assess endothelial cell angiogenesis (Arnaoutova et al., 2009).

Our results revealed that both HAGG and TNF-alpha suppressed GEC tube formation on Matrgel. The combination of HAGG and TNF-alpha further inhibited GEC tube formation. There were evidences supporting the inhibitory effects of TNF-alpha on endothelial cell tube formation. Hsu et al reported that TNF-alpha inhibited HUVEC migration and capillary tube formation. p38 MAPK (mitogen-activated protein kinase)-MNK1 (MAPK-activated protein kinase 1) axis contributed to these inhibitory effects (Hsu et al., 2016). Du et al also reported that TNF-alpha suppressed tube formation and induced cell apoptosis of endothelial progenitor cells (EPCs), which were endothelial precursors and crucial for angiogenesis and neovascularization (Siddique et al., 2010; Du et al., 2014; Laurenzana et al., 2015). However, the effects of TNF-alpha on angiogenesis are controversial. There are also reports indicating that TNF-alpha promoted angiogenesis (Vanderslice et al., 1998; Zhu et al., 2007; Yang et al., 2014).

Moreover, Sainson and colleagues reported that continuous stimulation of TNF-alpha inhibited angiogenesis, while a pulse stimulation of TNF-alpha followed by normal medium culture promoted angiogenesis (Sainson et al., 2008). Their results implicated that not only the type of cytokines, but also the duration of stimulation, affects angiogenesis. For acute inflammation *in vivo,* TNF-alpha is cleared rapidly, which resembles the pulse stimulation. Whereas in chronic inflammatory diseases and SLE, TNF-alpha is persistent in tissues and may cause suppressed angiogenesis.

The mechanisms for regulating angiogenesis are complex. Numerous factors, including proangiogenic factors and anti-angiogenic factors, orchestrate together to influence angiogenesis (Bikfalvi and Bicknell, 2002). Among them, vascular endothelial growth factor (VEGF) family members are key players (Carmeliet and Collen, 2000). In mammals, there are five members in VEGF family: VEGF-A to -D, and placenta growth factor (PlGF). Members of the VEGF family can bind to three receptors (VEGFR-1 to -3). VEGF-A is thought to be one of the major inducers of angiogenesis and VEGFR-2 (also known as KDR or FLK1) is the main receptor for VEGF-A to conduct the angiogenesis activities. The Notch receptors and their ligands are also crucial for sprouting in angiogenesis. Angiopoietins (Angs) and their Tie2 receptor are important for regulating endothelial integrity and homeostasis, showing a linkage between angiogenesis and inflammation (Fiedler and Augustin, 2006). Ang-1 and Ang-2 bind to the same site of Tie2 receptor with similar affinity and show antagonistic effects. Balance between Ang-1 and Ang-2 determines the status of vasculature.

Some clinical observations may implicate suppressed angiogenesis in LN. Messenger RNA expression of VEGF in the kidney biopsy samples from proliferative LN patients (Class III or IV) was lower than that from control samples. Reduced immunohistochemistry staining of VEGF was also observed in glomeruli from LN patients (Avihingsanon et al., 2009). Cross-species transcriptional network analysis revealed that decreased VEGF expression in kidney samples was commonly shared in

three murine LN models and human LN patients (Berthier et al., 2012). Transcriptional analysis of glomeruli isolated by laser-capture microscopy revealed that gene expression of VEGF was decreased in renal biopsies from LN patients, in comparison with control samples (Peterson et al., 2004). Wongpiyabovorn et al also reported that a SNP (+405 GG) at the exon 1 in *VEGF* gene was associated with LN patients with low VEGF mRNA expression and with LN with end-stage renal disease (Wongpiyabovorn et al., 2011). Besides, serum concentration of the anti-angiogenic Ang-2 was increased in LN patients compared with control subjects, and positively correlated with SLEDAI scores (Kumpers et al., 2009; El-Banawy et al., 2012; Bakr et al., 2014).

Our results showed that HAGG suppressed GEC tube formation, which may provide another explanation for the abnormal angiogenesis in LN. There are also evidences supporting the inhibitory effects of autoantibodies or ICs on endothelial angiogenesis. An endothelial-specific adhesion molecule, vascular endothelial cadherin (VE-cadherin), is important for endothelial junctions, integrity and angiogenesis. Autoantibodies to VE-cadherin (AAVEs) were detected in the circulation and the level of AAVEs was significantly higher in lupus patients and other patients with autoimmune diseases than that in healthy controls (Bouillet et al., 2013). Binding anti-VE-cadherin monoclonal antibodies (BV13 or BV14) to their target VE-cadherin inhibited endothelial tube formation in a gel of collagen (Corada et al., 2002). A high positive rate of angiotensin II type 1 receptor-activating autoantibody (AT1-AA) was detected in LN patients compared with healthy control (Xiong et al., 2013). AT1-AA led to increased synthesis and

secretion of soluble Fms-like tyrosine kinase-1 (sFlt-1, or sVEGFR-1), which was a circulating anti-angiogenic protein, and resulted in inhibition of capillary tube formation (Zhou et al., 2008a). However, considering that more than 180 autoantibodies and the subsequent ICs have been detected in lupus patients (Yaniv et al., 2015), further investigations are needed to decipher whether there is a universal effect of these diverse autoantibodies or ICs on endothelial angiogenesis, and whether the effects on angiogenesis are through universal or distinct mechanisms.

4.3.4 Intracellular NO production

NO is a soluble and versatile molecule. Physical concentration of NO is essential for remaining endothelial functions. However, over production of NO exhibits cytotoxic effects. There were evidences indicating that NO production was increased in LN and that this increased NO production might be damaging. Weinberg and colleagues reported elevated NO production in LN mice, by measuring urinary excretion of nitrite/nitrate (in mice receiving nitrate-free diet). Disease manifestations were alleviated by NOS inhibitors (Weinberg et al., 1994). Enhanced NO production was also reported in lupus patients (using serum nitrite and citrulline as surrogate markers), correlated with disease activities (Wanchu et al., 1998). Belmont and colleagues reported similar results that NO production was increased in lupus patients. Besides, they observed increased endothelial iNOS expression in lupus patients (Belmont et al., 1997). Our results revealed that HAGG increased NO production in GECs, which echoed the data from the above-mentioned studies.

In endothelial cells, NO is mainly synthesized by eNOS, which activity is highly regulated through different pathways and rapidly responds to a variety of stimuli. Among these regulatory mechanisms, the Akt-eNOS pathway has been reported to modulate NO production (Hemmings and Restuccia, 2012). Active Akt directly phosphorylates eNOS and augments enzyme activity to synthesize NO. Dimmeler et al demonstrated that eNOS and active Akt were co-immunoprecipitated from endothelial cells. Constitutively active Akt mutation Thr308Asp led to phosphorylation of eNOS, whereas inactive Akt mutation Thr308Ala did not affect phosphorylation of eNOS. Ser1177Asp mutation in eNOS mimic the continuous phosphorylation of eNOS by Akt and displayed significantly increased enzyme activity. In contrast, replacement of Ser1177 by alanine in eNOS prevented the phosphorylation on this site and inhibited the activation of eNOS activity (Dimmeler et al., 1999). The phosphorylation or aspartate replacement on Ser1177 introduced a negative charge on this site, accelerated the electron flux in the reductase domain of eNOS, and finally increased the enzyme activity (McCabe et al., 2000).

In our previous experiments, we have demonstrated that HAGG induced phosphorylation of Akt on Thr308 (Chapter 3, Figure 3.6, C). In this section, we also observed increased expression of p-eNOS (Ser1177) and NO production in HAGG-treated GECs. Similarly, the autophagy activator rapamycin suppressed the expressions of p-Akt (Thr308) and p-eNOS (Ser1177), and reduced NO production in GECs. Co-stimulation with rapamycin and HAGG attenuated the suppression effects, leading to increased expressions of p-Akt,

p-eNOS, and NO production in GECs, when compared with the effects of rapamycin alone.

3MA also suppressed eNOS phosphorylation and NO productions in GECs in our experiments. Actually, 3MA is a non-specific inhibitor for PI3K and has dual roles in the autophagy process. 3MA has persistent suppressive effects on Class I PI3K and transient suppressive effects on Class III PI3K (Wu et al., 2010). In mammalian cells, Class I PI3K can activate the downstream kinase Akt and is an inhibitor for autophagy. Whereas Class III PI3K, a homolog of yeast Vps34, is a key protein for the early nucleation step in autophagosome formation, and thus an activator for autophagy (Yang et al., 2013b). It has also been reported that 3MA inhibited the expression of p-Akt (Thr308) (Farkas et al., 2011; Wu et al., 2013b). This decreased p-Akt expression caused by 3MA may explain the decreased p-eNOS expression and NO production in 3MA-treated GECs in our results.

Intriguingly, we observed that TNF-alpha increased the expression of p-Akt. However, the phosphorylation of eNOS was suppressed and NO production was eventually increased in TNF-alpha-treated GECs in our experiments. TNF-alpha has been reported to stimulate the phosphorylation and activation of Akt in endothelial cells (Murao et al., 2000; Zhou et al., 2008b). As to the effects of TNF-alpha on eNOS activation and expression in endothelial cells, the involved mechanisms are complicated and we need to consider comprehensively. Clementi and his group reported that TNF-alpha increased p-eNOS (Ser1177) expression through sequential activation of neutral sphingomyelinase,

sphingosine-kinase-1, and Sphingosine-1-phosphate receptors in human endothelial cells (Barsacchi et al., 2003; De Palma et al., 2006). Kawanaka et al also reported that TNF-alpha stimulated p-eNOS expression in human microvascular endothelial cells (Kawanaka et al., 2002). In contrast, other evidences indicated that TNF-alpha reduced the expressions of p-eNOS in endothelial cells, which is similar as our results (Arita et al., 2013; Siefers, 2014). Dschietzig et al also reported that TNF-alpha increased the phosphorylation of eNOS on Thr495, which was a crucial marker for inactive eNOS. Their results indicated that the eNOS activity was inhibited by TNF-alpha (Dschietzig et al., 2012).

In addition, the effects of TNF-alpha on the total eNOS expressions in endothelial cells have also been investigated. Evidences supported that TNF-alpha suppressed the mRNA and protein expressions of total eNOS in endothelial cells (Barilli et al., 2008; Altorjay et al., 2011; Helbing et al., 2011; Dschietzig et al., 2012). TNF-alpha inhibited eNOS gene promoter activity in endothelial cells and thus reduced eNOS gene expression (Anderson et al., 2004). TNF-alpha also suppressed eNOS expression at the posttranscriptional level. TNF-alpha increased the expression of eEF1A1 (translation elongation factor 1-alpha 1), which interacted with eNOS 3'-UTR (untranslated region) and decreased eNOS mRNA stability (Yan et al., 2008). Taken together, these evidences remind us that TNF-alpha influenced eNOS expression and activity through complicated mechanisms.

When investigating the ultimate NO productions in endothelial cells, beside the roles of eNOS, the contributions of iNOS should also be considered. There were reports revealing

that iNOS expression and NO production were greatly upregulated by TNF-alpha in endothelial cells (Xia et al., 2006; Arai et al., 2008). This increased iNOS expression by TNF-alpha partly explained why we observed increased NO production in GECs while the p-eNOS expression was decreased.

In conclusion, in this chapter, we incubated GECs with HAGG and examined their effects on endothelial cell functions. Our results indicated that HAGG influenced different aspect of the GEC functions. HAGG changed cell morphology, suppressed cell viability, upregulated the expression of active caspase-3, inhibited angiogenesis, increased phosphorylation of eNOS and increased NO production in GECs.

Chapter 5 General Discussions and Conclusions

Lupus nephritis is a common and severe complication of SLE with poor prognosis. However, the pathogenesis and mechanisms for the tissue damage are not thoroughly understood. Both intrinsic and extrinsic renal factors contribute to the kidney impairments. Among these intricate factors, LN is initiated by IC deposition and regarded as an IC-mediated glomerulonephritis. Besides, chronic inflammation, activation of renal parenchymal cells, vascular dysfunctions, tissue hypoxia, abnormal metabolism, and aberrant tissue repair, all participate in the renal damage in LN (Davidson, 2016). Especially, there are accumulating evidences revealing vascular lesions and GEC injuries in LN. Thus, in our experiments, we investigated the effects of ICs on GECs, using HAGG as a surrogate for ICs.

5.1 Human glomerular endothelial cells

Endothelial cells are highly heterogeneous in different organs and species and temporally dynamic (Aird, 2005; Aird, 2007). GECs have specialized characteristics different from other endothelial cells. Particularly, GECs have large fenestrated area on the cell membranes, and thick endothelial cell surface layers. GECs are injured in LN and their impairments are involved in the LN pathogenesis. Therefore, it is important to conduct experiments on these unique human GECs.

However, compared with other kinds of endothelial cells, such as HUVECs, and compared with other kinds of renal parenchymal cells, such as podocytes and mesangial

cells, limited studies were performed on human GECs. We searched the database Web of Science with relevant keywords and found out that, in contrast to the total publications on “endothelial cells”, the publications mentioning “glomerular endothelial cells” were scanty accounting to only 1/66 of the former (Figure 5.1, A). Within the kidney, “mesangial cells” received much more concerns, although the relevant publications have declined in recent years (Figure 5.1, B, green line). Researches on “podocytes” developed more rapidly than those on “glomerular endothelial cells” (Figure 5.1, B, red line). Especially, for publications related to LN, similar results were observed. Very few publications were about GECs (Figure 5.1, C).

Historically, it was difficult to culture GECs *in vitro* and hindered the researches on GECs. In 1984, Striker et al first isolated and cultured human glomerular endothelial cells *in vitro* (Striker et al., 1984). In 1989, Ballermann et al established the *in vitro* culture method for bovine glomerular capillary endothelial cells (Ballermann, 1989). Around 1990, there was an obvious increase in the publications related to “glomerular endothelial cells” (Figure 5.1, B). In 1994, Nitta et al established an immortalized bovine glomerular endothelial cell line (Nitta et al., 1994). Around 2003, human glomerular endothelial cells were commercially available. In 2006, Satchell and colleagues generated a conditionally immortalized human GECs, which were then widely accepted (Satchell et al., 2006). These progressed biological technologies facilitate researches on human GECs. In our experiments, we purchased human GECs from Cell System Corporation.

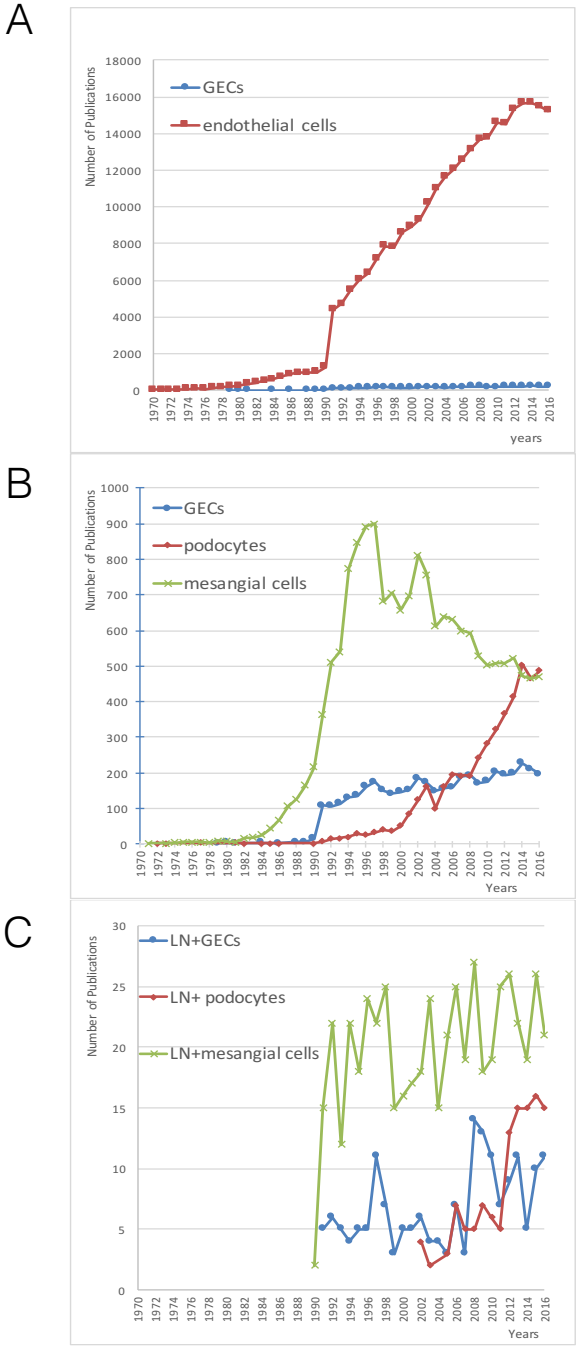

Figure 5.1 Limited researches were conducted on glomerular endothelial cells.

Yearly publication data were collected from Web of Science, using different keywords, from 1970 to 2016. (A) Publications with keywords “endothelial cells” and “glomerular endothelial cells”. (B) Search results with keywords about “renal parenchymal cells”, including glomerular endothelial cells, podocytes, and mesangial cells. (C) Search results with keywords “lupus nephritis” combined with “renal parenchymal cells”. Abbreviations: GECs: glomerular endothelial cells, LN: lupus nephritis.

5.2 Immune complexes preparation

In our experiments, we prepared HAGG and used it as a surrogate of ICs, to stimulate the human GECs, mimicking a simplified condition of the ICs deposition in LN. Obtaining ICs is important for researches on LN pathogenesis, especially for *in vitro* studies. However, some problems cannot be ignored for the IC preparation. So far, more than 180 different autoantibodies have been found in lupus patients (Yaniv et al., 2015). They combine with their target autoantigens and form various ICs. Although some of these autoantibodies or ICs are believed to be more related to lupus pathogenesis (for example, dsDNA/anti-dsDNA antibody ICs are associated with a high incidence of renal impairment in lupus), none of them has been proved to be the specific and decisive pathogenic autoantibody/ICs in lupus yet. And it is still not clear what are the effective parts within ICs and through which pathways and mechanism ICs lead to damages on cells and tissues. Thus, people need to decide whether to use blended ICs or a single kind of IC, and further decide to use which kinds of ICs, for *in vitro* stimulation. This was also the question that we faced when designing this project. Currently, there are at least four methods to prepare ICs.

5.2.1 Isolating total ICs from patient serum

Immune complexes can be isolated from serum by affinity column chromatography. A bacterial virulence factor Protein G (from Streptococcal origin), and similar proteins, have high affinity towards human gamma globulin/IgGs, and can be immobilized to Sepharose IC purification (Chenais et al., 1977; Means et al., 2005; Lande et al., 2011;

Wen et al., 2013). However, isolated ICs may be contaminated with trace amount of the Protein G.

Immune complexes can also be isolated from patient serum by polyethylene glycol (PEG)-6000 precipitation (Riha et al., 1979; Lopes-Virella et al., 1999; Elshafie et al., 2007; Lood et al., 2012). Cold low concentration of PEG-6000 borate solution can precipitate large proteins, including ICs. However, some non-gamma globulin proteins, including fibronectin, albumin, transferrin, alpha-2 macroglobulin and complements are also precipitated simultaneously (Smith et al., 1987; Robinson et al., 1989). Generally, ICs isolated from serum are closer to the native physiological situations. The defect is that the compositions of the isolated ICs are more complex. The quality of isolated ICs can be fluctuated. The sources of ICs are limited. Besides, the patients may be at different stages of disease with different manifestations and under different treatments, causing too many different components in the serum in addition to ICs.

5.2.2 Isolating or synthesizing specific IC related to LN

Although LN patients have a wide spectrum of autoantibodies and ICs, one may choose specific ICs and investigate their roles on LN pathogenesis separately. The preparation methods are based on the unique characteristics of the target ICs. For instance, to prepare the DNA/anti-DNA ICs, Means et al first isolated the total ICs from patient serum, as described in 5.2.1 above. Then they incubated the total ICs with DNA-coated magnetic microbeads. The magnetically labelled anti-DNA ICs were separated from other ICs in a magnetic field (Means et al., 2005). To prepare type II collagen (CII)/anti-CII

autoantibody IC, Manivel et al coated the purchased native human CII in ELISA plates. After blocking the plate with human albumin, they added and incubated patient serum to the coated plate wells, and obtained the solid phase IC (Manivel et al., 2015). To prepare the nucleosome/anti-nucleosome antibody IC, Boule et al first isolated nuclei from bovine thymus. Then, they physically disrupted the isolated nuclei and digested the nuclear materials with micrococcal nuclease. The digested nucleosome fragments were subsequently mixed with the nucleosome-specific monoclonal antibody PL2-3 to synthesize the nucleosome/anti-nucleosome IC (Boule et al., 2004). Using selected ICs is a simplification of the real problem associated with the complex autoimmune diseases. One may conduct systematic investigations and obtain plenty of information about the effects of the selected ICs in LN. However, the potential interactions between different ICs may be ignored.

5.2.3 Synthesizing single IC unrelated to the disease

To further simplify the situation, scientists have also synthesized ICs which are not reported in lupus patients, such as bovine serum albumin (BSA)/anti-BSA antibody IC, ovalbumin/anti-ovalbumin antibody IC, with arbitrary ratios of the antigen over antibody (Medof et al., 1981; Barrionuevo et al., 2003; Marzocchi-Machado et al., 2005; Denny et al., 2010; Chauhan and Moore, 2011; Clatworthy et al., 2014). One underlying assumption of using this simple antigen/antibody IC model to replace ICs in diseases is that the IC structure itself, regardless of the content of the antigens, is pathogenic to diseases. These artificial ICs can be easily synthesized. The composition of the ICs is

under control and homogeneous. One potential risk of using these synthesized ICs is that antigens could introduce extra effects on the immune system, hence the effects induced by the synthesized ICs may deviate from the authentic situations in diseases.

5.2.4 Heat aggregated gamma globulin (HAGG)

Different from the method described in Section 5.2.3, physical challenges including heat, freeze-thawed cycles, pH changes, and stir or shake, can lead to aggregation of gamma globulin, forming a large size structure similar to ICs (Mahler et al., 2005; Filipe et al., 2012a). A commonly accepted protocol to prepare HAGG is that heating monomeric IgG at 62-63 °C for 20-60 minutes, and cooling the samples on ice immediately. Then the aggregated IgG may be diluted to target concentrations in PBS (Kijlstra et al., 1979; Cines et al., 1984; Ptak et al., 1998; Blom et al., 2000; Haymann et al., 2004; Maeda et al., 2010; Yuan et al., 2011; Suwanichkul and Wenderfer, 2013). HAGGs generated by this method are covalent aggregates, with forming intermolecular disulphide bonds (Filipe et al., 2012b; Telikepalli et al., 2014). The dynamic aggregation of gamma globulins under heat stress, and the characterization of IgG monomers and HAGG, were monitored and analysed by multiple techniques, including size exclusion chromatography (SEC), asymmetrical flow field flow fractionation (AF4), nanoparticle tracking analysis (NTA), dynamic light scattering (DLS). The reported average diameter of monomeric IgG was approximate 11 nm, determined by DLS method (Bermudez and Forciniti, 2004; Hawe et al., 2008). The average size of HAGG (heated at 70 °C for 8 hours) was much larger than that of monomeric IgG (Domingues, 2011). The average size of HAGG (heated at

74 °C for 15 minutes) was 175 ±76 nm, detected by NTA method (Filipe et al., 2010). The authors also heated the monomeric IgG at 50 °C for 45 minutes and recorded the aggregation into a movie by NanoSight instruments. Increased size and number of aggregates were observed (Filipe et al., 2010). Compared with other methods, HAGG is easily generated from purified human gamma globulin, which could be purchased from companies. This artificial ICs have stable structures which are similar with antigen/antibody ICs and display multitude similarities with natural ICs in biological behaviours. Hence, in our experiments, we used HAGG as a surrogate for ICs to stimulate GECs.

5.3 The relationships between autophagy and GEC dysfunctions

In our study, we have demonstrated that HAGG suppressed autophagy in GECs, through Akt-mTOR-dependent pathways (Chapter 3). We also proved that HAGG induced injuries on GEC functions, including changing cell morphology, inhibiting proliferation and viability, suppressing tube formation, and inducing NO productions (Chapter 4). However, what is the relationships between autophagy and GEC dysfunctions? Are the HAGG-induced GEC dysfunctions resulted from the suppressed autophagy?

Regarding the relationship between autophagy and NO production, our results revealed that HAGG induced NO production in GECs. The autophagy activator Rapamycin suppressed NO productions in GECs. The combination of rapamycin and HAGG

alleviated the increased effect of HAGG alone on NO generation. This suggested that suppressed autophagy led to elevated NO production.

Kinase Akt is a key molecule involved in our results. On one hand, Akt can directly phosphorylate and activate eNOS and stimulated NO production in endothelial cells. On the other hand, Akt is an important upstream regulator for mTOR activity. Fully activated Akt results in suppressed autophagy. In our results, HAGG increased phosphorylation of Akt and the downstream target eNOS in GECs, while rapamycin inhibited Akt and eNOS phosphorylation. Similarly, although 3MA is a traditional autophagy suppressor by inhibiting Class III PI3K, long-time incubation with 3MA in nutrition-sufficient medium led to non-specific inhibition of Class I PI3K, which eventually inhibited the activations of Akt and eNOS and suppressed NO production in GECs.

There were other evidences supporting our results that rapamycin reduced NO production in endothelial cells, through various mechanisms apart from altering the Akt and eNOS activities (Long et al., 2007; Barilli et al., 2008; Fruhwurth et al., 2014; Reineke et al., 2015). Besides, chloroquine can suppress autophagy by increasing endo-lysosomal pH and inhibiting degradations of autophagosomes in the lysosomes. Pestana et al reported that serum deprivation induced autophagy and suppressed NO production in HUVECs. Chloroquine suppressed autophagy and increased NO production in the starved ECs (Pestana et al., 2015). Ghigo et al reported that chloroquine increased NO production in endothelial cells by activating NOS via impairment of the iron metabolism and did not

upregulate the NOS expression (Ghigo et al., 1998). McCarthy et al reported that chloroquine lowered blood pressure and increased artery NO production in spontaneously hypertensive rats, without affecting phosphorylation eNOS activation. They also demonstrated that chloroquine increased NO bioavailability via decreasing the ROS generation (McCarthy et al., 2016). These evidences of rapamycin and chloroquine indicated that autophagy regulators interfered different steps in autophagy and may interfere with NO production through different mechanisms.

Conflicting results were also reported in the literature, suggesting that impaired autophagy was associated with suppressed eNOS activation and NO production. LaRocca and colleagues reported that autophagy was impaired in aged vasculatures. Aged vasculatures had reduced eNOS expression and NO bioavailability. In cultured endothelial cells, activating autophagy by trehalose enhanced eNOS expression and NO production, while suppressing autophagy by Atg12-specific siRNA reduced NO production and suppressed the effects of trehalose (LaRocca et al., 2012). Fetterman et al reported that in endothelial cells isolated from diabetic patients, autophagy was impaired, and insulin-induced eNOS phosphorylation was suppressed. Treatment with autophagy activator, spermidine, in diabetic endothelial cells restored the eNOS activation and NO production (Fetterman et al., 2016). There were also reports stating that laminar shear stress induced autophagy in endothelial cell and increased eNOS phosphorylation, expression, and NO production. Pretreatment with autophagy activator rapamycin enhanced the eNOS expression in endothelial cells exposed to laminar shear stress.

Suppressing autophagy by Atg3-specific siRNA prevented increasing NO production in endothelia cells under shear stress (Bharath et al., 2014; Guo et al., 2014). For these studies, the authors described a reversed direction of the correlation between autophagy and NO productions from our results. We need to further investigate the detailed pathways through which the autophagy regulators (such as trehalose, spermidine, and Atg-specific siRNAs) interfere.

In addition, excess NO inhibited autophagy. Sarkar et al reported that NO-releasing chemicals (NO donors) inhibited autophagosome synthesis and autophagy flux in rat cortical neurons and Hela cells. NO donors S-nitrosylated JNK1 and inhibited JNK1 phosphorylation. This JNK1 inhibition led to reduced Bcl-2 phosphorylation and increased Bcl-2-Beclin1 association. Then the formation of Beclin1-Vps34 complex was disrupted and the autophagy was suppressed. Additionally, NO suppressed autophagy by activating mTORC1. The authors further demonstrated that apart from NO donors, overexpression of NOS suppressed autophagy (Sarkar et al., 2011). Shen and colleagues also reported that NO inhibited autophagy in meniscal cells, through the JNK pathway (Shen et al., 2014). Our results showed that HAGG increased NO production and suppressed autophagy in GECs, which could be supported by these evidences.

Till now, we can cautiously describe that HAGG incubation activated Akt, which subsequently activated mTOR-dependent pathway and suppressed autophagy. Meanwhile, activated Akt further elevated phosphorylation of eNOS, contributing to the

increased NO production in GECs. The effects of HAGG on GEC functions were summarized in Figure 5.2.

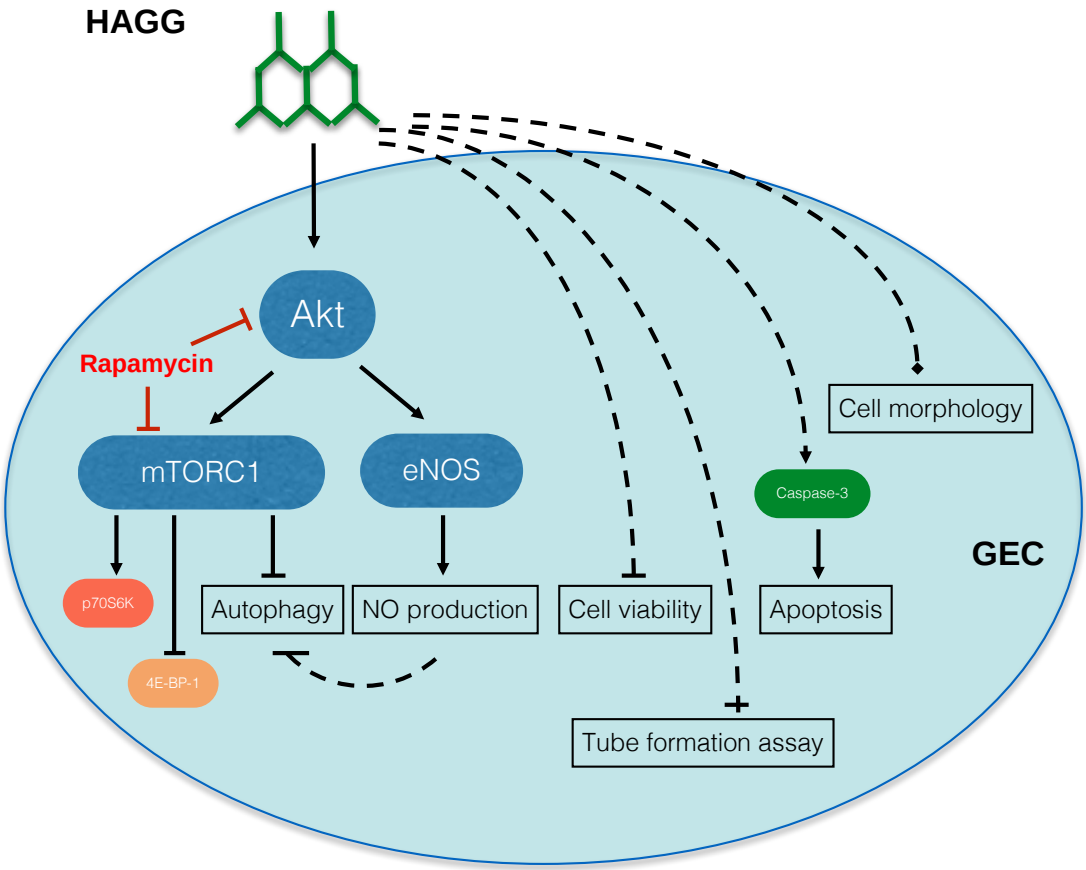

Figure 5.2 Summary of the effects of HAGG on GEC functions.

HAGG activated Akt, which subsequently activated mTOR and eventually suppressed autophagy. Meanwhile, activated Akt stimulated eNOS phosphorylation, contributing to the increased NO production in GECs. Besides, HAGG stimulation changed GEC morphology, upregulated active caspase-3 expression, suppressed cell viability and suppressed tube formation ability. Dotted lines indicate that the involved mechanisms are not clear. Abbreviations: HAGG: heat-aggregated gamma globulin; NO: nitric oxide; GEC: glomerular endothelial cell.

5.4 Limitations and future works

We have demonstrated that HAGG suppressed autophagy in GECs in an Akt-mTOR-dependent pathway. In addition, HAGG alone could damage GEC functions. In the future, we will continue to explore the effects of HAGG/ICs on GEC functions, and focus on the involved mechanisms of injures initiated by HAGG/ICs.

1. As we have detected that HAGG changed GEC morphology, we may further investigate the morphology-related factors, especially focus on cell-cell junctions, cell-ECM connections, and cytoskeleton arrangement. Besides, we should further examine the effects of changed cell morphology on vascular permeability and renal impairment.

2. In the current study, both rapamycin and 3MA are not specific regulators for autophagy. They have many side effects on cell metabolism. To improve, we may use more specific techniques to interfere the autophagy process, such as using siRNA. For LN, Atg5/7 show special important effects.

3. We have used artificial HAGG to simulate the ICs, and investigated their effects on cultured GECs *in vitro*. Next, we may isolate ICs from serum of LN patients to stimulate GECs and examine their effects. Besides, we may use the renal biopsy specimens collected from the LN patients, to examine the autophagy process and injuries in real tissues. Double immunostaining is a powerful tool to monitor the molecules within endothelia cells, as we can label the endothelial cells with cell-specific markers such as CD105 or CD31 with one fluorescent signal, and label the autophagy-related target such as phosphorylated mTOR or Akt with another fluorescent signal.

4. Podocytes and GECs are the two important cellular components for GFB and important for GFB integrity and renal functions. They are tightly connected based on spatial locations and functional interactions. Endothelial cell and podocyte autophagy synergistically protect from diabetes-induced glomerulosclerosis. Deletion of Atg5 specifically in podocytes or in GECs resulted in accelerated diabetic nephropathy (Lenoir et al., 2015). Our previous works also demonstrated that autophagy played a protective role in PAN-induced podocyte injuries (Kang et al., 2014). In this project, we proved that HAGG suppressed autophagy and impaired cell functions in GECs. This project may be expanded to investigate the interactions between podocytes and GECs under HAGG/ICs stimulation in co-culture environment and the role of autophagy in barrier characteristics.

5.5 Conclusions

Glomerular endothelial cell is one of the structural foundations of renal functions. Immune complex is involved in the pathogenesis of LN and can deposit on GECs. To better understand the mechanisms of renal damages in LN, we cultured the human GECs *in vitro* and stimulated them with ICs, using HAGG as a surrogate, to simulate and simplify the micro-pathological situation in LN. Our results revealed that HAGG suppressed autophagy in human GECs, through Akt-mTOR-dependent pathway. Meanwhile, HAGG influenced different aspect of the GEC functions. HAGG changed cell morphology, suppressed cell viability, induced apoptosis, inhibited angiogenesis, increased eNOS phosphorylation and eventually increased NO production in GECs. In

the presence of inflammatory cytokine, TNF-alpha, HAGG further damaged GEC functions.

Our study indicated that, HAGG deposit alone, without any other inflammatory cytokines, complements, nor other residential or infiltrating immune cells, can already lead to damages on GEC functions. Although some damage may be mild, their effects on cell functions cannot be ignored when considering chronic diseases such as LN. The effects of ICs on GEC functions provide a new view for disease mechanisms. Maintaining GEC functions may be a new target and method for LN therapy.

Appendix

Source of Reagents

Antibodies	Cat. No.	Suppliers
anti-4E-BP1 rabbit mAb	#9644	Cell Signaling Technology
anti-CD31/PECAM-1 mouse mAb	#BBA7	R&D Systems
anti-eNOS rabbit mAb	#9586	Cell Signaling Technology
anti-GAPDH rabbit mAb	#2118	Cell Signaling Technology
anti-ICAM-1 antibody	#4915	Cell Signaling Technology
anti-iNOS rabbit mAb	#13120	Cell Signaling Technology
anti-LC3B antibody	#2775	Cell Signaling Technology
anti-mouse IgG (Alexa Fluor 647 Conjugate) antibody	#4410	Cell Signaling Technology
anti-mTOR antibody	#2972	Cell Signaling Technology
anti-NOS (pan) antibody	#2977	Cell Signaling Technology
anti-p70 s6 kinase rabbit mAb	#2708	Cell Signaling Technology
anti-phopho-mTOR (Ser2448) rabbit mAb	#5536	Cell Signaling Technology
anti-phospho-4E-BP1 (Thr37/46) rabbit mAb	#2855	Cell Signaling Technology
anti-phospho-Akt (Thr308) rabbit mAb	#13038	Cell Signaling Technology
anti-phospho-eNOS (Ser1177) rabbit mAb	#9570	Cell Signaling Technology
anti-phospho-eNOS (Thr495) antibody	#9574	Cell Signaling Technology
anti-phospho-p70 s6 kinase (Thr389) rabbit mAb	#9234	Cell Signaling Technology

Antibodies	Cat. No.	Suppliers
anti-phospho-ULK1 (Ser757) antibody	#6888	Cell Signaling Technology
anti-rabbit IgG (Alexa Fluor 488 Conjugate) antibody	#4412	Cell Signaling Technology
anti-rabbit IgG, HRP-linked antibody	#7074	Cell Signaling Technology
anti-SQSTM1/p62 antibody	#5114	Cell Signaling Technology
anti-ULK1 antibody	#4773	Cell Signaling Technology
anti-VCAM-1 rabbit mAb	#13662	Cell Signaling Technology
anti-Von Willebrand Factor mouse mAb	#M0616	DakoCytomation

Reagents	Cat. No.	Suppliers
3-Methyladenine	#M9281	Sigma-Aldrich
Calbiochem Phosphotase Inihibitor Cocktail	#524625	Merck Millipore
Cell Counting Kit (CCK-8)	#CK-04	Dojindo
Chloroquine diphosphate salt	#6628	Sigma-Aldrich
Complete Classic Medium Kit with Serum & CultureBoost	#4Z0-500	Cell Systems Corporation
cOmplete Protease Inhibitor Cocktail Tablets	#05892791001	Roche Applied Science
CytoTox 96 Non-Radioactive Cytotoxicity Assay	#G1780	Promega Corporation
DAF-FM diacetate	#D-23844	Thermo Fisher Scientific
Dead Cell Apoptosis Kit with YO-PRO-1 and PI	#V13243	Thermo Fisher Scientific
Dimethyl Sulphoxide (DMSO, sterile-filtered)	#D2650	Sigma-Aldrich
Dulbecco's Phosphate Buffered Saline	#21600010	Thermo Fisher Scientific
Glycerol	#15523	Sigma-Aldrich
Human Glomerular Microvascular Endothelial Cells Vial	#ACBRI 128	Cell Systems Corporation
HyClone Bovine Serum Albumin (BSA)	#SH30574	GE Healthcare Life Sciences
IgG from human serum	#I4506	Sigma-Aldrich
Matrigel (Growth Factor Reduced)	#356231	Corning Incorporated
Matrigel (Standard)	#356237	Corning Incorporated
PE Active Caspase-3 Apoptosis Kit	#550914	BD Biosciences

Reagents	Cat. No.	Suppliers
Pierce BCA Protein Assay Kit	#23225	Thermo Fisher Scientific
Polyethylene glycol (PEG) 6000	#81260	Sigma-Aldrich
Prolong Gold Antifade Mountant with DAPI	#P36931	Thermo Fisher Scientific
Rapamycin	#R8781	Sigma-Aldrich
Sodium dodecyl sulfate (SDS)	#161-0302	Bio-Rad
TNF-alpha	#210-TA-005	R&D Systems
Tris	#161-0719	Bio-Rad
Triton X-100	#T9284	Sigma-Aldrich
Tween-20	#T/4206	Thermo Fisher Scientific
Western Lightning	#104001EA	Perkin Elmer

References

Abrass CK, Nies KM, Louie JS, Border WA and Glassock RJ (1980). "Correlation and predictive accuracy of circulating immune complexes with disease activity in patients with systemic lupus erythematosus." Arthritis Rheum **23**(3): 273-282.

Aguilera MO, Beron W and Colombo MI (2012). "The actin cytoskeleton participates in the early events of autophagosome formation upon starvation induced autophagy." Autophagy **8**(11): 1590-1603.

Aird WC (2005). "Spatial and temporal dynamics of the endothelium." J Thromb Haemost **3**(7): 1392-1406.

Aird WC (2007). "Phenotypic heterogeneity of the endothelium: I. Structure, function, and mechanisms." Circ Res **100**(2): 158-173.

Aktan F (2004). "iNOS-mediated nitric oxide production and its regulation." Life Sci **75**(6): 639-653.

Alderton WK, Cooper CE and Knowles RG (2001). "Nitric oxide synthases: structure, function and inhibition." Biochem J **357**(Pt 3): 593-615.

Alessi DR, James SR, Downes CP, Holmes AB, Gaffney PR, Reese CB, et al. (1997). "Characterization of a 3-phosphoinositide-dependent protein kinase which phosphorylates and activates protein kinase Balpha." Curr Biol **7**(4): 261-269.

Almeida JL, Cole KD and Plant AL (2016). "Standards for Cell Line Authentication and Beyond." PLoS Biol **14**(6): e1002476.

Altorjay I, Vereb Z, Serfozo Z, Bacskai I, Batori R, Erdodi F, et al. (2011). "Anti-TNF-alpha antibody (infliximab) therapy supports the recovery of eNOS and VEGFR2 protein expression in endothelial cells." Int J Immunopathol Pharmacol **24**(2): 323-335.

Anderson HD, Rahmutula D and Gardner DG (2004). "Tumor necrosis factor-alpha inhibits endothelial nitric-oxide synthase gene promoter activity in bovine aortic endothelial cells." J Biol Chem **279**(2): 963-969.

Arai S, Harada N, Kubo N, Shen J, Nakamura A, Ikeda H, et al. (2008). "Induction of inducible nitric oxide synthase and apoptosis by LPS and TNF-alpha in nasal microvascular endothelial cells." Acta Otolaryngol **128**(1): 78-85.

Arbuckle MR, McClain MT, Rubertone MV, Scofield RH, Dennis GJ, James JA, et al. (2003). "Development of autoantibodies before the clinical onset of systemic lupus erythematosus." N Engl J Med **349**(16): 1526-1533.

Arita R, Nakao S, Kita T, Kawahara S, Asato R, Yoshida S, et al. (2013). "A key role for ROCK in TNF-alpha-mediated diabetic microvascular damage." Invest Ophthalmol Vis Sci **54**(3): 2373-2383.

Arkill KP, Qvortrup K, Starborg T, Mantell JM, Knupp C, Michel CC, et al. (2014). "Resolution of the three dimensional structure of components of the glomerular filtration barrier." BMC Nephrol **15**: 24.

Armstead VE, Minchenko AG, Schuhl RA, Hayward R, Nossuli TO and Lefer AM (1997). "Regulation of P-selectin expression in human endothelial cells by nitric oxide." Am J Physiol **273**(2 Pt 2): H740-746.

Arnaoutova I, George J, Kleinman HK and Benton G (2009). "The endothelial cell tube formation assay on basement membrane turns 20: state of the science and the art." Angiogenesis **12**(3): 267-274.

Arnaoutova I and Kleinman HK (2010). "In vitro angiogenesis: endothelial cell tube formation on gelled basement membrane extract." Nat Protoc **5**(4): 628-635.

Arnaud L, Fagot JP, Mathian A, Paita M, Fagot-Campagna A and Amoura Z (2014). "Prevalence and incidence of systemic lupus erythematosus in France: a 2010 nation-wide population-based study." Autoimmun Rev **13**(11): 1082-1089.

Avihingsanon Y, Benjachat T, Tassanarong A, Sodsai P, Kittikovit V and Hirankarn N (2009). "Decreased renal expression of vascular endothelial growth factor in lupus nephritis is associated with worse prognosis." Kidney Int **75**(12): 1340-1348.

Bakr SI, Shehab AA-S, Shennawy DE, Ahmed R, Abo-shady, Zeitoun YA, et al. (2014). "Serum Angiopoietin-2 and Soluble Thrombomodulin in Patients with Systemic

Lupus Erythematosus and their Relation to Disease Activity and Renal Affection." JMSCR **2**(6): 14.

Ballermann BJ (1989). "Regulation of bovine glomerular endothelial cell growth in vitro." Am J Physiol **256**(1 Pt 1): C182-189.

Bar-Peled L, Schweitzer LD, Zoncu R and Sabatini DM (2012). "Ragulator is a GEF for the rag GTPases that signal amino acid levels to mTORC1." Cell **150**(6): 1196-1208.

Barilli A, Visigalli R, Sala R, Gazzola GC, Parolari A, Tremoli E, et al. (2008). "In human endothelial cells rapamycin causes mTORC2 inhibition and impairs cell viability and function." Cardiovasc Res **78**(3): 563-571.

Barrat FJ, Meeker T, Gregorio J, Chan JH, Uematsu S, Akira S, et al. (2005). "Nucleic acids of mammalian origin can act as endogenous ligands for Toll-like receptors and may promote systemic lupus erythematosus." J Exp Med **202**(8): 1131-1139.

Barrionuevo P, Beigier-Bompadre M, Fernandez GC, Gomez S, Alves-Rosa MF, Palermo MS, et al. (2003). "Immune complex-FcgammaR interaction modulates monocyte/macrophage molecules involved in inflammation and immune response." Clin Exp Immunol **133**(2): 200-207.

Barsacchi R, Perrotta C, Bulotta S, Moncada S, Borgese N and Clementi E (2003). "Activation of endothelial nitric-oxide synthase by tumor necrosis factor-alpha: a

novel pathway involving sequential activation of neutral sphingomyelinase, phosphatidylinositol-3' kinase, and Akt." Mol Pharmacol **63**(4): 886-895.

Bejarano E and Cuervo AM (2010). "Chaperone-mediated autophagy." Proc Am Thorac Soc **7**(1): 29-39.

Belmont HM, Levartovsky D, Goel A, Amin A, Giorno R, Rediske J, et al. (1997). "Increased nitric oxide production accompanied by the up-regulation of inducible nitric oxide synthase in vascular endothelium from patients with systemic lupus erythematosus." Arthritis Rheum **40**(10): 1810-1816.

Ben-Zvi I, Kivity S, Langevitz P and Shoenfeld Y (2012). "Hydroxychloroquine: from malaria to autoimmunity." Clin Rev Allergy Immunol **42**(2): 145-153.

Bermudez O and Forciniti D (2004). "Aggregation and denaturation of antibodies: a capillary electrophoresis, dynamic light scattering, and aqueous two-phase partitioning study." J Chromatogr B Analyt Technol Biomed Life Sci **807**(1): 17-24.

Berthier CC, Bethunaickan R, Gonzalez-Rivera T, Nair V, Ramanujam M, Zhang W, et al. (2012). "Cross-species transcriptional network analysis defines shared inflammatory responses in murine and human lupus nephritis." J Immunol **189**(2): 988-1001.

Bharath LP, Mueller R, Li Y, Ruan T, Kunz D, Goodrich R, et al. (2014). "Impairment of autophagy in endothelial cells prevents shear-stress-induced increases in nitric oxide bioavailability." Can J Physiol Pharmacol **92**(7): 605-612.

Bhaskar PT and Hay N (2007). "The two TORCs and Akt." Dev Cell **12**(4): 487-502.

Bhattacharya A and Eissa NT (2013). "Autophagy and autoimmunity crosstalks." Front Immunol **4**: 88.

Bikfalvi A and Bicknell R (2002). "Recent advances in angiogenesis, anti-angiogenesis and vascular targeting." Trends Pharmacol Sci **23**(12): 576-582.

Birmingham DJ and Hebert LA (2015). "The Complement System in Lupus Nephritis." Semin Nephrol **35**(5): 444-454.

Bjorkoy G, Lamark T, Brech A, Outzen H, Perander M, Overvatn A, et al. (2005). "p62/SQSTM1 forms protein aggregates degraded by autophagy and has a protective effect on huntingtin-induced cell death." J Cell Biol **171**(4): 603-614.

Blom AB, van Lent PL, van Vuuren H, Holthuysen AE, Jacobs C, van de Putte LB, et al. (2000). "Fc gamma R expression on macrophages is related to severity and chronicity of synovial inflammation and cartilage destruction during experimental immune-complex-mediated arthritis (ICA)." Arthritis Res **2**(6): 489-503.

Blommaart EF, Krause U, Schellens JP, Vreeling-Sindelarova H and Meijer AJ (1997). "The phosphatidylinositol 3-kinase inhibitors wortmannin and LY294002 inhibit autophagy in isolated rat hepatocytes." Eur J Biochem **243**(1-2): 240-246.

Boehme MW, Raeth U, Galle PR, Stremmel W and Scherbaum WA (2000). "Serum thrombomodulin-a reliable marker of disease activity in systemic lupus erythematosus (SLE): advantage over established serological parameters to indicate disease activity." Clin Exp Immunol **119**(1): 189-195.

Borchers AT, Leibushor N, Naguwa SM, Cheema GS, Shoenfeld Y and Gershwin ME (2012). "Lupus nephritis: a critical review." Autoimmun Rev **12**(2): 174-194.

Borchers AT, Naguwa SM, Shoenfeld Y and Gershwin ME (2010). "The geoepidemiology of systemic lupus erythematosus." Autoimmun Rev **9**(5): A277-287.

Bouillet L, Baudet AE, Deroux A, Sidibe A, Dumestre-Perard C, Mannic T, et al. (2013). "Auto-antibodies to vascular endothelial cadherin in humans: association with autoimmune diseases." Lab Invest **93**(11): 1194-1202.

Boule MW, Broughton C, Mackay F, Akira S, Marshak-Rothstein A and Rifkin IR (2004). "Toll-like receptor 9-dependent and -independent dendritic cell activation by chromatin-immunoglobulin G complexes." J Exp Med **199**(12): 1631-1640.

Bredt DS, Hwang PM, Glatt CE, Lowenstein C, Reed RR and Snyder SH (1991). "Cloned and expressed nitric oxide synthase structurally resembles cytochrome P-450 reductase." Nature **351**(6329): 714-718.

Brown EE, Edberg JC and Kimberly RP (2007). "Fc receptor genes and the systemic lupus erythematosus diathesis." Autoimmunity **40**(8): 567-581.

Canaud G, Bienaime F, Tabarin F, Bataillon G, Seilhean D, Noel LH, et al. (2014). "Inhibition of the mTORC pathway in the antiphospholipid syndrome." N Engl J Med **371**(4): 303-312.

Carmeliet P and Collen D (2000). "Molecular basis of angiogenesis. Role of VEGF and VE-cadherin." Ann N Y Acad Sci **902**: 249-262; discussion 262-244.

Carpenter JE, Jackson W, Benetti L and Grose C (2011). "Autophagosome formation during varicella-zoster virus infection following endoplasmic reticulum stress and the unfolded protein response." J Virol **85**(18): 9414-9424.

Carreno L, Lopez-Longo FJ, Monteagudo I, Rodriguez-Mahou M, Bascones M, Gonzalez CM, et al. (1999). "Immunological and clinical differences between juvenile and adult onset of systemic lupus erythematosus." Lupus **8**(4): 287-292.

Casali P, Bossus A, Carpentier NA and Lambert PH (1977). "Solid-phase enzyme immunoassay or radioimmunoassay for the detection of immune complexes based on their recognition by conglutinin: conglutinin-binding test. A comparative study

with 125I-labelled Clq binding and Raji-cell RIA tests." Clin Exp Immunol **29**(2): 342-354.

Chan FK, Moriwaki K and De Rosa MJ (2013). "Detection of necrosis by release of lactate dehydrogenase activity." Methods Mol Biol **979**: 65-70.

Chan RW, Lai FM, Li EK, Tam LS, Chow KM, Lai KB, et al. (2007). "Intrarenal cytokine gene expression in lupus nephritis." Ann Rheum Dis **66**(7): 886-892.

Chan RW, Tam LS, Li EK, Lai FM, Chow KM, Lai KB, et al. (2003). "Inflammatory cytokine gene expression in the urinary sediment of patients with lupus nephritis." Arthritis Rheum **48**(5): 1326-1331.

Chauhan AK and Moore TL (2011). "T cell activation by terminal complex of complement and immune complexes." J Biol Chem **286**(44): 38627-38637.

Chenais F, Virella G, Patrick CC and Fudenberg HH (1977). "Isolation of soluble immune complexes by affinity chromatography using staphylococcal protein A--Sepharose as substrate." J Immunol Methods **18**(1-2): 183-192.

Cheng F (2013). ATG5 and autophagy in the pathogenesis of systemic lupus erythematosus. Doctor Degree Thesis, Peking University.

Choi J, Chen J, Schreiber SL and Clardy J (1996). "Structure of the FKBP12-rapamycin complex interacting with the binding domain of human FRAP." Science **273**(5272): 239-242.

Choi YJ, Park YJ, Park JY, Jeong HO, Kim DH, Ha YM, et al. (2012). "Inhibitory effect of mTOR activator MHY1485 on autophagy: suppression of lysosomal fusion." PLoS One **7**(8): e43418.

Chresta CM, Davies BR, Hickson I, Harding T, Cosulich S, Critchlow SE, et al. (2010). "AZD8055 is a potent, selective, and orally bioavailable ATP-competitive mammalian target of rapamycin kinase inhibitor with in vitro and in vivo antitumor activity." Cancer Res **70**(1): 288-298.

Cines DB, Lyss AP, Reeber M, Bina M and DeHoratius RJ (1984). "Presence of complement-fixing anti-endothelial cell antibodies in systemic lupus erythematosus." J Clin Invest **73**(3): 611-625.

Clarke AJ, Ellinghaus U, Cortini A, Stranks A, Simon AK, Botto M, et al. (2015). "Autophagy is activated in systemic lupus erythematosus and required for plasmablast development." Ann Rheum Dis **74**(5): 912-920.

Clatworthy MR, Harford SK, Mathews RJ and Smith KG (2014). "FcgammaRIIb inhibits immune complex-induced VEGF-A production and intranodal lymphangiogenesis." Proc Natl Acad Sci U S A **111**(50): 17971-17976.

Corada M, Zanetta L, Orsenigo F, Breviario F, Lampugnani MG, Bernasconi S, et al. (2002). "A monoclonal antibody to vascular endothelial-cadherin inhibits tumor angiogenesis without side effects on endothelial permeability." Blood **100**(3): 905-911.

Corning. (2017). "Corning Matrigel Matrix: frequently asked questions." http://csmedia2.corning.com/LifeSciences/Media/pdf/faq_DL_026_Corning_Matrigel_Matrix.pdf.

Crazzolara R, Bradstock KF and Bendall LJ (2009). "RAD001 (Everolimus) induces autophagy in acute lymphoblastic leukemia." Autophagy **5**(5): 727-728.

Criollo A, Maiuri MC, Tasdemir E, Vitale I, Fiebig AA, Andrews D, et al. (2007). "Regulation of autophagy by the inositol trisphosphate receptor." Cell Death Differ **14**(5): 1029-1039.

Danchenko N, Satia JA and Anthony MS (2006). "Epidemiology of systemic lupus erythematosus: a comparison of worldwide disease burden." Lupus **15**(5): 308-318.

Davidson A (2016). "What is damaging the kidney in lupus nephritis?" Nat Rev Rheumatol **12**(3): 143-153.

Davis LS, Hutcheson J and Mohan C (2011). "The role of cytokines in the pathogenesis and treatment of systemic lupus erythematosus." J Interferon Cytokine Res **31**(10): 781-789.

De Palma C, Meacci E, Perrotta C, Bruni P and Clementi E (2006). "Endothelial nitric oxide synthase activation by tumor necrosis factor alpha through neutral sphingomyelinase 2, sphingosine kinase 1, and sphingosine 1 phosphate receptors:

a novel pathway relevant to the pathophysiology of endothelium." Arterioscler Thromb Vasc Biol **26**(1): 99-105.

Deanfield JE, Halcox JP and Rabelink TJ (2007). "Endothelial function and dysfunction: testing and clinical relevance." Circulation **115**(10): 1285-1295.

Dengjel J, Schoor O, Fischer R, Reich M, Kraus M, Muller M, et al. (2005). "Autophagy promotes MHC class II presentation of peptides from intracellular source proteins." Proc Natl Acad Sci U S A **102**(22): 7922-7927.

Denninger JW and Marletta MA (1999). "Guanylate cyclase and the .NO/cGMP signaling pathway." Biochim Biophys Acta **1411**(2-3): 334-350.

Denny MF, Yalavarthi S, Zhao W, Thacker SG, Anderson M, Sandy AR, et al. (2010). "A distinct subset of proinflammatory neutrophils isolated from patients with systemic lupus erythematosus induces vascular damage and synthesizes type I IFNs." J Immunol **184**(6): 3284-3297.

Deretic V, Kimura T, Timmins G, Moseley P, Chauhan S and Mandell M (2015). "Immunologic manifestations of autophagy." J Clin Invest **125**(1): 75-84.

Deretic V, Saitoh T and Akira S (2013). "Autophagy in infection, inflammation and immunity." Nat Rev Immunol **13**(10): 722-737.

Dibble CC, Elis W, Menon S, Qin W, Klekota J, Asara JM, et al. (2012). "TBC1D7 is a third subunit of the TSC1-TSC2 complex upstream of mTORC1." Mol Cell **47**(4): 535-546.

Dimmeler S, Fleming I, Fisslthaler B, Hermann C, Busse R and Zeiher AM (1999). "Activation of nitric oxide synthase in endothelial cells by Akt-dependent phosphorylation." Nature **399**(6736): 601-605.

Doekes G, van Es LA and Daha MR (1984). "Binding and activation of the first complement component by soluble immune complexes: effect of complex size and composition." Scand J Immunol **19**(2): 99-110.

Domingues JB (2011). Stability Assessment of Biopharmaceutical Formulations. Master's degree in Biological Engineering Thesis, Universidade Técnica de Lisboa.

Dorrello NV, Peschiaroli A, Guardavaccaro D, Colburn NH, Sherman NE and Pagano M (2006). "S6K1- and betaTRCP-mediated degradation of PDCD4 promotes protein translation and cell growth." Science **314**(5798): 467-471.

Dschietzig T, Brecht A, Bartsch C, Baumann G, Stangl K and Alexiou K (2012). "Relaxin improves TNF-alpha-induced endothelial dysfunction: the role of glucocorticoid receptor and phosphatidylinositol 3-kinase signalling." Cardiovasc Res **95**(1): 97-107.

Du G, Song Y, Zhang T, Ma L, Bian N, Chen X, et al. (2014). "Simvastatin attenuates TNFalphainduced apoptosis in endothelial progenitor cells via the upregulation of SIRT1." Int J Mol Med **34**(1): 177-182.

Dunlop EA and Tee AR (2013). "The kinase triad, AMPK, mTORC1 and ULK1, maintains energy and nutrient homoeostasis." Biochem Soc Trans **41**(4): 939-943.

El-Banawy HS, Gaber EW, Maharem DA and Matrawy KA (2012). "Angiopoietin-2, endothelial dysfunction and renal involvement in patients with systemic lupus erythematosus." J Nephrol **25**(4): 541-550.

Elshafie AI, Ahlin E, Mathsson L, ElGhazali G and Ronnelid J (2007). "Circulating immune complexes (IC) and IC-induced levels of GM-CSF are increased in sudanese patients with acute visceral Leishmania donovani infection undergoing sodium stibogluconate treatment: implications for disease pathogenesis." J Immunol **178**(8): 5383-5389.

Elshal M, Abdelaziz A, Abbas A, Mahmoud K, Fathy H, El Mongy S, et al. (2009). "Quantification of circulating endothelial cells in peripheral blood of systemic lupus erythematosus patients: a simple and reproducible method of assessing endothelial injury and repair." Nephrol Dial Transplant **24**(5): 1495-1499.

Fan QW, Cheng C, Hackett C, Feldman M, Houseman BT, Nicolaides T, et al. (2010). "Akt and autophagy cooperate to promote survival of drug-resistant glioma." Sci Signal **3**(147): ra81.

Farkas T, Daugaard M and Jaattela M (2011). "Identification of small molecule inhibitors of phosphatidylinositol 3-kinase and autophagy." J Biol Chem **286**(45): 38904-38912.

Faurschou M, Dreyer L, Kamper AL, Starklint H and Jacobsen S (2010). "Long-term mortality and renal outcome in a cohort of 100 patients with lupus nephritis." Arthritis Care Res (Hoboken) **62**(6): 873-880.

Feldman CH, Hiraki LT, Liu J, Fischer MA, Solomon DH, Alarcon GS, et al. (2013). "Epidemiology and sociodemographics of systemic lupus erythematosus and lupus nephritis among US adults with Medicaid coverage, 2000-2004." Arthritis Rheum **65**(3): 753-763.

Feldman ME, Apsel B, Uotila A, Loewith R, Knight ZA, Ruggero D, et al. (2009). "Active-site inhibitors of mTOR target rapamycin-resistant outputs of mTORC1 and mTORC2." PLoS Biol **7**(2): e38.

Feng J, Park J, Cron P, Hess D and Hemmings BA (2004). "Identification of a PKB/Akt hydrophobic motif Ser-473 kinase as DNA-dependent protein kinase." J Biol Chem **279**(39): 41189-41196.

Fernandez D, Bonilla E, Mirza N, Niland B and Perl A (2006). "Rapamycin reduces disease activity and normalizes T cell activation-induced calcium fluxing in patients with systemic lupus erythematosus." Arthritis Rheum **54**(9): 2983-2988.

Feron O and Michel T (2000). Cell and Molecular Biology of Nitric Oxide Synthases. Contemporary Cardiology. J. Loscalzo and J. A. Vita, Humana Press Inc. **4:** 11-31.

Fetterman JL, Holbrook M, Flint N, Feng B, Breton-Romero R, Linder EA, et al. (2016). "Restoration of autophagy in endothelial cells from patients with diabetes mellitus improves nitric oxide signaling." Atherosclerosis **247**: 207-217.

Fiedler U and Augustin HG (2006). "Angiopoietins: a link between angiogenesis and inflammation." Trends Immunol **27**(12): 552-558.

Filipe V, Hawe A and Jiskoot W (2010). "Critical evaluation of Nanoparticle Tracking Analysis (NTA) by NanoSight for the measurement of nanoparticles and protein aggregates." Pharm Res **27**(5): 796-810.

Filipe V, Jiskoot W, Basmeleh AH, Halim A, Schellekens H and Brinks V (2012a). "Immunogenicity of different stressed IgG monoclonal antibody formulations in immune tolerant transgenic mice." MAbs **4**(6): 740-752.

Filipe V, Poole R, Oladunjoye O, Braeckmans K and Jiskoot W (2012b). "Detection and characterization of subvisible aggregates of monoclonal IgG in serum." Pharm Res **29**(8): 2202-2212.

Fischmann TO, Hruza A, Niu XD, Fossetta JD, Lunn CA, Dolphin E, et al. (1999). "Structural characterization of nitric oxide synthase isoforms reveals striking active-site conservation." Nat Struct Biol **6**(3): 233-242.

Fleming A, Noda T, Yoshimori T and Rubinsztein DC (2011). "Chemical modulators of autophagy as biological probes and potential therapeutics." Nat Chem Biol **7**(1): 9-17.

Fleming I (2010). "Molecular mechanisms underlying the activation of eNOS." Pflugers Arch **459**(6): 793-806.

Fogo AB and Kon V (2010). "The glomerulus--a view from the inside--the endothelial cell." Int J Biochem Cell Biol **42**(9): 1388-1397.

Forstermann U and Munzel T (2006). "Endothelial nitric oxide synthase in vascular disease: from marvel to menace." Circulation **113**(13): 1708-1714.

Forstermann U and Sessa WC (2012). "Nitric oxide synthases: regulation and function." Eur Heart J **33**(7): 829-837, 837a-837d.

Freedman BI, Langefeld CD, Andringa KK, Croker JA, Williams AH, Garner NE, et al. (2014). "End-stage renal disease in African Americans with lupus nephritis is associated with APOL1." Arthritis Rheumatol **66**(2): 390-396.

Frijns R, Fijnheer R, Schiel A, Donders R, Sixma J and Derksen R (2001). "Persistent increase in plasma thrombomodulin in patients with a history of lupus nephritis: endothelial cell activation markers." J Rheumatol **28**(3): 514-519.

Fruhwurth S, Krieger S, Winter K, Rosner M, Mikula M, Weichhart T, et al. (2014). "Inhibition of mTOR down-regulates scavenger receptor, class B, type I (SR-BI)

expression, reduces endothelial cell migration and impairs nitric oxide production." Biochim Biophys Acta **1841**(7): 944-953.

Fujii H, Nakatani K, Arita N, Ito MR, Terada M, Miyazaki T, et al. (2003). "Internalization of antibodies by endothelial cells via fibronectin implicating a novel mechanism in lupus nephritis." Kidney Int **64**(5): 1662-1670.

Fujita E, Nagahama K, Shimizu A, Aoki M, Higo S, Yasuda F, et al. (2015). "Glomerular capillary and endothelial cell injury is associated with the formation of necrotizing and crescentic lesions in crescentic glomerulonephritis." J Nippon Med Sch **82**(1): 27-35.

Garcia-Martinez JM, Moran J, Clarke RG, Gray A, Cosulich SC, Chresta CM, et al. (2009). "Ku-0063794 is a specific inhibitor of the mammalian target of rapamycin (mTOR)." Biochem J **421**(1): 29-42.

Gateva V, Sandling JK, Hom G, Taylor KE, Chung SA, Sun X, et al. (2009). "A large-scale replication study identifies TNIP1, PRDM1, JAZF1, UHRF1BP1 and IL10 as risk loci for systemic lupus erythematosus." Nat Genet **41**(11): 1228-1233.

Ghigo D, Aldieri E, Todde R, Costamagna C, Garbarino G, Pescarmona G, et al. (1998). "Chloroquine stimulates nitric oxide synthesis in murine, porcine, and human endothelial cells." J Clin Invest **102**(3): 595-605.

Gianchecchi E, Delfino DV and Fierabracci A (2014). "Recent insights on the putative role of autophagy in autoimmune diseases." Autoimmun Rev **13**(3): 231-241.

Gigante A, Gasperini ML, Afeltra A, Barbano B, Margiotta D, Cianci R, et al. (2011). "Cytokines expression in SLE nephritis." Eur Rev Med Pharmacol Sci **15**(1): 15-24.

Gilkeson GS, Mashmoushi AK, Ruiz P, Caza TN, Perl A and Oates JC (2013). "Endothelial nitric oxide synthase reduces crescentic and necrotic glomerular lesions, reactive oxygen production, and MCP1 production in murine lupus nephritis." PLoS One **8**(5): e64650.

Gimbrone MA, Jr. and Garcia-Cardena G (2016). "Endothelial Cell Dysfunction and the Pathobiology of Atherosclerosis." Circ Res **118**(4): 620-636.

Goilav B and Putterman C (2015). "The Role of Anti-DNA Antibodies in the Development of Lupus Nephritis: A Complementary, or Alternative, Viewpoint?" Semin Nephrol **35**(5): 439-443.

Goldblatt F and O'Neill SG (2013). "Clinical aspects of autoimmune rheumatic diseases." Lancet **382**(9894): 797-808.

Gomes LC and Dikic I (2014). "Autophagy in antimicrobial immunity." Mol Cell **54**(2): 224-233.

Groenewoud MJ and Zwartkruis FJ (2013). "Rheb and Rags come together at the lysosome to activate mTORC1." Biochem Soc Trans **41**(4): 951-955.

Grootscholten C, Dieker JW, McGrath FD, Roos A, Derksen RH, van der Vlag J, et al. (2007). "A prospective study of anti-chromatin and anti-C1q autoantibodies in patients with proliferative lupus nephritis treated with cyclophosphamide pulses or azathioprine/methylprednisolone." Ann Rheum Dis **66**(5): 693-696.

Gros F, Arnold J, Page N, Decossas M, Korganow AS, Martin T, et al. (2012). "Macroautophagy is deregulated in murine and human lupus T lymphocytes." Autophagy **8**(7): 1113-1123.

Guo F, Li X, Peng J, Tang Y, Yang Q, Liu L, et al. (2014). "Autophagy regulates vascular endothelial cell eNOS and ET-1 expression induced by laminar shear stress in an ex vivo perfused system." Ann Biomed Eng **42**(9): 1978-1988.

Gwinn DM, Shackelford DB, Egan DF, Mihaylova MM, Mery A, Vasquez DS, et al. (2008). "AMPK phosphorylation of raptor mediates a metabolic checkpoint." Mol Cell **30**(2): 214-226.

Hagele H, Allam R, Pawar RD, Reichel CA, Krombach F and Anders HJ (2009). "Double-stranded DNA activates glomerular endothelial cells and enhances albumin permeability via a toll-like receptor-independent cytosolic DNA recognition pathway." Am J Pathol **175**(5): 1896-1904.

Hanly JG, Su L, Urowitz MB, Romero-Diaz J, Gordon C, Bae SC, et al. (2016). "A Longitudinal Analysis of Outcomes of Lupus Nephritis in an International

Inception Cohort Using a Multistate Model Approach." Arthritis Rheumatol **68**(8): 1932-1944.

Hara T, Nakamura K, Matsui M, Yamamoto A, Nakahara Y, Suzuki-Migishima R, et al. (2006). "Suppression of basal autophagy in neural cells causes neurodegenerative disease in mice." Nature **441**(7095): 885-889.

Haraldsson B, Nystrom J and Deen WM (2008). "Properties of the glomerular barrier and mechanisms of proteinuria." Physiol Rev **88**(2): 451-487.

Harkiss GD, Hazleman BL and Brown DL (1979). "A longitudinal study of circulating immune complexes, dna antibodies and complement in patients with systemic lupus erythematosus: an analysis of their relationship to disease activity." J Clin Lab Immunol **2**(4): 275-283.

Harr MW, McColl KS, Zhong F, Molitoris JK and Distelhorst CW (2010). "Glucocorticoids downregulate Fyn and inhibit IP(3)-mediated calcium signaling to promote autophagy in T lymphocytes." Autophagy **6**(7): 912-921.

Hawe A, Friess W, Sutter M and Jiskoot W (2008). "Online fluorescent dye detection method for the characterization of immunoglobulin G aggregation by size exclusion chromatography and asymmetrical flow field flow fractionation." Anal Biochem **378**(2): 115-122.

Hay FC, Nineham LJ and Roitt IM (1976). "Routine assay for the detection of immune complexes of known immunoglobulin class using solid phase C1q." Clin Exp Immunol **24**(3): 396-400.

Hayashi S, Yamamoto A, You F, Yamashita K, Ikegame Y, Tawada M, et al. (2009). "The stent-eluting drugs sirolimus and paclitaxel suppress healing of the endothelium by induction of autophagy." Am J Pathol **175**(5): 2226-2234.

Haymann JP, Delarue F, Baud L and Sraer JD (2004). "Aggregated IgG bind to glomerular epithelial cells to stimulate urokinase release through an endocytosis-independent process." Nephron Exp Nephrol **98**(1): e13-21.

He C and Klionsky DJ (2009). "Regulation mechanisms and signaling pathways of autophagy." Annu Rev Genet **43**: 67-93.

Helbing T, Rothweiler R, Ketterer E, Goetz L, Heinke J, Grundmann S, et al. (2011). "BMP activity controlled by BMPER regulates the proinflammatory phenotype of endothelium." Blood **118**(18): 5040-5049.

Hemmings BA and Restuccia DF (2012). "PI3K-PKB/Akt pathway." Cold Spring Harb Perspect Biol **4**(9): a011189.

Henault J, Martinez J, Riggs JM, Tian J, Mehta P, Clarke L, et al. (2012). "Noncanonical autophagy is required for type I interferon secretion in response to DNA-immune complexes." Immunity **37**(6): 986-997.

Henry CM, Hollville E and Martin SJ (2013). "Measuring apoptosis by microscopy and flow cytometry." Methods **61**(2): 90-97.

Hillmann A, Wardemann H, Pap T and Jacobi A (2012). "Uptake of SLE autoantibodies by podocytes." Ann Rheum Dis **71**(Suppl 1): A32-33.

Hsu KS, Guan BJ, Cheng X, Guan D, Lam M, Hatzoglou M, et al. (2016). "Translational control of PML contributes to TNFalpha-induced apoptosis of MCF7 breast cancer cells and decreased angiogenesis in HUVECs." Cell Death Differ **23**(3): 469-483.

Huang J and Brumell JH (2014). "Bacteria-autophagy interplay: a battle for survival." Nat Rev Microbiol **12**(2): 101-114.

Inguscio V, Panzarini E and Dini L (2012). "Autophagy Contributes to the Death/Survival Balance in Cancer PhotoDynamic Therapy." Cells **1**(3): 464-491.

Inoki K, Li Y, Zhu T, Wu J and Guan KL (2002). "TSC2 is phosphorylated and inhibited by Akt and suppresses mTOR signalling." Nat Cell Biol **4**(9): 648-657.

Inoki K, Ouyang H, Zhu T, Lindvall C, Wang Y, Zhang X, et al. (2006). "TSC2 integrates Wnt and energy signals via a coordinated phosphorylation by AMPK and GSK3 to regulate cell growth." Cell **126**(5): 955-968.

Inoki K, Zhu T and Guan KL (2003). "TSC2 mediates cellular energy response to control cell growth and survival." Cell **115**(5): 577-590.

Isenberg DA, Manson JJ, Ehrenstein MR and Rahman A (2007). "Fifty years of anti-ds DNA antibodies: are we approaching journey's end?" Rheumatology (Oxford) **46**(7): 1052-1056.

Itakura A and McCarty OJ (2013). "Pivotal role for the mTOR pathway in the formation of neutrophil extracellular traps via regulation of autophagy." Am J Physiol Cell Physiol **305**(3): C348-354.

Iwata Y, Furuichi K, Kaneko S and Wada T (2011). "The role of cytokine in the lupus nephritis." J Biomed Biotechnol **2011**: 594809.

Jacinto E, Facchinetti V, Liu D, Soto N, Wei S, Jung SY, et al. (2006). "SIN1/MIP1 maintains rictor-mTOR complex integrity and regulates Akt phosphorylation and substrate specificity." Cell **127**(1): 125-137.

Jain MV, Paczulla AM, Klonisch T, Dimgba FN, Rao SB, Roberg K, et al. (2013). "Interconnections between apoptotic, autophagic and necrotic pathways: implications for cancer therapy development." J Cell Mol Med **17**(1): 12-29.

Jarukitsopa S, Hoganson DD, Crowson CS, Sokumbi O, Davis MD, Michet CJ, Jr., et al. (2015). "Epidemiology of systemic lupus erythematosus and cutaneous lupus erythematosus in a predominantly white population in the United States." Arthritis Care Res (Hoboken) **67**(6): 817-828.

Jin C, Zhao Y, Yu L, Xu S and Fu G (2013). "MicroRNA-21 mediates the rapamycin-induced suppression of endothelial proliferation and migration." FEBS Lett **587**(4): 378-385.

Jindra PT, Jin YP, Rozengurt E and Reed EF (2008). "HLA class I antibody-mediated endothelial cell proliferation via the mTOR pathway." J Immunol **180**(4): 2357-2366.

Jounai N, Takeshita F, Kobiyama K, Sawano A, Miyawaki A, Xin KQ, et al. (2007). "The Atg5 Atg12 conjugate associates with innate antiviral immune responses." Proc Natl Acad Sci U S A **104**(35): 14050-14055.

Ju H, Zou R, Venema VJ and Venema RC (1997). "Direct interaction of endothelial nitric-oxide synthase and caveolin-1 inhibits synthase activity." J Biol Chem **272**(30): 18522-18525.

Jung CH, Jun CB, Ro SH, Kim YM, Otto NM, Cao J, et al. (2009). "ULK-Atg13-FIP200 complexes mediate mTOR signaling to the autophagy machinery." Mol Biol Cell **20**(7): 1992-2003.

Kabeya Y, Mizushima N, Ueno T, Yamamoto A, Kirisako T, Noda T, et al. (2000). "LC3, a mammalian homologue of yeast Apg8p, is localized in autophagosome membranes after processing." EMBO J **19**(21): 5720-5728.

Kabeya Y, Mizushima N, Yamamoto A, Oshitani-Okamoto S, Ohsumi Y and Yoshimori T (2004). "LC3, GABARAP and GATE16 localize to autophagosomal membrane depending on form-II formation." J Cell Sci **117**(Pt 13): 2805-2812.

Kang SA, Pacold ME, Cervantes CL, Lim D, Lou HJ, Ottina K, et al. (2013). "mTORC1 phosphorylation sites encode their sensitivity to starvation and rapamycin." Science **341**(6144): 1236566.

Kang YL, Saleem MA, Chan KW, Yung BY and Law HK (2014). "The cytoprotective role of autophagy in puromycin aminonucleoside treated human podocytes." Biochem Biophys Res Commun **443**(2): 628-634.

Karbach S, Wenzel P, Waisman A, Munzel T and Daiber A (2014). "eNOS uncoupling in cardiovascular diseases--the role of oxidative stress and inflammation." Curr Pharm Des **20**(22): 3579-3594.

Katsuyama K, Shichiri M, Marumo F and Hirata Y (1998). "NO inhibits cytokine-induced iNOS expression and NF-kappaB activation by interfering with phosphorylation and degradation of IkappaB-alpha." Arterioscler Thromb Vasc Biol **18**(11): 1796-1802.

Kawanaka H, Jones MK, Szabo IL, Baatar D, Pai R, Tsugawa K, et al. (2002). "Activation of eNOS in rat portal hypertensive gastric mucosa is mediated by TNF-alpha via the PI 3-kinase-Akt signaling pathway." Hepatology **35**(2): 393-402.

Kijlstra A, van Es LA and Daha MR (1979). "The role of complement in the binding and degradation of immunoglobulin aggregates by macrophages." J Immunol **123**(6): 2488-2493.

Kim J and Kim E (2016). "Rag GTPase in amino acid signaling." Amino Acids **48**(4): 915-928.

Kim J, Kundu M, Viollet B and Guan KL (2011). "AMPK and mTOR regulate autophagy through direct phosphorylation of Ulk1." Nat Cell Biol **13**(2): 132-141.

Kim YC and Guan KL (2015). "mTOR: a pharmacologic target for autophagy regulation." J Clin Invest **125**(1): 25-32.

Kingsmore SF, Thompson JM, Crockard AD, Todd D, McKirgan J, Patterson C, et al. (1989). "Measurement of circulating immune complexes containing IgG, IgM, IgA and IgE by flow cytometry: correlation with disease activity in patients with systemic lupus erythematosus." J Clin Lab Immunol **30**(1): 45-52.

Kleinert H, Schwarz PM and Forstermann U (2003). "Regulation of the expression of inducible nitric oxide synthase." Biol Chem **384**(10-11): 1343-1364.

Kleinman HK and Martin GR (2005). "Matrigel: basement membrane matrix with biological activity." Semin Cancer Biol **15**(5): 378-386.

Klionsky DJ, Abdelmohsen K, Abe A, Abedin MJ, Abeliovich H, Acevedo Arozena A, et al. (2016). "Guidelines for the use and interpretation of assays for monitoring autophagy (3rd edition)." Autophagy **12**(1): 1-222.

Kojima K, Kitaoka Y, Munemasa Y, Hirano A, Sase K and Takagi H (2014). "Axonal protection by modulation of p62 expression in TNF-induced optic nerve degeneration." Neurosci Lett **581**: 37-41.

Kubes P, Suzuki M and Granger DN (1991). "Nitric oxide: an endogenous modulator of leukocyte adhesion." Proc Natl Acad Sci U S A **88**(11): 4651-4655.

Kumpers P, David S, Haubitz M, Hellpap J, Horn R, Brocker V, et al. (2009). "The Tie2 receptor antagonist angiopoietin 2 facilitates vascular inflammation in systemic lupus erythematosus." Ann Rheum Dis **68**(10): 1638-1643.

Kunanopparat A, Hirankarn N, Kittigul C, Tangkijvanich P and Kimkong I (2016). "Autophagy machinery impaired interferon signalling pathways to benefit hepatitis B virus replication." Asian Pac J Allergy Immunol **34**(1): 77-85.

Kyogoku C, Langefeld CD, Ortmann WA, Lee A, Selby S, Carlton VE, et al. (2004). "Genetic association of the R620W polymorphism of protein tyrosine phosphatase PTPN22 with human SLE." Am J Hum Genet **75**(3): 504-507.

Lamas S, Marsden PA, Li GK, Tempst P and Michel T (1992). "Endothelial nitric oxide synthase: molecular cloning and characterization of a distinct constitutive enzyme isoform." Proc Natl Acad Sci U S A **89**(14): 6348-6352.

Lamb CA, Yoshimori T and Tooze SA (2013). "The autophagosome: origins unknown, biogenesis complex." Nat Rev Mol Cell Biol **14**(12): 759-774.

Lande R, Ganguly D, Facchinetti V, Frasca L, Conrad C, Gregorio J, et al. (2011). "Neutrophils activate plasmacytoid dendritic cells by releasing self-DNA-peptide complexes in systemic lupus erythematosus." Sci Transl Med **3**(73): 73ra19.

LaRocca TJ, Henson GD, Thorburn A, Sindler AL, Pierce GL and Seals DR (2012). "Translational evidence that impaired autophagy contributes to arterial ageing." J Physiol **590**(Pt 14): 3305-3316.

Laurenzana A, Fibbi G, Margheri F, Biagioni A, Luciani C, Del Rosso M, et al. (2015). "Endothelial Progenitor Cells in Sprouting Angiogenesis: Proteases Pave the Way." Curr Mol Med **15**(7): 606-620.

Lavallard VJ, Meijer AJ, Codogno P and Gual P (2012). "Autophagy, signaling and obesity." Pharmacol Res **66**(6): 513-525.

Lech M and Anders HJ (2013). "The pathogenesis of lupus nephritis." J Am Soc Nephrol **24**(9): 1357-1366.

Lee DF, Kuo HP, Chen CT, Hsu JM, Chou CK, Wei Y, et al. (2007a). "IKK beta suppression of TSC1 links inflammation and tumor angiogenesis via the mTOR pathway." Cell **130**(3): 440-455.

Lee HK, Lund JM, Ramanathan B, Mizushima N and Iwasaki A (2007b). "Autophagy-dependent viral recognition by plasmacytoid dendritic cells." Science **315**(5817): 1398-1401.

Lee SJ, Silverman E and Bargman JM (2011). "The role of antimalarial agents in the treatment of SLE and lupus nephritis." Nat Rev Nephrol **7**(12): 718-729.

Lee YH, Kim HJ, Rho YH, Choi SJ, Ji JD and Song GG (2004). "Intron 4 polymorphism of the endothelial nitric oxide synthase gene is associated with the development of lupus nephritis." Lupus **13**(3): 188-191.

Lenoir O, Jasiek M, Henique C, Guyonnet L, Hartleben B, Bork T, et al. (2015). "Endothelial cell and podocyte autophagy synergistically protect from diabetes-induced glomerulosclerosis." Autophagy **11**(7): 1130-1145.

Levine B and Kroemer G (2008). "Autophagy in the pathogenesis of disease." Cell **132**(1): 27-42.

Levine B, Mizushima N and Virgin HW (2011). "Autophagy in immunity and inflammation." Nature **469**(7330): 323-335.

Li B, Yue Y, Dong C, Shi Y and Xiong S (2014). "Blockade of macrophage autophagy ameliorates activated lymphocytes-derived DNA induced murine lupus possibly via inhibition of proinflammatory cytokine production." Clin Exp Rheumatol **32**(5): 705-714.

Li M, Zhang W, Leng X, Li Z, Ye Z, Li C, et al. (2013a). "Chinese SLE Treatment and Research group (CSTAR) registry: I. Major clinical characteristics of Chinese patients with systemic lupus erythematosus." Lupus **22**(11): 1192-1199.

Li R, Sun J, Ren LM, Wang HY, Liu WH, Zhang XW, et al. (2012). "Epidemiology of eight common rheumatic diseases in China: a large-scale cross-sectional survey in Beijing." Rheumatology (Oxford) **51**(4): 721-729.

Li S, Wang L, Hu Y and Sheng R (2015). "Autophagy regulators as potential cancer therapeutic agents: a review." Curr Top Med Chem **15**(8): 720-744.

Li Y, Fang X and Li QZ (2013b). "Biomarker profiling for lupus nephritis." Genomics Proteomics Bioinformatics **11**(3): 158-165.

Li Y, Lee PY and Reeves WH (2010). "Monocyte and macrophage abnormalities in systemic lupus erythematosus." Arch Immunol Ther Exp (Warsz) **58**(5): 355-364.

Lim SS, Bayakly AR, Helmick CG, Gordon C, Easley KA and Drenkard C (2014). "The incidence and prevalence of systemic lupus erythematosus, 2002-2004: The Georgia Lupus Registry." Arthritis Rheumatol **66**(2): 357-368.

Lin JR, Shen WL, Yan C and Gao PJ (2015). "Downregulation of dynamin-related protein 1 contributes to impaired autophagic flux and angiogenic function in senescent endothelial cells." Arterioscler Thromb Vasc Biol **35**(6): 1413-1422.

Liu Q, Xu C, Kirubakaran S, Zhang X, Hur W, Liu Y, et al. (2013). "Characterization of Torin2, an ATP-competitive inhibitor of mTOR, ATM, and ATR." Cancer Res **73**(8): 2574-2586.

Liu TJ, Koul D, LaFortune T, Tiao N, Shen RJ, Maira SM, et al. (2009). "NVP-BEZ235, a novel dual phosphatidylinositol 3-kinase/mammalian target of rapamycin inhibitor, elicits multifaceted antitumor activities in human gliomas." Mol Cancer Ther **8**(8): 2204-2210.

Long C, Cook LG, Wu GY and Mitchell BM (2007). "Removal of FKBP12/12.6 from endothelial ryanodine receptors leads to an intracellular calcium leak and endothelial dysfunction." Arterioscler Thromb Vasc Biol **27**(7): 1580-1586.

Lood C, Allhorn M, Lood R, Gullstrand B, Olin AI, Ronnblom L, et al. (2012). "IgG glycan hydrolysis by endoglycosidase S diminishes the proinflammatory properties of immune complexes from patients with systemic lupus erythematosus: a possible new treatment?" Arthritis Rheum **64**(8): 2698-2706.

Lopes-Virella MF, Virella G, Orchard TJ, Koskinen S, Evans RW, Becker DJ, et al. (1999). "Antibodies to oxidized LDL and LDL-containing immune complexes as risk factors for coronary artery disease in diabetes mellitus." Clin Immunol **90**(2): 165-172.

Lui SL, Tsang R, Chan KW, Zhang F, Tam S, Yung S, et al. (2008a). "Rapamycin attenuates the severity of established nephritis in lupus-prone NZB/W F1 mice." Nephrol Dial Transplant **23**(9): 2768-2776.

Lui SL, Yung S, Tsang R, Zhang F, Chan KW, Tam S, et al. (2008b). "Rapamycin prevents the development of nephritis in lupus-prone NZB/W F1 mice." Lupus **17**(4): 305-313.

Lyons CR, Orloff GJ and Cunningham JM (1992). "Molecular cloning and functional expression of an inducible nitric oxide synthase from a murine macrophage cell line." J Biol Chem **267**(9): 6370-6374.

Ma XM and Blenis J (2009). "Molecular mechanisms of mTOR-mediated translational control." Nat Rev Mol Cell Biol **10**(5): 307-318.

Mack HI, Zheng B, Asara JM and Thomas SM (2012). "AMPK-dependent phosphorylation of ULK1 regulates ATG9 localization." Autophagy **8**(8): 1197-1214.

Maeda K, Mehta H, Drevets DA and Coggeshall KM (2010). "IL-6 increases B-cell IgG production in a feed-forward proinflammatory mechanism to skew hematopoiesis and elevate myeloid production." Blood **115**(23): 4699-4706.

Mahler HC, Muller R, Friess W, Delille A and Matheus S (2005). "Induction and analysis of aggregates in a liquid IgG1-antibody formulation." Eur J Pharm Biopharm **59**(3): 407-417.

Mak A and Kow NY (2014). "Imbalance between endothelial damage and repair: a gateway to cardiovascular disease in systemic lupus erythematosus." Biomed Res Int **2014**: 178721.

Manivel VA, Sohrabian A, Wick MC, Mullazehi M, Hakansson LD and Ronnelid J (2015). "Anti-type II collagen immune complex-induced granulocyte reactivity is associated with joint erosions in RA patients with anti-collagen antibodies." Arthritis Res Ther **17**: 8.

Manning BD and Cantley LC (2007). "AKT/PKB signaling: navigating downstream." Cell **129**(7): 1261-1274.

Maroz N and Segal MS (2013). "Lupus nephritis and end-stage kidney disease." Am J Med Sci **346**(4): 319-323.

Marquez-Curtis LA, Sultani AB, McGann LE and Elliott JA (2016). "Beyond membrane integrity: Assessing the functionality of human umbilical vein endothelial cells after cryopreservation." Cryobiology **72**(3): 183-190.

Marti HP and Frey FJ (2005). "Nephrotoxicity of rapamycin: an emerging problem in clinical medicine." Nephrol Dial Transplant **20**(1): 13-15.

Marzocchi-Machado CM, Alves CM, Azzolini AE, Polizello AC, Carvalho IF and Lucisano-Valim YM (2005). "CR1 on erythrocytes of Brazilian systemic lupus erythematosus patients: the influence of disease activity on expression and ability

of this receptor to bind immune complexes opsonized with complement from normal human serum." J Autoimmun **25**(4): 289-297.

Mauvezin C and Neufeld TP (2015). "Bafilomycin A1 disrupts autophagic flux by inhibiting both V-ATPase-dependent acidification and Ca-P60A/SERCA-dependent autophagosome-lysosome fusion." Autophagy **11**(8): 1437-1438.

McCabe TJ, Fulton D, Roman LJ and Sessa WC (2000). "Enhanced electron flux and reduced calmodulin dissociation may explain "calcium-independent" eNOS activation by phosphorylation." J Biol Chem **275**(9): 6123-6128.

McCarthy CG, Wenceslau CF, Goulopoulou S, Ogbi S, Matsumoto T and Webb RC (2016). "Autoimmune therapeutic chloroquine lowers blood pressure and improves endothelial function in spontaneously hypertensive rats." Pharmacol Res **113**(Pt A): 384-394.

McIlwain DR, Berger T and Mak TW (2013). "Caspase functions in cell death and disease." Cold Spring Harb Perspect Biol **5**(4): a008656.

McLeod IX, Jia W and He YW (2012). "The contribution of autophagy to lymphocyte survival and homeostasis." Immunol Rev **249**(1): 195-204.

Means TK, Latz E, Hayashi F, Murali MR, Golenbock DT and Luster AD (2005). "Human lupus autoantibody-DNA complexes activate DCs through cooperation of CD32 and TLR9." J Clin Invest **115**(2): 407-417.

Medof ME, Scarborough D and Miller G (1981). "Ability of complement to release systemic lupus erythematosus immune complexes from cell receptors." Clin Exp Immunol **44**(2): 416-425.

Menon MC, Chuang PY and He CJ (2012). "The glomerular filtration barrier: components and crosstalk." Int J Nephrol **2012**: 749010.

Mihaylova MM and Shaw RJ (2011). "The AMPK signalling pathway coordinates cell growth, autophagy and metabolism." Nat Cell Biol **13**(9): 1016-1023.

Mijaljica D, Prescott M and Devenish RJ (2011). "Microautophagy in mammalian cells: revisiting a 40-year-old conundrum." Autophagy **7**(7): 673-682.

Mineo C, Gormley AK, Yuhanna IS, Osborne-Lawrence S, Gibson LL, Hahner L, et al. (2005). "FcgammaRIIB mediates C-reactive protein inhibition of endothelial NO synthase." Circ Res **97**(11): 1124-1131.

Mizushima N, Levine B, Cuervo AM and Klionsky DJ (2008). "Autophagy fights disease through cellular self-digestion." Nature **451**(7182): 1069-1075.

Mizushima N, Yamamoto A, Hatano M, Kobayashi Y, Kabeya Y, Suzuki K, et al. (2001). "Dissection of autophagosome formation using Apg5-deficient mouse embryonic stem cells." J Cell Biol **152**(4): 657-668.

Mizushima N, Yoshimori T and Ohsumi Y (2011). "The role of Atg proteins in autophagosome formation." Annu Rev Cell Dev Biol **27**: 107-132.

Mohan C and Putterman C (2015). "Genetics and pathogenesis of systemic lupus erythematosus and lupus nephritis." Nat Rev Nephrol **11**(6): 329-341.

Mok CC (2010). "Biomarkers for lupus nephritis: a critical appraisal." J Biomed Biotechnol **2010**: 638413.

Mok CC (2011). "Epidemiology and survival of systemic lupus erythematosus in Hong Kong Chinese." Lupus **20**(7): 767-771.

Monneaux F, Lozano JM, Patarroyo ME, Briand JP and Muller S (2003). "T cell recognition and therapeutic effect of a phosphorylated synthetic peptide of the 70K snRNP protein administered in MR/lpr mice." Eur J Immunol **33**(2): 287-296.

Mortensen DS, Sapienza J, Lee BG, Perrin-Ninkovic SM, Harris R, Shevlin G, et al. (2013). "Use of core modification in the discovery of CC214-2, an orally available, selective inhibitor of mTOR kinase." Bioorg Med Chem Lett **23**(6): 1588-1591.

Moss SC, Lightell DJ, Jr., Marx SO, Marks AR and Woods TC (2010). "Rapamycin regulates endothelial cell migration through regulation of the cyclin-dependent kinase inhibitor p27Kip1." J Biol Chem **285**(16): 11991-11997.

Mostowy S, Sancho-Shimizu V, Hamon MA, Simeone R, Brosch R, Johansen T, et al. (2011). "p62 and NDP52 proteins target intracytosolic Shigella and Listeria to different autophagy pathways." J Biol Chem **286**(30): 26987-26995.

Munz C (2012). "Antigen Processing for MHC Class II Presentation via Autophagy." Front Immunol **3**: 9.

Murao K, Ohyama T, Imachi H, Ishida T, Cao WM, Namihira H, et al. (2000). "TNF-alpha stimulation of MCP-1 expression is mediated by the Akt/PKB signal transduction pathway in vascular endothelial cells." Biochem Biophys Res Commun **276**(2): 791-796.

Nakatani K, Fujii H, Hasegawa H, Terada M, Arita N, Ito MR, et al. (2004). "Endothelial adhesion molecules in glomerular lesions: association with their severity and diversity in lupus models." Kidney Int **65**(4): 1290-1300.

Nangaku M and Couser WG (2005). "Mechanisms of immune-deposit formation and the mediation of immune renal injury." Clin Exp Nephrol **9**(3): 183-191.

Nazio F, Strappazzon F, Antonioli M, Bielli P, Cianfanelli V, Bordi M, et al. (2013). "mTOR inhibits autophagy by controlling ULK1 ubiquitylation, self-association and function through AMBRA1 and TRAF6." Nat Cell Biol **15**(4): 406-416.

Nitta K, Horiba N, Uchida K, Tsutsui T, Horita S, Murai K, et al. (1994). "Establishment and characterization of an immortalized bovine glomerular endothelial cell line." Nihon Jinzo Gakkai Shi **36**(8): 883-889.

Nixon RA (2013). "The role of autophagy in neurodegenerative disease." Nat Med **19**(8): 983-997.

Norman MU, Lister KJ, Yang YH, Issekutz A and Hickey MJ (2005). "TNF regulates leukocyte-endothelial cell interactions and microvascular dysfunction during immune complex-mediated inflammation." Br J Pharmacol **144**(2): 265-274.

Nowling TK and Gilkeson GS (2011). "Mechanisms of tissue injury in lupus nephritis." Arthritis Res Ther **13**(6): 250.

Oates JC (2010). "The biology of reactive intermediates in systemic lupus erythematosus." Autoimmunity **43**(1): 56-63.

Ohsumi Y (2014). "Historical landmarks of autophagy research." Cell Res **24**(1): 9-23.

Opperman CM and Sishi BJ (2015). "Tumor necrosis factor alpha stimulates p62 accumulation and enhances proteasome activity independently of ROS." Cell Biol Toxicol **31**(2): 83-94.

Page N, Gros F, Schall N, Decossas M, Bagnard D, Briand JP, et al. (2011). "HSC70 blockade by the therapeutic peptide P140 affects autophagic processes and endogenous MHCII presentation in murine lupus." Ann Rheum Dis **70**(5): 837-843.

Pan L, Kreisle RA and Shi Y (1999). "Expression of endothelial cell IgG Fc receptors and markers on various cultures." Chin Med J (Engl) **112**(2): 157-161.

Pan LF, Kreisle RA and Shi YD (1998). "Detection of Fcgamma receptors on human endothelial cells stimulated with cytokines tumour necrosis factor-alpha (TNF-alpha) and interferon-gamma (IFN-gamma)." Clin Exp Immunol **112**(3): 533-538.

Pankiv S, Clausen TH, Lamark T, Brech A, Bruun JA, Outzen H, et al. (2007). "p62/SQSTM1 binds directly to Atg8/LC3 to facilitate degradation of ubiquitinated protein aggregates by autophagy." J Biol Chem **282**(33): 24131-24145.

Park D, Jeong H, Lee MN, Koh A, Kwon O, Yang YR, et al. (2016). "Resveratrol induces autophagy by directly inhibiting mTOR through ATP competition." Sci Rep **6**: 21772.

Parry TJ, Brosius R, Thyagarajan R, Carter D, Argentieri D, Falotico R, et al. (2005). "Drug-eluting stents: sirolimus and paclitaxel differentially affect cultured cells and injured arteries." Eur J Pharmacol **524**(1-3): 19-29.

Pautz A, Art J, Hahn S, Nowag S, Voss C and Kleinert H (2010). "Regulation of the expression of inducible nitric oxide synthase." Nitric Oxide **23**(2): 75-93.

Periyasamy-Thandavan S, Jiang M, Schoenlein P and Dong Z (2009). "Autophagy: molecular machinery, regulation, and implications for renal pathophysiology." Am J Physiol Renal Physiol **297**(2): F244-256.

Pestana CR, Oishi JC, Salistre-Araujo HS and Rodrigues GJ (2015). "Inhibition of autophagy by chloroquine stimulates nitric oxide production and protects

endothelial function during serum deprivation." Cell Physiol Biochem **37**(3): 1168-1177.

Peterson KS, Huang JF, Zhu J, D'Agati V, Liu X, Miller N, et al. (2004). "Characterization of heterogeneity in the molecular pathogenesis of lupus nephritis from transcriptional profiles of laser-captured glomeruli." J Clin Invest **113**(12): 1722-1733.

Petri M, Orbai AM, Alarcon GS, Gordon C, Merrill JT, Fortin PR, et al. (2012). "Derivation and validation of the Systemic Lupus International Collaborating Clinics classification criteria for systemic lupus erythematosus." Arthritis Rheum **64**(8): 2677-2686.

Pierdominici M, Vomero M, Barbati C, Colasanti T, Maselli A, Vacirca D, et al. (2012). "Role of autophagy in immunity and autoimmunity, with a special focus on systemic lupus erythematosus." FASEB J **26**(4): 1400-1412.

Pincus Z and Theriot JA (2007). "Comparison of quantitative methods for cell-shape analysis." J Microsc **227**(Pt 2): 140-156.

Potente M, Gerhardt H and Carmeliet P (2011). "Basic and therapeutic aspects of angiogenesis." Cell **146**(6): 873-887.

Ptak W, Paliwal V, Bryniarski K, Ptak M and Askenase PW (1998). "Aggregated immunoglobulin protects immune T cells from suppression: dependence on

isotype, Fc portion, and macrophage FcgammaR." Scand J Immunol **47**(2): 136-145.

Rafikov R, Fonseca FV, Kumar S, Pardo D, Darragh C, Elms S, et al. (2011). "eNOS activation and NO function: structural motifs responsible for the posttranslational control of endothelial nitric oxide synthase activity." J Endocrinol **210**(3): 271-284.

Rajendran P, Rengarajan T, Thangavel J, Nishigaki Y, Sakthisekaran D, Sethi G, et al. (2013). "The vascular endothelium and human diseases." Int J Biol Sci **9**(10): 1057-1069.

Ramser B, Kokot A, Metze D, Weiss N, Luger TA and Bohm M (2009). "Hydroxychloroquine modulates metabolic activity and proliferation and induces autophagic cell death of human dermal fibroblasts." J Invest Dermatol **129**(10): 2419-2426.

Rashid HO, Yadav RK, Kim HR and Chae HJ (2015). "ER stress: Autophagy induction, inhibition and selection." Autophagy **11**(11): 1956-1977.

Raught B, Peiretti F, Gingras AC, Livingstone M, Shahbazian D, Mayeur GL, et al. (2004). "Phosphorylation of eucaryotic translation initiation factor 4B Ser422 is modulated by S6 kinases." EMBO J **23**(8): 1761-1769.

Rees F, Doherty M, Grainge M, Davenport G, Lanyon P and Zhang W (2016). "The incidence and prevalence of systemic lupus erythematosus in the UK, 1999-2012." Ann Rheum Dis **75**(1): 136-141.

Reineke DC, Muller-Schweinitzer E, Winkler B, Kunz D, Konerding MA, Grussenmeyer T, et al. (2015). "Rapamycin impairs endothelial cell function in human internal thoracic arteries." Eur J Med Res **20**: 59.

Rekvig OP (2015). "The anti-DNA antibody: origin and impact, dogmas and controversies." Nat Rev Rheumatol **11**(9): 530-540.

Riha I, Haskova V, Kaslik J, Maierova M and Stransky J (1979). "The use of polyethyleneglycol for immune complex detection in human sera." Mol Immunol **16**(7): 489-493.

Rioux JD, Xavier RJ, Taylor KD, Silverberg MS, Goyette P, Huett A, et al. (2007). "Genome-wide association study identifies new susceptibility loci for Crohn disease and implicates autophagy in disease pathogenesis." Nat Genet **39**(5): 596-604.

Robinson MW, Scott DG, Bacon PA, Walton KW, Coppock JS and Scott DL (1989). "What proteins are present in polyethylene glycol precipitates from rheumatic sera?" Ann Rheum Dis **48**(6): 496-501.

Roca-Cusachs P, Alcaraz J, Sunyer R, Samitier J, Farre R and Navajas D (2008). "Micropatterning of single endothelial cell shape reveals a tight coupling between nuclear volume in G1 and proliferation." Biophys J **94**(12): 4984-4995.

Rodrik-Outmezguine VS, Chandarlapaty S, Pagano NC, Poulikakos PI, Scaltriti M, Moskatel E, et al. (2011). "mTOR kinase inhibition causes feedback-dependent biphasic regulation of AKT signaling." Cancer Discov **1**(3): 248-259.

Russell RC, Tian Y, Yuan H, Park HW, Chang YY, Kim J, et al. (2013). "ULK1 induces autophagy by phosphorylating Beclin-1 and activating VPS34 lipid kinase." Nat Cell Biol **15**(7): 741-750.

Sabatel C, Malvaux L, Bovy N, Deroanne C, Lambert V, Gonzalez ML, et al. (2011). "MicroRNA-21 exhibits antiangiogenic function by targeting RhoB expression in endothelial cells." PLoS One **6**(2): e16979.

Sainson RC, Johnston DA, Chu HC, Holderfield MT, Nakatsu MN, Crampton SP, et al. (2008). "TNF primes endothelial cells for angiogenic sprouting by inducing a tip cell phenotype." Blood **111**(10): 4997-5007.

Saitoh T, Fujita N, Jang MH, Uematsu S, Yang BG, Satoh T, et al. (2008). "Loss of the autophagy protein Atg16L1 enhances endotoxin-induced IL-1beta production." Nature **456**(7219): 264-268.

Sarbassov DD, Guertin DA, Ali SM and Sabatini DM (2005). "Phosphorylation and regulation of Akt/PKB by the rictor-mTOR complex." Science **307**(5712): 1098-1101.

Sarkar S (2013). "Regulation of autophagy by mTOR-dependent and mTOR-independent pathways: autophagy dysfunction in neurodegenerative diseases and therapeutic application of autophagy enhancers." Biochem Soc Trans **41**(5): 1103-1130.

Sarkar S, Davies JE, Huang Z, Tunnacliffe A and Rubinsztein DC (2007). "Trehalose, a novel mTOR-independent autophagy enhancer, accelerates the clearance of mutant huntingtin and alpha-synuclein." J Biol Chem **282**(8): 5641-5652.

Sarkar S, Floto RA, Berger Z, Imarisio S, Cordenier A, Pasco M, et al. (2005). "Lithium induces autophagy by inhibiting inositol monophosphatase." J Cell Biol **170**(7): 1101-1111.

Sarkar S, Korolchuk VI, Renna M, Imarisio S, Fleming A, Williams A, et al. (2011). "Complex inhibitory effects of nitric oxide on autophagy." Mol Cell **43**(1): 19-32.

Satchell SC and Braet F (2009). "Glomerular endothelial cell fenestrations: an integral component of the glomerular filtration barrier." Am J Physiol Renal Physiol **296**(5): F947-956.

Satchell SC, Tasman CH, Singh A, Ni L, Geelen J, von Ruhland CJ, et al. (2006). "Conditionally immortalized human glomerular endothelial cells expressing fenestrations in response to VEGF." Kidney Int **69**(9): 1633-1640.

Saxena R, Mahajan T and Mohan C (2011). "Lupus nephritis: current update." Arthritis Res Ther **13**(5): 240.

Schafer A, Wiesmann F, Neubauer S, Eigenthaler M, Bauersachs J and Channon KM (2004). "Rapid regulation of platelet activation in vivo by nitric oxide." Circulation **109**(15): 1819-1822.

Schall N and Muller S (2015). "Resetting the autoreactive immune system with a therapeutic peptide in lupus." Lupus **24**(4-5): 412-418.

Schmeding A and Schneider M (2013). "Fatigue, health-related quality of life and other patient-reported outcomes in systemic lupus erythematosus." Best Pract Res Clin Rheumatol **27**(3): 363-375.

Schmeisser H, Bekisz J and Zoon KC (2014). "New function of type I IFN: induction of autophagy." J Interferon Cytokine Res **34**(2): 71-78.

Schmeisser H, Fey SB, Horowitz J, Fischer ER, Balinsky CA, Miyake K, et al. (2013). "Type I interferons induce autophagy in certain human cancer cell lines." Autophagy **9**(5): 683-696.

Searles CD (2006). "Transcriptional and posttranscriptional regulation of endothelial nitric oxide synthase expression." Am J Physiol Cell Physiol **291**(5): C803-816.

Seglen PO and Gordon PB (1982). "3-Methyladenine: specific inhibitor of autophagic/lysosomal protein degradation in isolated rat hepatocytes." Proc Natl Acad Sci U S A **79**(6): 1889-1892.

Seglen PO, Grinde B and Solheim AE (1979). "Inhibition of the lysosomal pathway of protein degradation in isolated rat hepatocytes by ammonia, methylamine, chloroquine and leupeptin." Eur J Biochem **95**(2): 215-225.

Seredkina N and Rekvig OP (2011). "Acquired loss of renal nuclease activity is restricted to DNaseI and is an organ-selective feature in murine lupus nephritis." Am J Pathol **179**(3): 1120-1128.

Sesin CA, Yin X, Esmon CT, Buyon JP and Clancy RM (2005). "Shedding of endothelial protein C receptor contributes to vasculopathy and renal injury in lupus: in vivo and in vitro evidence." Kidney Int **68**(1): 110-120.

Shang L, Chen S, Du F, Li S, Zhao L and Wang X (2011). "Nutrient starvation elicits an acute autophagic response mediated by Ulk1 dephosphorylation and its subsequent dissociation from AMPK." Proc Natl Acad Sci U S A **108**(12): 4788-4793.

Shaul PW, Smart EJ, Robinson LJ, German Z, Yuhanna IS, Ying Y, et al. (1996). "Acylation targets emdothelial nitric-oxide synthase to plasmalemmal caveolae." J Biol Chem **271**(11): 6518-6522.

Shen C, Yan J, Erkocak OF, Zheng XF and Chen XD (2014). "Nitric oxide inhibits autophagy via suppression of JNK in meniscal cells." Rheumatology (Oxford) **53**(6): 1022-1033.

Shi CS, Shenderov K, Huang NN, Kabat J, Abu-Asab M, Fitzgerald KA, et al. (2012a). "Activation of autophagy by inflammatory signals limits IL-1beta production by targeting ubiquitinated inflammasomes for destruction." Nat Immunol **13**(3): 255-263.

Shi WY, Xiao D, Wang L, Dong LH, Yan ZX, Shen ZX, et al. (2012b). "Therapeutic metformin/AMPK activation blocked lymphoma cell growth via inhibition of mTOR pathway and induction of autophagy." Cell Death Dis **3**: e275.

Shibutani ST, Saitoh T, Nowag H, Munz C and Yoshimori T (2015). "Autophagy and autophagy-related proteins in the immune system." Nat Immunol **16**(10): 1014-1024.

Shimobayashi M and Hall MN (2014). "Making new contacts: the mTOR network in metabolism and signalling crosstalk." Nat Rev Mol Cell Biol **15**(3): 155-162.

Shiojima I and Walsh K (2002). "Role of Akt signaling in vascular homeostasis and angiogenesis." Circ Res **90**(12): 1243-1250.

Siddique A, Shantsila E, Lip GY and Varma C (2010). "Endothelial progenitor cells: what use for the cardiologist?" J Angiogenes Res **2**: 6.

Siefers KJ (2014). Sodium salicylate prevents in ammation- associated decreases in phosphorylated-Enos SER1177 in human aortic endothelial cells through an AMPK-dependent mechanism. MS (Master of Science) Thesis, University of Iowa. http://ir.uiowa.edu/etd/4753.

Singh S, Wu T, Xie C, Vanarsa K, Han J, Mahajan T, et al. (2012). "Urine VCAM-1 as a marker of renal pathology activity index in lupus nephritis." Arthritis Research & Therapy **14**(4).

Siragusa M and Fleming I (2016). "The eNOS signalosome and its link to endothelial dysfunction." Pflugers Arch **468**(7): 1125-1137.

Skeoch S, Haque S, Pemberton P and Bruce IN (2014). "Cell adhesion molecules as potential biomarkers of nephritis, damage and accelerated atherosclerosis in patients with SLE." Lupus **23**(8): 819-824.

Smith AJ, Kyle V, Cawston TE and Hazleman BL (1987). "Isolation and analysis of immune complexes from sera of patients with polymyalgia rheumatica and giant cell arteritis." Ann Rheum Dis **46**(6): 468-474.

Smith SM, Wunder MB, Norris DA and Shellman YG (2011). "A simple protocol for using a LDH-based cytotoxicity assay to assess the effects of death and growth inhibition at the same time." PLoS One **6**(11): e26908.

St John PL and Abrahamson DR (2001). "Glomerular endothelial cells and podocytes jointly synthesize laminin-1 and -11 chains." Kidney Int **60**(3): 1037-1046.

Striker GE, Soderland C, Bowen-Pope DF, Gown AM, Schmer G, Johnson A, et al. (1984). "Isolation, characterization, and propagation in vitro of human glomerular endothelial cells." J Exp Med **160**(1): 323-328.

Stroka KM, Vaitkus JA and Aranda-Espinoza H (2012). "Endothelial cells undergo morphological, biomechanical, and dynamic changes in response to tumor necrosis factor-alpha." Eur Biophys J **41**(11): 939-947.

Stuehr DJ (1997). "Structure-function aspects in the nitric oxide synthases." Annu Rev Pharmacol Toxicol **37**: 339-359.

Stylianou K, Petrakis I, Mavroeidi V, Stratakis S, Vardaki E, Perakis K, et al. (2011). "The PI3K/Akt/mTOR pathway is activated in murine lupus nephritis and downregulated by rapamycin." Nephrol Dial Transplant **26**(2): 498-508.

Sun S, Rao NL, Venable J, Thurmond R and Karlsson L (2007). "TLR7/9 antagonists as therapeutics for immune-mediated inflammatory disorders." Inflamm Allergy Drug Targets **6**(4): 223-235.

Sun W, Jiao Y, Cui B, Gao X, Xia Y and Zhao Y (2013). "Immune complexes activate human endothelium involving the cell-signaling HMGB1-RAGE axis in the pathogenesis of lupus vasculitis." Lab Invest **93**(6): 626-638.

Suwanichkul A and Wenderfer SE (2013). "Differential expression of functional Fc-receptors and additional immune complex receptors on mouse kidney cells." Mol Immunol **56**(4): 369-379.

Szczygiel AM, Brzezinka G, Targosz-Korecka M, Chlopicki S and Szymonski M (2012). "Elasticity changes anti-correlate with NO production for human endothelial cells stimulated with TNF-alpha." Pflugers Arch **463**(3): 487-496.

Taguchi-Atarashi N, Hamasaki M, Matsunaga K, Omori H, Ktistakis NT, Yoshimori T, et al. (2010). "Modulation of local PtdIns3P levels by the PI phosphatase MTMR3 regulates constitutive autophagy." Traffic **11**(4): 468-478.

Tan Y, Yu F and Liu G (2014). "Diverse vascular lesions in systemic lupus erythematosus and clinical implications." Curr Opin Nephrol Hypertens **23**(3): 218-223.

Tanida I, Minematsu-Ikeguchi N, Ueno T and Kominami E (2005). "Lysosomal turnover, but not a cellular level, of endogenous LC3 is a marker for autophagy." Autophagy **1**(2): 84-91.

Tanigaki K, Sundgren N, Khera A, Vongpatanasin W, Mineo C and Shaul PW (2015). "Fcgamma receptors and ligands and cardiovascular disease." Circ Res **116**(2): 368-384.

Tannenbaum SH, Finko R and Cines DB (1986). "Antibody and immune complexes induce tissue factor production by human endothelial cells." J Immunol **137**(5): 1532-1537.

Telikepalli SN, Kumru OS, Kalonia C, Esfandiary R, Joshi SB, Middaugh CR, et al. (2014). "Structural characterization of IgG1 mAb aggregates and particles generated under various stress conditions." J Pharm Sci **103**(3): 796-809.

Teruel M and Alarcon-Riquelme ME (2016). "The genetic basis of systemic lupus erythematosus: What are the risk factors and what have we learned." J Autoimmun **74**: 161-175.

Theofilopoulos AN, Wilson CB and Dixon FJ (1976). "The Raji cell radioimmune assay for detecting immune complexes in human sera." J Clin Invest **57**(1): 169-182.

Tsioni V, Andreoli L, Meini A, Frassi M, Raffetti E, Airo P, et al. (2015). "The prevalence and incidence of systemic lupus erythematosus in children and adults: a population-based study in a mountain community in northern Italy." Clin Exp Rheumatol **33**(5): 681-687.

Tsokos GC (2011). "Systemic lupus erythematosus." N Engl J Med **365**(22): 2110-2121.

van Bavel CC, Fenton KA, Rekvig OP, van der Vlag J and Berden JH (2008). "Glomerular targets of nephritogenic autoantibodies in systemic lupus erythematosus." Arthritis Rheum **58**(7): 1892-1899.

Vander Haar E, Lee SI, Bandhakavi S, Griffin TJ and Kim DH (2007). "Insulin signalling to mTOR mediated by the Akt/PKB substrate PRAS40." Nat Cell Biol **9**(3): 316-323.

Vanderslice P, Munsch CL, Rachal E, Erichsen D, Sughrue KM, Truong AN, et al. (1998). "Angiogenesis induced by tumor necrosis factor-agr; is mediated by alpha4 integrins." Angiogenesis **2**(3): 265-275.

Vicencio JM, Ortiz C, Criollo A, Jones AW, Kepp O, Galluzzi L, et al. (2009). "The inositol 1,4,5-trisphosphate receptor regulates autophagy through its interaction with Beclin 1." Cell Death Differ **16**(7): 1006-1017.

Wanchu A, Khullar M, Deodhar SD, Bambery P and Sud A (1998). "Nitric oxide synthesis is increased in patients with systemic lupus erythematosus." Rheumatol Int **18**(2): 41-43.

Wang GR, Zhu Y, Halushka PV, Lincoln TM and Mendelsohn ME (1998). "Mechanism of platelet inhibition by nitric oxide: in vivo phosphorylation of thromboxane receptor by cyclic GMP-dependent protein kinase." Proc Natl Acad Sci U S A **95**(9): 4888-4893.

Watanabe-Asano T, Kuma A and Mizushima N (2014). "Cycloheximide inhibits starvation-induced autophagy through mTORC1 activation." Biochem Biophys Res Commun **445**(2): 334-339.

Weckerle CE, Mangale D, Franek BS, Kelly JA, Kumabe M, James JA, et al. (2012). "Large-scale analysis of tumor necrosis factor alpha levels in systemic lupus erythematosus." Arthritis Rheum **64**(9): 2947-2952.

Weening JJ, D'Agati VD, Schwartz MM, Seshan SV, Alpers CE, Appel GB, et al. (2004). "The classification of glomerulonephritis in systemic lupus erythematosus revisited." Kidney Int **65**(2): 521-530.

Wei Y, Pattingre S, Sinha S, Bassik M and Levine B (2008). "JNK1-mediated phosphorylation of Bcl-2 regulates starvation-induced autophagy." Mol Cell **30**(6): 678-688.

Weinberg JB, Granger DL, Pisetsky DS, Seldin MF, Misukonis MA, Mason SN, et al. (1994). "The role of nitric oxide in the pathogenesis of spontaneous murine autoimmune disease: increased nitric oxide production and nitric oxide synthase expression in MRL-lpr/lpr mice, and reduction of spontaneous glomerulonephritis and arthritis by orally administered NG-monomethyl-L-arginine." J Exp Med **179**(2): 651-660.

Wen Z, Xu L, Chen X, Xu W, Yin Z, Gao X, et al. (2013). "Autoantibody induction by DNA-containing immune complexes requires HMGB1 with the TLR2/microRNA-155 pathway." J Immunol **190**(11): 5411-5422.

Williams A, Sarkar S, Cuddon P, Ttofi EK, Saiki S, Siddiqi FH, et al. (2008). "Novel targets for Huntington's disease in an mTOR-independent autophagy pathway." Nat Chem Biol **4**(5): 295-305.

Williams RS, Cheng L, Mudge AW and Harwood AJ (2002). "A common mechanism of action for three mood-stabilizing drugs." Nature **417**(6886): 292-295.

Wink DA, Miranda KM, Espey MG, Pluta RM, Hewett SJ, Colton C, et al. (2001). "Mechanisms of the antioxidant effects of nitric oxide." Antioxid Redox Signal **3**(2): 203-213.

Winkler DG, Faia KL, DiNitto JP, Ali JA, White KF, Brophy EE, et al. (2013). "PI3K-delta and PI3K-gamma inhibition by IPI-145 abrogates immune responses and suppresses activity in autoimmune and inflammatory disease models." Chem Biol **20**(11): 1364-1374.

Wirth M, Joachim J and Tooze SA (2013). "Autophagosome formation--the role of ULK1 and Beclin1-PI3KC3 complexes in setting the stage." Semin Cancer Biol **23**(5): 301-309.

Wong PM, Puente C, Ganley IG and Jiang X (2013). "The ULK1 complex: sensing nutrient signals for autophagy activation." Autophagy **9**(2): 124-137.

Wongpiyabovorn J, Hirankarn N, Ruchusatsawat K, Yooyongsatit S, Benjachat T and Avihingsanon Y (2011). "The association of single nucleotide polymorphism within vascular endothelial growth factor gene with systemic lupus erythematosus and lupus nephritis." Int J Immunogenet **38**(1): 63-67.

Wu LH, Yu F, Tan Y, Qu Z, Chen MH, Wang SX, et al. (2013a). "Inclusion of renal vascular lesions in the 2003 ISN/RPS system for classifying lupus nephritis improves renal outcome predictions." Kidney Int **83**(4): 715-723.

Wu Y, Wang X, Guo H, Zhang B, Zhang XB, Shi ZJ, et al. (2013b). "Synthesis and screening of 3-MA derivatives for autophagy inhibitors." Autophagy **9**(4): 595-603.

Wu YT, Tan HL, Shui G, Bauvy C, Huang Q, Wenk MR, et al. (2010). "Dual role of 3-methyladenine in modulation of autophagy via different temporal patterns of inhibition on class I and III phosphoinositide 3-kinase." J Biol Chem **285**(14): 10850-10861.

Xavier RJ and Rioux JD (2008). "Genome-wide association studies: a new window into immune-mediated diseases." Nat Rev Immunol **8**(8): 631-643.

Xia X, Kar R, Gluhak-Heinrich J, Yao W, Lane NE, Bonewald LF, et al. (2010). "Glucocorticoid-induced autophagy in osteocytes." J Bone Miner Res **25**(11): 2479-2488.

Xia Z, Liu M, Wu Y, Sharma V, Luo T, Ouyang J, et al. (2006). "N-acetylcysteine attenuates TNF-alpha-induced human vascular endothelial cell apoptosis and restores eNOS expression." Eur J Pharmacol **550**(1-3): 134-142.

Xiang YJ and Dai SM (2009). "Prevalence of rheumatic diseases and disability in China." Rheumatol Int **29**(5): 481-490.

Xie R, Nguyen S, McKeehan WL and Liu L (2010). "Acetylated microtubules are required for fusion of autophagosomes with lysosomes." BMC Cell Biol **11**: 89.

Xiong J, Liang Y, Yang H, Zhu F and Wang Y (2013). "The role of angiotensin II type 1 receptor-activating antibodies in patients with lupus nephritis." Int J Clin Pract **67**(10): 1066-1067.

Xu J, Wang Y, Tan X and Jing H (2012). "MicroRNAs in autophagy and their emerging roles in crosstalk with apoptosis." Autophagy **8**(6): 873-882.

Yamamoto K, Takahashi T, Asahara T, Ohura N, Sokabe T, Kamiya A, et al. (2003). "Proliferation, differentiation, and tube formation by endothelial progenitor cells in response to shear stress." J Appl Physiol (1985) **95**(5): 2081-2088.

Yan G, You B, Chen SP, Liao JK and Sun J (2008). "Tumor necrosis factor-alpha downregulates endothelial nitric oxide synthase mRNA stability via translation elongation factor 1-alpha 1." Circ Res **103**(6): 591-597.

Yang HL, Chang HC, Lin SW, Senthil Kumar KJ, Liao CH, Wang HM, et al. (2014). "Antrodia salmonea inhibits TNF-alpha-induced angiogenesis and atherogenesis in human endothelial cells through the down-regulation of NF-kappaB and up-regulation of Nrf2 signaling pathways." J Ethnopharmacol **151**(1): 394-406.

Yang W, Tang H, Zhang Y, Tang X, Zhang J, Sun L, et al. (2013a). "Meta-analysis followed by replication identifies loci in or near CDKN1B, TET3, CD80, DRAM1, and ARID5B as associated with systemic lupus erythematosus in Asians." Am J Hum Genet **92**(1): 41-51.

Yang YP, Hu LF, Zheng HF, Mao CJ, Hu WD, Xiong KP, et al. (2013b). "Application and interpretation of current autophagy inhibitors and activators." Acta Pharmacol Sin **34**(5): 625-635.

Yang Z, Goronzy JJ and Weyand CM (2015). "Autophagy in autoimmune disease." J Mol Med (Berl) **93**(7): 707-717.

Yang Z and Klionsky DJ (2010). "Mammalian autophagy: core molecular machinery and signaling regulation." Curr Opin Cell Biol **22**(2): 124-131.

Yaniv G, Twig G, Shor DB, Furer A, Sherer Y, Mozes O, et al. (2015). "A volcanic explosion of autoantibodies in systemic lupus erythematosus: a diversity of 180 different antibodies found in SLE patients." Autoimmun Rev **14**(1): 75-79.

Yano K, Gale D, Massberg S, Cheruvu PK, Monahan-Earley R, Morgan ES, et al. (2007). "Phenotypic heterogeneity is an evolutionarily conserved feature of the endothelium." Blood **109**(2): 613-615.

Yap DY, Ma MK, Tang CS and Chan TM (2012a). "Proliferation signal inhibitors in the treatment of lupus nephritis: preliminary experience." Nephrology (Carlton) **17**(8): 676-680.

Yap DY, Tang CS, Ma MK, Lam MF and Chan TM (2012b). "Survival analysis and causes of mortality in patients with lupus nephritis." Nephrol Dial Transplant **27**(8): 3248-3254.

Yazbeck VY, Georgakis GV, Li Y and Younes A (2006). "The mTOR inhibitor CCI-779 (temsirolimus) downregulates p21 and induces cell cycle arrest and autophagy in mantle cell lymphoma (MCL)." J Clin Oncol **24**(18_suppl): 7573.

Yeh KW, Yu CH, Chan PC, Horng JT and Huang JL (2013). "Burden of systemic lupus erythematosus in Taiwan: a population-based survey." Rheumatol Int **33**(7): 1805-1811.

Yu M, Selvaraj SK, Liang-Chu MM, Aghajani S, Busse M, Yuan J, et al. (2015a). "A resource for cell line authentication, annotation and quality control." Nature **520**(7547): 307-311.

Yu M, Song Y, Zhu MX, Liang W, Long Q, Ding PW, et al. (2015b). "B10 Cells Ameliorate the Progression of Lupus Nephritis by Attenuating Glomerular Endothelial Cell Injury." Cell Physiol Biochem **36**(6): 2161-2169.

Yuan W, DiMartino SJ, Redecha PB, Ivashkiv LB and Salmon JE (2011). "Systemic lupus erythematosus monocytes are less responsive to interleukin-10 in the presence of immune complexes." Arthritis Rheum **63**(1): 212-218.

Yuk JM, Shin DM, Lee HM, Yang CS, Jin HS, Kim KK, et al. (2009). "Vitamin D3 induces autophagy in human monocytes/macrophages via cathelicidin." Cell Host Microbe **6**(3): 231-243.

Yung S and Chan TM (2012). "Autoantibodies and resident renal cells in the pathogenesis of lupus nephritis: getting to know the unknown." Clin Dev Immunol **2012**: 139365.

Zeng QY, Chen R, Darmawan J, Xiao ZY, Chen SB, Wigley R, et al. (2008). "Rheumatic diseases in China." Arthritis Res Ther **10**(1): R17.

Zhang J, Defelice AF, Hanig JP and Colatsky T (2010). "Biomarkers of endothelial cell activation serve as potential surrogate markers for drug-induced vascular injury." Toxicol Pathol **38**(6): 856-871.

Zhou CC, Ahmad S, Mi T, Abbasi S, Xia L, Day MC, et al. (2008a). "Autoantibody from women with preeclampsia induces soluble Fms-like tyrosine kinase-1 production via angiotensin type 1 receptor and calcineurin/nuclear factor of activated T-cells signaling." Hypertension **51**(4): 1010-1019.

Zhou XJ, Lu XL, Lv JC, Yang HZ, Qin LX, Zhao MH, et al. (2011). "Genetic association of PRDM1-ATG5 intergenic region and autophagy with systemic lupus erythematosus in a Chinese population." Ann Rheum Dis **70**(7): 1330-1337.

Zhou XJ, Nath SK, Qi YY, Cheng FJ, Yang HZ, Zhang Y, et al. (2014). "Brief Report: identification of MTMR3 as a novel susceptibility gene for lupus nephritis in northern Han Chinese by shared-gene analysis with IgA nephropathy." Arthritis Rheumatol **66**(10): 2842-2848.

Zhou Z, Gengaro P, Wang W, Wang XQ, Li C, Faubel S, et al. (2008b). "Role of NF-kappaB and PI 3-kinase/Akt in TNF-alpha-induced cytotoxicity in microvascular endothelial cells." Am J Physiol Renal Physiol **295**(4): F932-941.

Zhu XY, Daghini E, Chade AR, Napoli C, Ritman EL, Lerman A, et al. (2007). "Simvastatin prevents coronary microvascular remodeling in renovascular hypertensive pigs." J Am Soc Nephrol **18**(4): 1209-1217.

Zubler RH, Lange G, Lambert PH and Miescher PA (1976). "Detection of immune complexes in unheated sera by modified 125I-Clq binding test. Effect of heating on the binding of Clq by immune complexes and application of the test to systemic lupus erythematosus." J Immunol **116**(1): 232-235.

Zykova SN, Tveita AA and Rekvig OP (2010). "Renal Dnase1 enzyme activity and protein expression is selectively shut down in murine and human membranoproliferative lupus nephritis." PLoS One **5**(8).